Design of Multi-Degree-of-Freedom Tuned-Mass Dampers using Perturbation Techniques

by

Justin Matthew Verdirame

Bachelor of Science, Mechanical Engineering
Massachusetts Institute of Technology, 2000

Submitted to the Department of Mechanical Engineering
in partial fulfillment of the requirements for the degree of

Master of Science in Mechanical Engineering

at the

MASSACHUSETTS INSTITUTE OF TECHNOLOGY

June 2003

Author .....
Department of Mechanical Engineering
June 5, 2003

Certified by .....
Samir A. Nayfeh
Assistant Professor
Thesis Supervisor

Accepted by .....
Ain A. Sonin
Chairman, Department Committee on Graduate Students

Design of Multi-Degree-of-Freedom Tuned-Mass Dampers using Perturbation Techniques

by

Justin Matthew Verdirame

Submitted to the Department of Mechanical Engineering
on June 5, 2003, in partial fulfillment of the
requirements for the degree of
Master of Science in Mechanical Engineering

Abstract

In precision assemblies, components must be aligned relative to another with high accuracy. The components are typically supported on flexures, which exhibit negligible damping; therefore, vibration of the components becomes an issue. In this thesis (and in concert with Zuo and Nayfeh [50]), we develop the concept of the multi-degree-of-freedom (MDOF) tuned-mass damper (TMD) to damp multiple modes of vibration of a primary structure. A MDOF TMD consists of a rigid mass connected to a primary mass with damping and stiffness tuned to suppress vibration in as many as six modes of vibration of the primary structure. Zuo and Nayfeh [50] have shown that, given size and location of the absorber mass, numerical optimization can efficiently determine the values of the springs and dampers but not their locations.

The goal of this thesis is to develop analytical approximations for the design and attainable performance of MDOF TMDs. The use of perturbation methods allows the locations of the springs and dampers to be optimized, in addition to their values. First, we examine the single-degree-of-freedom tuned-mass damper and use eigenvalue perturbation, with the mass ratio as the small parameter, to determine the approximate eigenvalues and eigenvectors. To demonstrate the application of the approximate eigenvalues and eigenvectors for design, we show that perturbation results for the minimax design, which maximizes the minimum damping coefficient, are a Maclaurin series expansion of the exact solution. Then, we extend the method to multiple degrees of freedom. Approximate eigenvalues and eigenvectors are determined for the coupled system. We use the minimax criterion to illustrate the design procedure using the expansion. The method is applied to a two-DOF system and a three-DOF system, and for the two-DOF system the results are compared with those of a numerical optimization procedure.

Thesis Supervisor: Samir A. Nayfeh
Title: Assistant Professor

Acknowledgments

This thesis has taken me so long to complete and so many people have helped me that I hope I do not forget anyone.

First, I must thank my advisor, Prof. Samir Nayfeh, for his instruction, insight, and unwaivering support. His excellence in all areas, from theory to practice, never ceases to amaze me. His ability to teach such varied and complicated topics have made him a great teacher. Furthermore, his creativity, enthusiasm, motivation, and kindness have made him an even better mentor. Finally, he must be commended for never getting frustrated by my inability to do algebra or write Matlab scripts.

Next, I must thank my labmates for providing encouragement, advice, and instruction. The "weavies," Jonathan Rohrs, Mauricio Diaz, and Emily Warmann have suffered tremendously by sharing office space with me for the past two years. Jonathan is faithfully answers my questions on everything ranging from software to math to design to current events. prepared to answer my questions (99% of which are stupid) and provide a discussion of current events. Mauricio answered many of my machine design and math questions and introduced me to Tacos Lupita. Lei Zuo has provided valuable insight on a number of fronts, but most importantly in my work on MDOF TMDs. Kripa Varanasi provided instruction in a variety of tasks and techniques. Dhanushkodi Mariappan always tried to make me stronger by helping him lift heavy machinery around the lab. Andrew Wilson provided excitement and kept me awake by yelling "Dood!" Maggie Beucler, Prof Nayfeh's administrative assistant, has been kind and encouraging throughout.

Countless others have made the last three years a lot fun. I am indebted to my fellow 2.003 TAs, Vijay Shilpiekandula, Xiaodong Lu, and Yi Xie, because their hard work and enthusiasm made the experience fun and educational (special thanks to Yi for her instruction in the "art" of using chopsticks). Joe Cattell and I started our own "company," and Joe taught me controls for the quals. Jeff Dahmus always had time for a conversation whenever I felt like procrastinating. Every game was exciting with the Neanderthals hockey team. Max Berniker is a fearless leader, as well as a

good roommate. I would like to thank all of my friends for their camaraderie and support.

I would also like to thank everyone else, too many to name here, who aided me in this research.

Most of all, I would like to thank my family especially my parents, Joe and Nancy. Their support and encouragement in all of my endeavors is relentless and greatly appreciated. My brother, Mike, and sister, Claudia, have provided constant "encouragement" with their incessant MIT jokes and fighting beaver impersonations. Nick and White Sox have provided me with an endless supply of white hairs to bring back from each visit home.

Contents

List of Figures

List of Tables

Chapter 1

Introduction

1.1 Motivation

In the design of precision machines and precision assemblies, components must be positioned to within tight tolerances. Furthermore, the support structures must not deform these components by applying unnecessary stresses. Therefore, the components must be kinematically constrained. In other words, the structure must be statically determinate. To accomplish this task, components are often supported on flexures, elastic elements which are relatively stiff in usually one direction and compliant in the other directions. Because these flexures are elastic and typically have negligible damping, vibration of the components relative to the support structure becomes a problem. Therefore, a method of introducing damping into the system must be found.

An example of such a system is the optical assembly of a lithography system. A mock-up of a beam splitter supported on flexures is shown in Figure 1-1. Its vibration mode shapes are shown in Figure 1-2. To maximize performance of the lithography system, the vibration of the optical elements should be well damped.

A number of methods exist for adding damping, but precision systems have special requirements that impose limitations. Typical methods such as adding viscoelastic materials are unacceptable in precision applications because creep is introduced into the system. Electromagnetic dampers are often difficult to use when retrofitting a

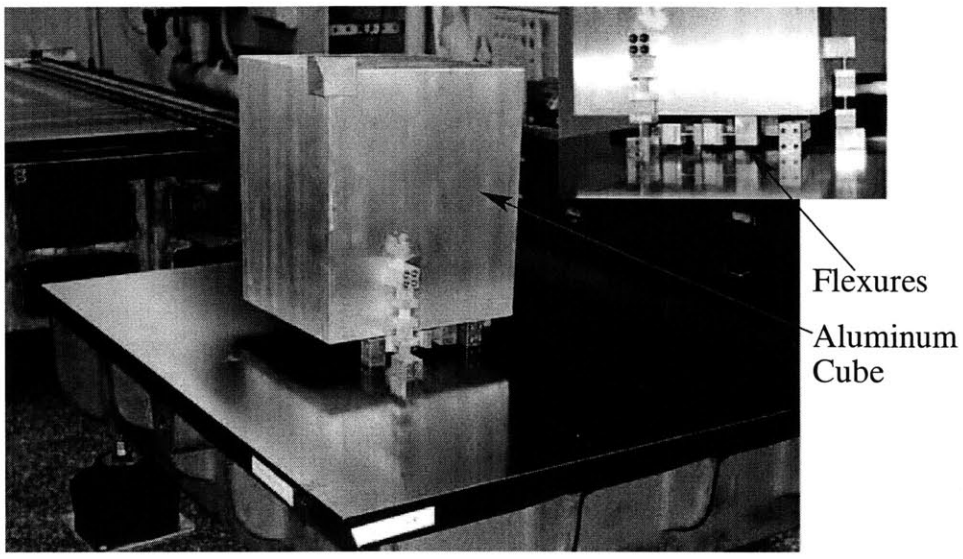

Figure 1-1: An aluminum block supported on flexures serves as a mock-up of an optical assembly typical of a lithography system. Aluminum has approximately the same density as glass.

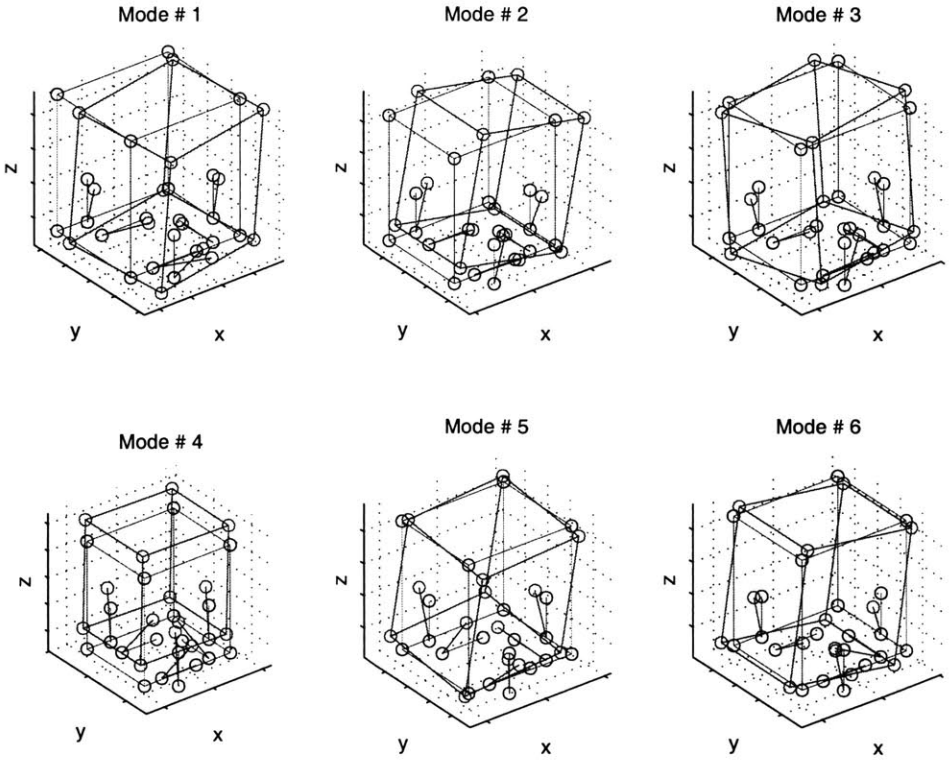

Figure 1-2: Vibration mode shapes of the mock-up shown in Figure 1-2.

system. Fluid dampers are unacceptable in systems where cleanliness is a concern. An inertial, or tuned-mass, damper is a good alternative because it is easy to retrofit; and it does not introduce creep.

1.2 Terminology

A tuned-mass damper (TMD), or dynamic vibration absorber (DVA), consists of a rigid mass connected to a primary mass with damping and stiffness tuned to suppress vibration of the primary mass (see Figure 1-3). There are three common tuning methods (see Figure 1-4). The H_∞ optimal tuning minimizes the maximum response to harmonic excitation, which for the single-degree-of-freedom (SDOF) TMD, sets the two peaks in the frequency response to be of equal and minimum height (see Figure 1-4). The $H2$ optimal design minimizes the energy in the system, or equivalently, minimizes the variance to white-noise (random) excitation. The third common tuning method is obtained from "minimax" optimization of the damping; the minimum damping coefficient is maximized. This design differs from the H_∞ and $H2$ tunings because it is not input-output based. When the input, or disturbance(s), are not well known, the minimax design is often preferable to the H_∞ and $H2$ optimal designs. This design maximizes the stability margin and robustness of the system. A result of this design for the SDOF TMD is that the system has one repeated eigenvalue instead of two distinct eigenvalues (see Figure 1-5). Therefore, the frequency response has a single peak (see Figure 1-4). This thesis focuses primarily on the minimax design.

1.3 Previous Literature

The concept of the tuned-mass damper was created by Frahm [9], who received a patent for the idea in 1909. The first analysis of the TMD was performed by Den Hartog and Ormondroyd in 1929 [26]. Their idea for the optimal tuned-mass damper was based on the idea of "equal peaks." They derived a simple tuning which very

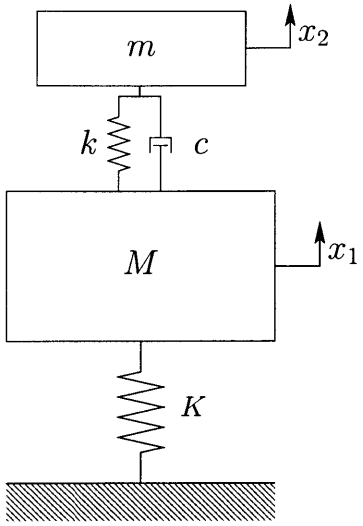

Figure 1-3: Diagram of a vibratory system comprising a mass M to which a single-degree-of-freedom tuned-mass damper m is attached.

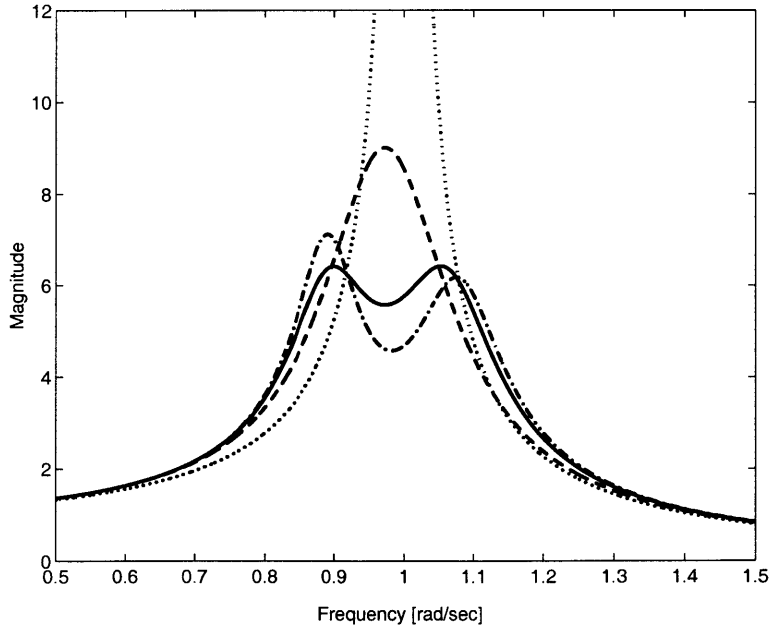

Figure 1-4: Frequency responses for various tuned-mass damper tuning methods: undamped (dots), solid (Den Hartog, approximate H_∞), minimax (dashed), $H2$ (dash-dot)

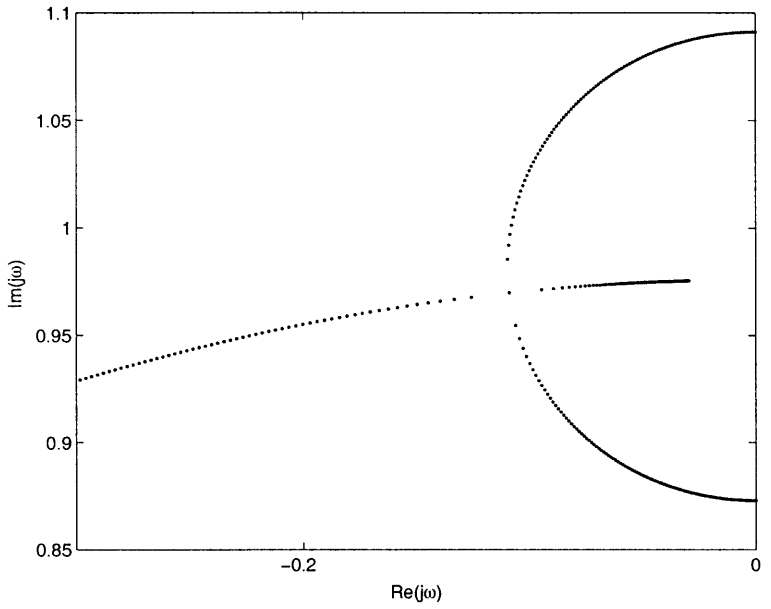

Figure 1-5: Eigenvalue locations for the minimax tuned SDOF TMD as the damping is varied. Only the upper half-plane pole locations are shown because the eigenvalues form complex conjugate pairs. The poles coalesce for the minimax damping value.

nearly approximates the H_∞ optimal tuning and is given by

$$f = \frac{1}{1+\mu} \tag{1.1}$$

where f is the ratio of the natural frequency of the TMD to the primary system and μ is the mass ratio (m/M). In 1946, Brock [4] derived the optimal damping coefficient of the absorber for Den Hartog and Ormondroyd's method of equal peaks:

$$\zeta = \sqrt{\frac{3\mu}{8(1+\mu)}} \tag{1.2}$$

More recently, researchers have expanded on the work of Den Hartog by finding the optimal tuning and damping based on time and frequency domain techniques [34] [40]x including the H_∞ and $H2$ optimal designs [3] and considered systems where the primary structure has light damping [10] [42]. Tsai [35] [36], Igusa and Kiureghian [13], and Pacheco and Fujino [27] used perturbation techniques to study the response of systems with SDOF TMDs. Fujino and Abé [10] expanded on this work and de-

veloped expressions for the design of SDOF TMDs using perturbation techniques. The presence of multiple modes in a primary structure affects the performance and optimal design of SDOF TMDs; this has been studied in continuous and discrete structures (e.g., [15, 42, 37]).

A fundamental difficulty in the use of a TMD is its sensitivity to tuning. Researchers have attempted to improve the performance robustness by tuning many SDOF TMDs to a single mode of the primary structure [12, 1, 18, 28, 21, 11]. Abé and Fujino [1] employed a perturbation method to develop some design rules for the multiple-TMD systems.

Most common structures have more than one vibrational mode of importance, and it is often desired to attenuate the response in many or all modes of a structure. Multiple SDOF TMDs can be employed to damp more than one mode of a primary structure (e.g., [41, 22, 20]). Rice [30] used the Simplex Algorithm to minimize the peak of the frequency response over a designated frequency range for two SDOF TMDs attached to a cantilever beam, optimizing the location as well as the stiffness and damping of the absorbers. Chen and Wu [5] studied the optimal placement of multiple SDOF TMDs on a model of a multi-story shear building. Many others (e.g., [29, 25, 33, 2, 49]) have used numerical methods, including genetic algorithms and LQG/H2 optimization, to design SDOF TMDs for MDOF structures.

Several researchers have examined the dynamics of MDOF structures coupled to other MDOF structures to obtain simple or closed-form approximations for the dynamic response [17, 7, 14, 43], but relatively few have used these results to design the secondary structures in order to attenuate vibration of the primary structure. Igusa and Kiureghian [14] used perturbation techniques to find approximate expressions for the behavior of primary-secondary structures. Snowdon *et al.* [32] developed the cruciform absorber which consists of two mass-loaded beams connected at right angles to one another and tuned to damp one or two modes of the primary structure. Yamaguchi [44] and Kawazoe *et al.* [19] both examined the use of beam-like absorbers to damp the vibration of primary beam structures.

Verdirame *et al.* [39] considered a MDOF TMD comprising a rigid body sup-

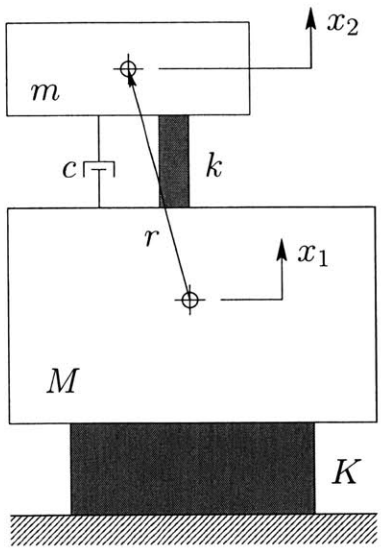

Figure 1-6: Diagram of a vibratory system comprising a mass M to which a tuned-mass damper m is attached.

ported by several springs and dampers relative to a primary structure and tuned this MDOF connection to maximize the minimal damping among as many as six modes (see Figure 1-6). A two-term perturbation expansion was used to obtain an approximate tuning, which was further refined using non-smooth numerical optimization. More recently, Zuo and Nayfeh [50] have shown that a single MDOF TMD can be more effective than multiple SDOF TMDs of the same total mass in maximizing the damping in many modes of a structure. Verdirame *et al.* [39] found that a two-term expansion yields a reasonable approximation for initial sizing and location of a MDOF TMD, but does not produce accurate enough frequency detunings or damping coefficients to build a nearly optimal absorber. The numerical optimization of Zuo and Nayfeh [50] efficiently determines the optimal spring and damping values for the absorber once their locations are given. However, their method is unable to determine their locations, which is an important parameter in determining the optimal design. In this thesis and similarly in Verdirame and Nayfeh [38], an eigenvalue perturbation is used to approximately determine the optimal springs, dampers, and their locations. Once the approximate design including locations is found, the methods of Zuo and Nayfeh [50] can efficiently determine the optimal spring and damper values.

1.3.1 Concept of the Multi-Degree-of-Freedom Tuned-Mass Damper

Assuming that the mounted component, such as the cube shown in Figure 1-1, is relatively more stiff than the flexures, the system has in general six modes of vibration in which the mounted component moves as a rigid body relative to the base. Therefore, we would like to be able to damp up to six modes of vibration. To accomplish this task, one could use six single-degree-of-freedom tuned-mass dampers. However, when six single-degree-of-freedom tuned-mass dampers are used, the inertia of the absorbers is not fully utilized. Instead as demonstrated by Zuo [45], Zuo and Nayfeh [50], and Verdirame *et al* [39], a multi-degree-of-freedom TMD may achieve better performance because the inertia of the single absorber mass is utilized to damp vibrations in many modes. A MDOF TMD consists of a single rigid body connected to a primary structure with damping and stiffness tuned to suppress vibration in as many as six modes of vibration of the primary structure.

Take as a simple example the two-degree-of-freedom system shown in Figure 1-7. If the total amount of mass added by the tuned-mass damper(s) is limited to μM, then two SDOF TMDs will each have a mass ratio of $\mu M/2$. However, a two-degree-of-freedom TMD consisting of a single body can have a mass of μM. The performance of a tuned-mass damper is limited by the magnitude of the mass ratio. Therefore, one expects that the two-DOF TMD is capable of better performance than two SDOF TMDs. Zuo [45] has shown that in many cases the MDOF TMD outperforms multiple SDOF TMDs.

1.4 Overview

The goal of this thesis is to improve on the methods developed by Zuo and Nayfeh. We develop analytical formulas for the approximate locations of the eigenvalues and eigenvectors of the MDOF TMD system. To demonstrate how these formulas may be used for design, we develop approximate analytical formulas for the minimax optimal

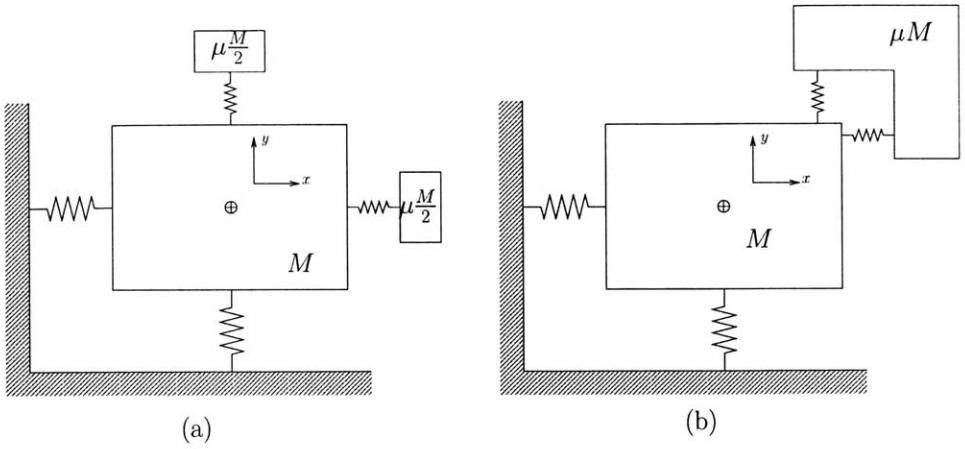

Figure 1-7: Diagram of a two-DOF system with (a) two SDOF TMDs and (b) one two-DOF TMD

design, a somewhat simple case.

1.4.1 Single-Degree-of-Freedom Tuned-Mass Damper

In Chapter 2, the single-degree-of-freedom primary system with a single-degree-of-freedom tuned-mass damper is studied in detail to provide insight for the multi-degree-of-freedom case. The equations of motion are nondimensionalized and then scaled appropriately. A three term eigenvalue perturbation expansion results in approximations with satisfactorily small error. An approximate minimax design is derived and compared to the exact minimax optimal design. The approximate design converges to the exact design. The approximate H_∞ optimal design for a SDOF TMD is discussed in Appendix A. The approximate $H2$ optimal design is discussed in Appendix B.

1.4.2 Multi-Degree-of-Freedom Tuned-Mass Damper

Building on the work of Chapter 1, the MDOF TMD is analyzed using a perturbation expansion. First, the general equations of motion are derived for two connected bodies. Then, the equations are scaled analogously to the SDOF case. Eigenvalue perturbation is used to derive analytical formulas for approximate eigenvalues and

eigenvectors. An approximate minimax design technique is given, and design examples are demonstrated for two-DOF and three-DOF systems.

1.5 Summary of Contributions

1. Developed the concept of the multi-degree-of-freedom tuned-mass damper along with Zuo and Nayfeh [50]

2. Eigenvalue perturbation: derivation of approximations for the eigenvalues and eigenvectors of systems containing multi-degree-of-freedom tuned-mass dampers

3. Approximate minimax design: a simple and direct method for designing MDOF TMDs to maximize the minimum damping coefficient

Chapter 2

Single-Degree-of-Freedom Tuned-Mass Damper

Consider the system in Figure 2-1 consisting of a single-degree-of-freedom primary system and a single-degree-of-freedom tuned-mass damper. The equations of motion for the free vibration problem are

$$\begin{bmatrix} M & 0 \\ 0 & m \end{bmatrix} \begin{pmatrix} \ddot{\tilde{x}}_1 \\ \ddot{\tilde{x}}_2 \end{pmatrix} + \begin{bmatrix} \tilde{c} & -\tilde{c} \\ -\tilde{c} & \tilde{c} \end{bmatrix} \begin{pmatrix} \dot{\tilde{x}}_1 \\ \dot{\tilde{x}}_2 \end{pmatrix} + \begin{bmatrix} K+\tilde{k} & -\tilde{k} \\ -\tilde{k} & \tilde{k} \end{bmatrix} \begin{pmatrix} \tilde{x}_1 \\ \tilde{x}_2 \end{pmatrix} = \begin{pmatrix} 0 \\ 0 \end{pmatrix} \tag{2.1}$$

2.1 Scaling

The scaling of the parameters is determined using distinguished limits [24]. The first step is to nondimensionalize the equations of motion. Then, the mass ratio, eigenvalues, and stiffness scaling are determined from the undamped equations of motion. Finally, the scaling of the damping is determined by looking at the full equations of motion, including damping.

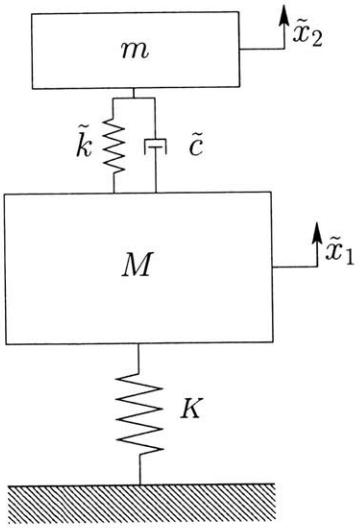

Figure 2-1: Diagram of a vibratory system comprising a mass M to which a single-degree-of-freedom tuned-mass damper m is attached.

2.1.1 Undamped SDOF TMD

Introducing nondimensional time $T = \Omega_n t$ where Ω_n is the natural frequency of the primary system, mass ratio $\epsilon^N = m/M$, and frequency ratio $k = (\omega_a/\Omega_n)^2$, we write the undamped equations of motion in the form

$$\begin{bmatrix} 1 & 0 \\ 0 & 1 \end{bmatrix} \begin{pmatrix} D^2\tilde{x}_1 \\ D^2\tilde{x}_2 \end{pmatrix} + \begin{bmatrix} 1+\epsilon^N k & -\epsilon^N k \\ -k & k \end{bmatrix} \begin{pmatrix} \tilde{x}_1 \\ \tilde{x}_2 \end{pmatrix} = \begin{pmatrix} 0 \\ 0 \end{pmatrix} \tag{2.2}$$

where D^2 is the operator denoting the second derivative with respect to nondimensional time T. The characteristic equation (whose solutions are the eigenvalues) is

$$\omega^4 - \omega^2(1+\epsilon^N k + k) + k = 0 \tag{2.3}$$

Tuning rules [8] suggest that the natural frequency of the absorber must be close to the natural frequency of the primary system. Therefore, we write the natural frequency ratio k as

$$k = 1 + k_1 \epsilon^p \tag{2.4}$$

where k_1 is O(1) and represents the detuning. Defining $\lambda = \omega^2$, the characteristic polynomial becomes

$$\lambda^2 - \lambda(2 + \epsilon^N + k_1\epsilon^p(1 + \epsilon^N)) + 1 + k_1\epsilon^p = 0$$

We are concerned with the relative scaling so we set $p = 1$, without loss of generality. The characteristic equation becomes

$$(\lambda - 1)^2 = \lambda(\epsilon^N + k_1\epsilon^{N+1} + k_1\epsilon) - k_1\epsilon \tag{2.5}$$

We assume a solution of the form

$$\lambda = 1 + \epsilon^v\lambda_1 + \epsilon^{2v}\lambda_2 + \ldots \tag{2.6}$$

We substitute (2.6) into (2.5). To retain the most dominant terms, we set $N = 2$:

$$\epsilon^{2v}\lambda_1^2 = \epsilon^2 + k_1\epsilon^{v+1}\lambda_1 \tag{2.7}$$

Therefore, we obtain the $v = 1$, and the tuning is written as

$$k = 1 + \epsilon k_1 + \epsilon^2 k_2 + \ldots \tag{2.8}$$

2.1.2 Damped SDOF TMD

Tuning rules [8] require that the damping of the absorber be light, or equivalently, that the absorber should be underdamped. Therefore, we write $\tilde{c} = \epsilon^q cm\Omega_n$ where $c = O(1)$. Nondimensionalizing the governing equation but taking advantage of the scaling of the mass ratio and the scaling of the detunings from the undamped case, the characteristic equation becomes

$$(\omega^2 - 1)^2 = j\epsilon^q c\omega^3 + \omega^2(k_1\epsilon + \epsilon^2 + k_1\epsilon^3 - c^2\epsilon^{2+2q}) + j\omega c\epsilon^q(\epsilon^2 + k_1\epsilon^3 - 1) - k_1\epsilon \tag{2.9}$$

We assume a solution of the form

$$\omega = 1 + \epsilon^v \omega_1 + \epsilon^{2v} \lambda_2 + \dots \tag{2.10}$$

There is also a pair of roots near $\omega = -1$, but we may ignore them because they are the complex conjugates of the pair near $\omega = 1$. Extracting the dominant terms, we obtain

$$4\epsilon^{2v}\omega_1^2 = 2jc\omega_1\epsilon^{q+v} + 2k_1\lambda_1\epsilon^{v+1} + \epsilon^2 \tag{2.11}$$

Therefore, we obtain the scaling to be $q = 1$ and $v = 1$. Thus, the damping is written as

$$c = \epsilon c_0 + \epsilon^2 c_1 + \dots \tag{2.12}$$

Using either row of the matrix form of the equations of motion, the scaling of the eigenvectors is shown to be

$$\begin{pmatrix} \tilde{x}_1 \\ \tilde{x}_2 \end{pmatrix} = \begin{pmatrix} \epsilon x_{10} \\ x_{20} \end{pmatrix} \tag{2.13}$$

2.1.3 Scaling of Higher Order Terms

Further analysis using either distinguished limits or the perturbation expansion shows that the second correction to the eigenvalue is at $O(\epsilon^{3/2})$. As well, the higher corrections scale with $\epsilon^{1/2}$ powers. The eigenvalue expansion is written in the form

$$\omega = 1 + \epsilon\omega_2 + \epsilon^{3/2}\omega_3 + \epsilon^2\omega_4 + \dots \tag{2.14}$$

If one performs a Taylor expansion of the tuning, one naively expects only terms in integer powers of ϵ. The reason for the half-power terms is that when the eigenvalues come close together, their sensitivities to parameter changes becomes large, and the half-power terms are necessary to capture this rapidly changing behavior. When the absorber is sufficiently detuned, the half-power terms go to zero.

Corresponding to the half-power scaling of the eigenvalues, the scaling of the higher order eigenvector corrections scale with powers of $\epsilon^{1/2}$. Thus, the expansion of

the eigenvectors may be written as

$$\begin{pmatrix} \tilde{x}_1 \\ \tilde{x}_2 \end{pmatrix} = \begin{pmatrix} \epsilon x_{10} + \epsilon^{3/2} x_{11} + \dots \\ x_{20} + \epsilon^{1/2} x_{21} + \dots \end{pmatrix} \tag{2.15}$$

This scaling agrees with expectations that the primary mass has small amplitude vibrations compared to the absorber. As in the eigenvalue expansion when the absorber is sufficiently detuned, the half-power corrections of the eigenvectors become zero.

2.2 Perturbation Expansion

We write the equations of motion in nondimensional form as

$$\begin{bmatrix} 1 & 0 \\ 0 & 1 \end{bmatrix} \begin{pmatrix} D^2 x_1 \\ D^2 x_2 \end{pmatrix} + \begin{bmatrix} \epsilon^3 c & -\epsilon^2 c \\ -\epsilon^2 c & \epsilon c \end{bmatrix} \begin{pmatrix} D x_1 \\ D x_2 \end{pmatrix} + \begin{bmatrix} 1 + \epsilon^2 k_1 & -\epsilon k \\ -\epsilon k & k \end{bmatrix} \begin{pmatrix} x_1 \\ x_2 \end{pmatrix} = \begin{pmatrix} 0 \\ 0 \end{pmatrix} \tag{2.16}$$

where $k = 1 + \epsilon k_1 + \epsilon^2 k_2 + \dots$, $c = c_0 + \epsilon c_1 + \epsilon^2 c_2 + \dots$ and the displacements have been scaled to reflect the eigenvector scaling such that $\tilde{x}_1 = \epsilon x_1$ and $\tilde{x_2} = x_2$.

To solve the eigenvalue problem, we assume a solution of the form

$$\begin{pmatrix} x_1 \\ x_2 \end{pmatrix} = \begin{pmatrix} x_{10} + \epsilon^{1/2} x_{11} + \epsilon x_{12} + \dots \\ x_{20} + \epsilon^{1/2} x_{21} + \epsilon x_{22} + \dots \end{pmatrix} e^{j\omega T} \tag{2.17}$$

where ω is given by

$$\omega = \omega_0 + \epsilon \omega_2 + \epsilon^{3/2} \omega_3 + \dots \tag{2.18}$$

Next, we perform the perform the perturbation expansion by separating terms of equal order in ϵ.

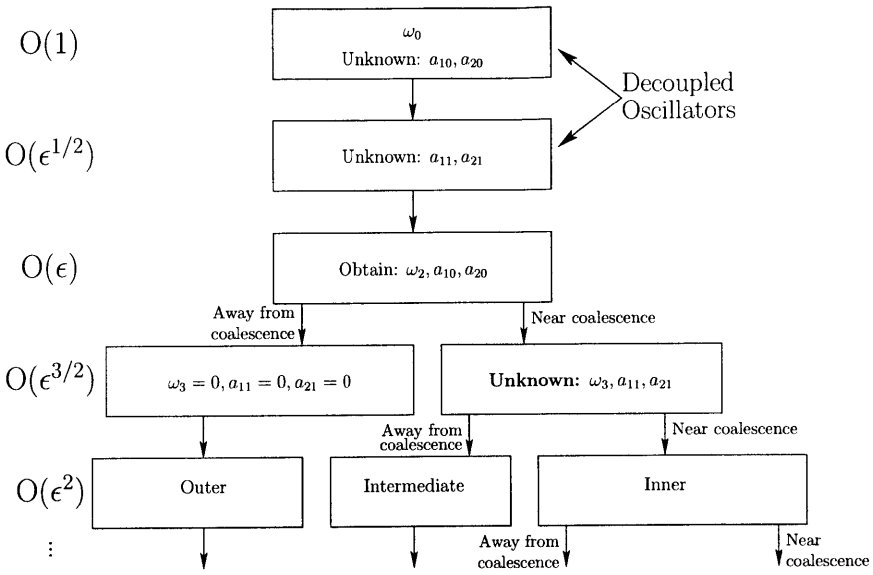

Figure 2-2: Diagram indicating the various steps in the perturbation expansion.

Expansion to O(1)

At this order, we obtain

$$\begin{bmatrix} 1-\omega_0^2 & 0 \\ 0 & 1-\omega_0^2 \end{bmatrix} \begin{pmatrix} x_{10} \\ x_{20} \end{pmatrix} = \begin{pmatrix} 0 \\ 0 \end{pmatrix} \tag{2.19}$$

Therefore, we obtain $\omega_0 = 1$ and the eigenvector

$$\begin{pmatrix} x_{10} \\ x_{20} \end{pmatrix} = \begin{pmatrix} a_{10} \\ a_{20} \end{pmatrix} \tag{2.20}$$

where a_{10} and a_{20} are unknown scalars.

Expansion to $O(\epsilon^{1/2})$

At this order, the equations are of a form similar to those at O(1):

$$\begin{bmatrix} 1-\omega_0^2 & 0 \\ 0 & 1-\omega_0^2 \end{bmatrix} \begin{pmatrix} x_{11} \\ x_{21} \end{pmatrix} = \begin{pmatrix} 0 \\ 0 \end{pmatrix} \tag{2.21}$$

We obtain corrections to the eigenvectors in the form

$$\begin{pmatrix} x_{11} \\ x_{21} \end{pmatrix} = \begin{pmatrix} a_{11} \\ a_{21} \end{pmatrix} \tag{2.22}$$

where a_{11} and a_{21} are unknown scalars. These terms will only be non-zero when the eigenvalues are close to each other.

The homogeneous solution of (2.21) is $(a_{10} \;\; a_{20})^T$. An arbitrary multiple of the homogeneous solution may always be added to the particular solution. For simplicity, we set this arbitrary constant to zero so that all multiples of the homogeneous solution are contained in the O(1) solution. The total solution of (2.21) can be written in the form

$$\begin{pmatrix} x_{11} \\ x_{21} \end{pmatrix} = \alpha_1 \begin{pmatrix} a_{10} \\ a_{20} \end{pmatrix} + \begin{pmatrix} a_{11} \\ a_{21} \end{pmatrix} \tag{2.23}$$

We set $\alpha_1 = 0$ without loss of generality. As a result, $(a_{11} \;\; a_{21})^T$ is orthogonal to $(a_{10} \;\; a_{20})^T$. As will be shown later, a_{11} and a_{21} are zero when the eigenvalues are sufficiently separated.

Expansion to O(ϵ)

At this order the equations become coupled and are given by

$$\begin{bmatrix} 1-\omega_0^2 & 0 \\ 0 & 1-\omega_0^2 \end{bmatrix} \begin{pmatrix} x_{12} \\ x_{22} \end{pmatrix} = \begin{bmatrix} 2\omega_0\omega_2 & 1 \\ 1 & 2\omega_0\omega_2 - (k_1 + j\omega_0 c_0) \end{bmatrix} \begin{pmatrix} x_{10} \\ x_{20} \end{pmatrix} \tag{2.24}$$

The coefficient matrix on the left-hand side is singular; therefore, solutions of the inhomogeneous problem exist if and only if the inhomogeneous terms are orthogonal to each solution of the adjoint homogeneous problem. Noting that the homogeneous problem is self-adjoint, we write the solvability condition as

$$\begin{bmatrix} 2\omega_0\omega_2 & 1 \\ 1 & 2\omega_0\omega_2 - (k_1 + j\omega_0 c_0) \end{bmatrix} \begin{pmatrix} x_{10} \\ x_{20} \end{pmatrix} = \begin{pmatrix} 0 \\ 0 \end{pmatrix} \tag{2.25}$$

Non-trivial solutions exist only if the determinant is zero. This requirement results in an equation for the first correction to the natural frequency:

$$\omega_2 = \frac{(j\omega_0 c_0 + k_1) \pm \sqrt{(j\omega_0 c_0 + k_1)^2 + 4}}{4\omega_0} \tag{2.26}$$

Equation (2.25) yields a relation between the scalars a_{10} and a_{20}:

$$\frac{a_{20}}{a_{10}} = -2\omega_0\omega_2 \tag{2.27}$$

Either a_{10} or a_{20} may be set arbitrarily.

In the same manner as at $O(\epsilon^{1/2})$, the total solution of (2.25) can be written in the form

$$\begin{pmatrix} x_{12} \\ x_{22} \end{pmatrix} = \alpha_2 \begin{pmatrix} a_{10} \\ a_{20} \end{pmatrix} + \begin{pmatrix} b_{12} \\ b_{22} \end{pmatrix} \tag{2.28}$$

where α_2 may be set to zero without loss of generality because $(a_{10} \;\; a_{20})^T$ is the homogeneous solution at each order and b_{12} and b_{22} are scalars chosen so that $(b_{12} \;\; b_{22})^T$ is orthogonal to $(a_{10} \;\; a_{20})^T$.

Figure 2-3 shows a plot of the exact and approximate eigenvalues ω as the damping is varied and the tuning is held fixed. (Only the upper half of the plot is shown because the eigenvalues form complex-conjugate pairs.) From the figure, we see that the $O(\epsilon)$ approximation is not accurate enough for use in design, and we therefore proceed to a higher order.

Expansion to $O(\epsilon^{3/2})$

At this order, we obtain

$$\begin{bmatrix} 1-\omega_0^2 & 0 \\ 0 & 1-\omega_0^2 \end{bmatrix} \begin{pmatrix} x_{13} \\ x_{23} \end{pmatrix} = \begin{bmatrix} 2\omega_0\omega_2 & 1 \\ 1 & 2\omega_0\omega_2 - (k_1 + j\omega_0 c_0) \end{bmatrix} \begin{pmatrix} x_{11} \\ x_{21} \end{pmatrix} + \begin{bmatrix} 2\omega_0\omega_3 & 0 \\ 0 & 2\omega_0\omega_3 \end{bmatrix} \begin{pmatrix} x_{10} \\ x_{20} \end{pmatrix} \tag{2.29}$$

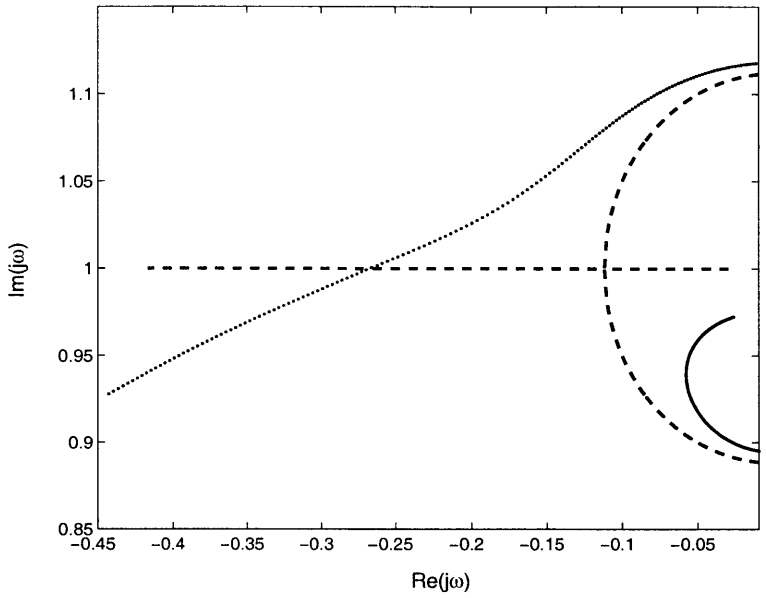

Figure 2-3: Comparison of the actual eigenvalues (dots) and O(ϵ) approximations to the eigenvalues (dashed) for a perfectly tuned ($k_1 = 0$) SDOF TMD with a mass ratio of 5% ($\epsilon = 0.22$) as the damping (c_0) is varied.

Imposing the solvability conditions, we obtain

$$\begin{bmatrix} 2\omega_0\omega_2 & 1 \\ 1 & 2\omega_0\omega_2 - (k_1 + j\omega_0 c_0) \end{bmatrix} \begin{pmatrix} a_{11} \\ a_{21} \end{pmatrix} = -2\omega_0\omega_3 \begin{bmatrix} 1 & 0 \\ 0 & 1 \end{bmatrix} \begin{pmatrix} a_{10} \\ a_{20} \end{pmatrix} \tag{2.30}$$

where a_{11} and a_{21} are still unknown. The coefficient matrix of the LHS is singular so we must impose that the RHS be orthogonal to the solution of the adjoint homogeneous problem $(a_{10} \;\; a_{20})'$ where the prime indicates conjugate transpose. Imposing this solvability condition, we obtain

$$2\omega_0\omega_3(a_{10}^2 + a_{20}^2) = 0 \tag{2.31}$$

This equation leads to the different solution regions shown in Figure 2-2. Usually, (2.31) requires that $\omega_3 = 0$. However, if the eigenvalues come close together (i.e., if the two values of ω_2 obtained from (2.26) are identical), then $a_{10}^2 + a_{20}^2 = 0$ and ω_3 remains unknown until the next order.

The corresponding eigenvector correction $(a_{11} \;\; a_{21})^T$ can only be found once ω_3 is known. To solve for the eigenvector corrections a_{11} and a_{21}, we must also impose the requirement given earlier that $(a_{11} \;\; a_{21})^T$ be orthogonal to $(a_{10} \;\; a_{20})^T$. Therefore, the equation for a_{11} and a_{21} is

$$\begin{bmatrix} 2\omega_0\omega_2 & 1 \\ \overline{a}_{10} & \overline{a}_{20} \end{bmatrix} \begin{pmatrix} b_{11} \\ b_{21} \end{pmatrix} = \begin{pmatrix} -2\omega_0\omega_3 a_{10} \\ 0 \end{pmatrix} \tag{2.32}$$

where the bar indicates the complex conjugate. Thus, if $\omega_3 = 0$, then a_{11} and a_{21} are zero.

If the eigenvalues of the coupled system come close together, the perturbation expansion becomes singular. This singularity leads to different solution regions (see Figure 2-2) depending on the closeness of the eigenvalues. First, we perform an "outer expansion" for the case where the TMD is sufficiently detuned that the expansion never becomes singular.

Outer Expansion to $O(\epsilon^2)$

In this case, the TMD is detuned and hence $\omega_3 = 0$, and we proceed to solve for ω_4 at this order. The governing equations at $O(\epsilon^2)$ are

$$\begin{aligned} \begin{bmatrix} 1-\omega_0^2 & 0 \\ 0 & 1-\omega_0^2 \end{bmatrix} \begin{pmatrix} x_{14} \\ x_{24} \end{pmatrix} = & \begin{bmatrix} 2\omega_0\omega_2 & 1 \\ 1 & 2\omega_0\omega_2 - (k_1 + j\omega_0 c_0) \end{bmatrix} \begin{pmatrix} x_{12} \\ x_{22} \end{pmatrix} \\ & + 2\omega_0\omega_3 \begin{bmatrix} 1 & 0 \\ 0 & 1 \end{bmatrix} \begin{pmatrix} x_{11} \\ x_{21} \end{pmatrix} \\ & + \begin{bmatrix} 2\omega_0\omega_4 + \omega_2^2 - 1 & k_1 + j\omega_0 c_0 \\ k_1 + j\omega_0 c_0 & 2\omega_0\omega_4 + \omega_2^2 - (k_2 + j\omega_2 c_0 + j\omega_0 c_1) \end{bmatrix} \begin{pmatrix} x_{10} \\ x_{20} \end{pmatrix} \end{aligned} \tag{2.33}$$

Making use of $\omega_3 = 0$ and imposing solvability conditions in the same manner as at $O(\epsilon^{3/2})$, we obtain an expression for ω_4:

$$\omega_4 = \frac{1 + 4\omega_0\omega_2(k_1 + j\omega_0 c_0) + 4\omega_0^2\omega_2^2(k_2 + j\omega_0 c_1 + j\omega_2 c_0) - \omega_2^2(1 + 4\omega_0^2\omega_2^2)}{2\omega_0(a_{10}^2 + a_{20}^2)} \tag{2.34}$$

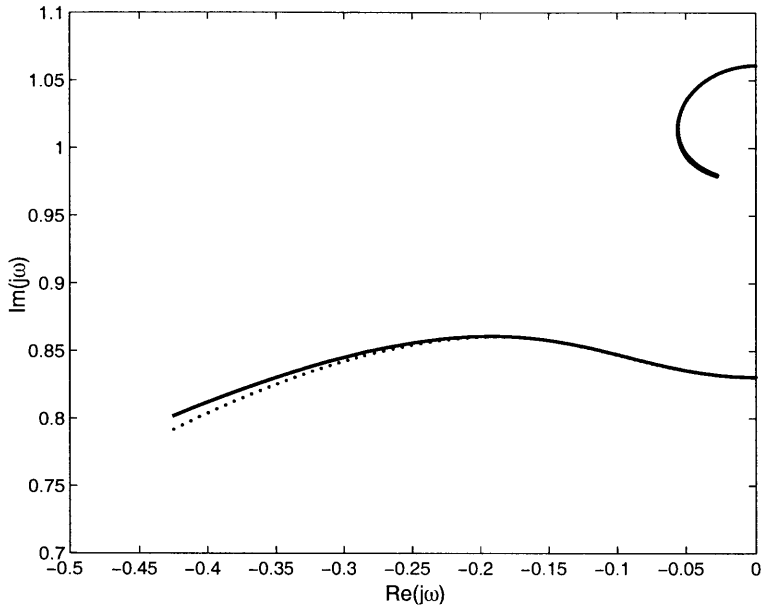

Figure 2-4: Outer expansion: Comparison of actual eigenvalues (dots) and $O(\epsilon^2)$ approximations to the eigenvalues (solid) for a SDOF TMD with a mass ratio of 5% with $k1 = -1$, $k_2 = 0$, and $c_1 = 0$ as the damping (c_0) is varied.

Figure 2-4 shows a comparison of the exact and approximate eigenvalues (to $O(\epsilon^2)$) as the damping is varied for a SDOF TMD for $\epsilon = 0.22$. Based on this figure, we conclude that the approximation to this order is of sufficient accuracy for practical design. In this case, the stiffness has been sufficiently detuned to keep the expansion regular, or uniform. We observe from (2.34) that the expansion becomes nonuniform when the denominator $a_{10}^2 + a_{20}^2$ becomes small, which occurs as the two eigenvalues come close together.

Intermediate Expansion to $O(\epsilon^2)$

In this case the eigenvalues are relatively close together, the two solutions for ω_2 given by (2.26) are identical and ω_3 cannot be found using (2.31). Instead, the solvability condition for (2.33) results in an expression for ω_3:

$$\omega_3 = \pm\sqrt{\frac{1 + 4\omega_0\omega_2(k_1 + j\omega_0 c_0) + 4\omega_0^2\omega_2^2(k_2 + j\omega_0 c_1 + j\omega_2 c_0)}{8\omega_0^3\omega_2}} \tag{2.35}$$

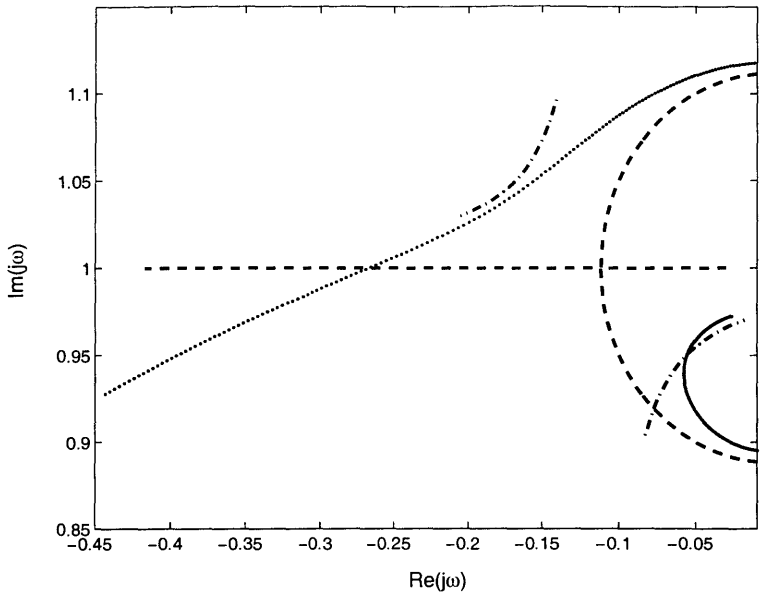

Figure 2-5: Comparison of actual and approximate eigenvalues including ω_3 for a perfectly tuned ($k_1 = 0$) SDOF TMD with a mass ratio of 5% as the damping (c_0) is varied: outer expansion (dashed), intermediate expansion (dashdot), exact (dots).

Figure 2-5 shows the variation of the eigenvalues as the damping is varied where the approximation includes ω_3. The exact and approximate solutions are not in close agreement; then we proceed to solve for ω_4 by imposing solvability conditions (as before) at $O(\epsilon^{5/2})$. Figure 2-6 shows the combination of the outer and intermediate approximations to the eigenvalues of the SDOF TMD as the damping is varied. The intermediate expansion closely approximates the eigenvalue locations in the region of non-uniformity where the outer expansion becomes singular.

Inner Expansion to $O(\epsilon^2)$

If the numerator of the expression for ω_3 given by (2.35) is zero, the eigenvalues are very close together. In this case, we can determine ω_4 from the solvability condition at $O(\epsilon^3)$. The resulting expression is valid only in a small region where the distance between the eigenvalues is smaller than $O(\epsilon^{3/2})$.

A case of particular interest is that in which the numerator and denominator in the expression for ω_4 given by (2.34) are both zero. As c_0 (or k_1) is varied, the numerator

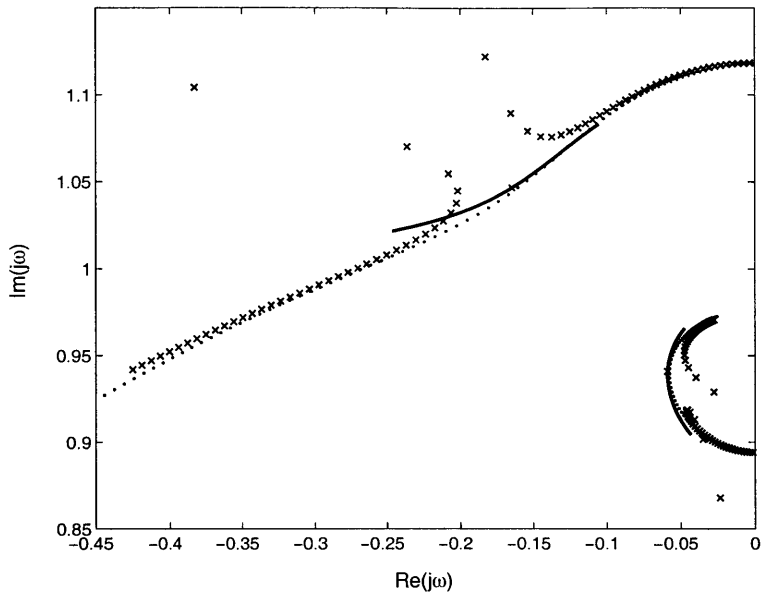

Figure 2-6: Comparison of actual and approximate eigenvalues including ω_4 for a SDOF TMD with a mass ratio of 5%, $k_1 = 0$, $c_1 = 0$, and $k_2 = 0$ as the damping (c_0) is varied: outer expansion ($\times$), intermediate expansion (solid), exact (dots).

and the denominator $2\omega_0(a_{10}^2 + a_{20}^2)$ approach zero at the same rate and the limit remains finite. Thus, the outer expansion remains valid even as the denominator goes to zero. For the SDOF TMD, in the limit as we approach $k_1 = 0$, $k_2 = -2$, $c_0 = 2$, and $c_1 = 0$, the expression for ω_4 given in (2.34) approaches $-5/8$. If we hold $k_1 = 0$, $k_2 = -2$, and $c_1 = 0$ as we vary c_0, we obtain Figure 2-7, where the expansion agrees closely with the exact solution even as the eigenvalues com very close together.

As shown by Figures 2-4, 2-6, and 2-7, the outer, intermediate, and inner expansions approximate well the eigenvalues and eigenvectors of the coupled systems despite a relatively large perturbation parameter ($\epsilon = 0.22$).

2.3 Approximate Minimax Design

The minimax design maximizes the minimum damping coefficient. As a consequence, the poles must coalesce for the SDOF case. To obtain an approximate minimax design, the approximations of the eigenvalues must coalesce at each order.

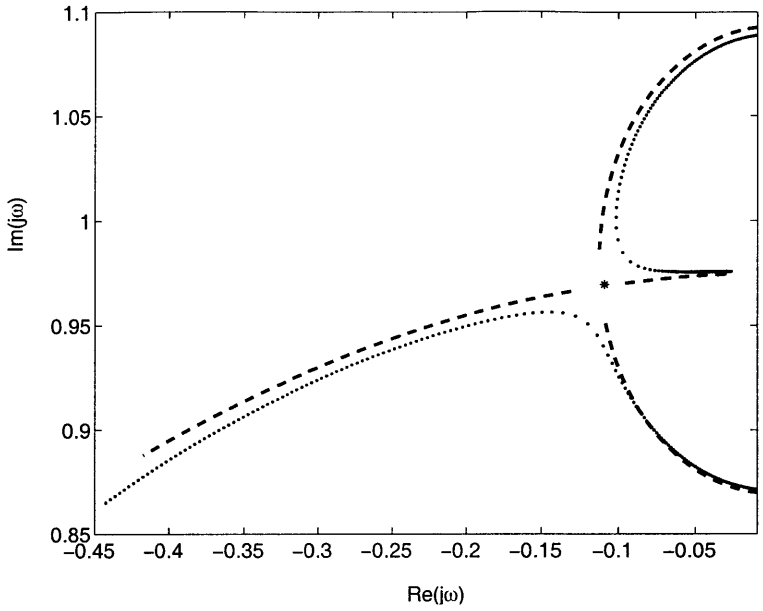

Figure 2-7: Outer expansion when the eigenvalues are close to coalescence ($k_0 = 1$, $k_1 = 0$, $k_2 = -2$, $c_1 = 0$) as the damping (c_0) is varied: $O(\epsilon^2)$ approximate eigenvalue locations (dashed), exact eigenvalue locations (dots).

The first correction to the natural frequency ω_2 is the solution of a quadratic equation given by (2.26). For ω_2 to have only one value, the radicand must be zero. Therefore, we obtain $\omega_2 = j/2$, $k_1 = 0$, and $c_0 = 2$. Setting $a_{10} = 1$, we require $a_{20} = -j$. The next correction for the design is found from forcing ω_3 to coalesce. Equivalently, we may use the outer expression for ω_{p4} and force the numerator to be zero. (The $O(\epsilon)$ design causes the denominator to be zero.) Thus, we obtain $k_2 = -2$, $c_1 = 0$, and $\omega_4 = -5/8$.

2.3.1 Comparison to the Exact Minimax Design

The exact solution for the tuning, damping, and eigenvalue of the minimax tuned-mass damper is derived by solving for the coefficients of the terms in the characteristic polynomial [10]. For the minimax optimal design, the eigenvalues must be a complex-conjugate pair of repeated roots. Therefore, the characteristic equation has the form

$$(\omega - \omega^*)^2(\omega - \overline{\omega}^*)^2 = 0 \tag{2.36}$$

where ω^* is the location of the repeated eigenvalue of the minimax TMD in the complex plane and the overline indicates the complex conjugate. This equation is a fourth-order polynomial in ω. The characteristic equation derived from (2.1) is also a fourth-order polynomial in ω. Equating coefficients, we obtain four equations for four unknown quantities: tuning, damping, and real and imaginary parts of the eigenvalue. Solving these equations for the case of zero damping in the primary structure, the exact solutions as given by Fujino and Abé [10] are

$$\omega^* = -\frac{\epsilon}{2\sqrt{1+\epsilon^2}} + j\sqrt{\frac{1-\epsilon^2/4}{1+\epsilon^2}} \tag{2.37}$$

$$k^* = \left(\frac{1}{1+\epsilon^2}\right)^2 \tag{2.38}$$

$$c^* = 2\frac{\epsilon}{\sqrt{1+\epsilon^2}} \tag{2.39}$$

Expanding the exact solutions in a Maclaurin series (Taylor series about zero) in ϵ, we obtain

$$\omega^* = j - \frac{1}{2}\epsilon - j\frac{5}{8}\epsilon^2 + \frac{1}{4}\epsilon^3 - \ldots \tag{2.40}$$

$$k^* = 1 - 2\epsilon^2 + \epsilon^4 - \ldots \tag{2.41}$$

$$c^* = 2\left(1 - \frac{3}{2}\epsilon^2 + \frac{15}{8}\epsilon^4 - \ldots\right) \tag{2.42}$$

Comparing coefficients of the expansion to the approximate design, we find that the perturbation design gives the same results as the expansion of the exact solution. We conclude that the perturbation expansion yields a uniform approximation to the exact solution. In the next chapter, we examine the multi-degree-of-freedom tuned-mass damper in the same manner.

Chapter 3

Multi-Degree-of-Freedom Tuned-Mass Damper

In this chapter, we extend the methods of the preceding chapter to a multi-degree-of-freedom (MDOF) tuned-mass damper (TMD).

3.1 Equations of Motion and Scaling

Consider small-amplitude vibration of the body M shown in Figure 3-1 with $N \leq 6$ degrees of freedom relative to an inertially fixed base. With reference to its center of mass, we arrange the non-dimensional displacements and rotations of the rigid body M into a coordinate vector x_1, which for the case of $N = 6$ takes the form $[u_{11}, u_{12}, u_{13}, \theta_{11}, \theta_{12}, \theta_{13}]^T$. Before the addition of the TMD, the governing equation can be written as

$$M\ddot{x}_1 + Kx_1 = 0$$

where M and K are, respectively, the non-dimensional mass and stiffness matrices associated with free vibration of the body described by the coordinate vector x_1.

The tuned-mass damper m has N degrees of freedom relative to the main mass. If the body M is restrained from motion, the equations of motion for the absorber

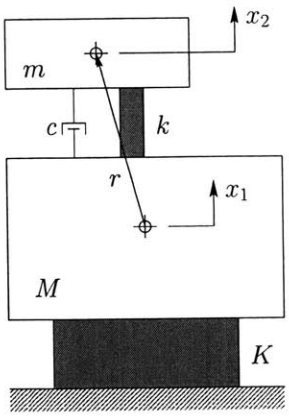

Figure 3-1: Diagram of a vibratory system comprising a mass M to which a tuned-mass damper m is attached.

mass can be written as

$$m\ddot{x}_2 + c\dot{x}_2 + kx_2 = 0$$

where m, c, and k are the non-dimensional mass, damping, and stiffness matrices, respectively, of the absorber when it is decoupled from the primary mass.

If the coordinate systems of the absorber and the primary mass are parallel, the dimensionless equations of motion of the coupled system can be written as

$$\begin{bmatrix} M & 0 \\ 0 & \epsilon^2 m \end{bmatrix} \begin{pmatrix} \ddot{x}_1 \\ \ddot{x}_2 \end{pmatrix} + \epsilon^2 \begin{bmatrix} GcG' & -Gc \\ -cG' & c \end{bmatrix} \begin{pmatrix} \dot{x}_1 \\ \dot{x}_2 \end{pmatrix} + \begin{bmatrix} K + \epsilon^2 GkG' & -\epsilon^2 Gk \\ -\epsilon^2 kG' & \epsilon^2 k \end{bmatrix} \begin{pmatrix} x_1 \\ x_2 \end{pmatrix} = \begin{pmatrix} 0 \\ 0 \end{pmatrix} \quad (3.1)$$

where the small parameter

$$\epsilon = \sqrt{\frac{m}{M}} \quad (3.2)$$

is the square-root of the mass ratio and the matrix G is given by

$$G = \begin{bmatrix} I & 0 \\ R & I \end{bmatrix}$$

where I is the identity matrix and R is a skew-symmetric matrix comprising the

elements of the vector from the center of mass of the primary system to the center of mass of the absorber:

$$R = \begin{bmatrix} 0 & -r_3 & r_2 \\ r_3 & 0 & -r_1 \\ -r_2 & r_1 & 0 \end{bmatrix}$$

A more detailed derivation of the coupled equations of motion is given in Appendix C. Assuming harmonic response of the form $e^{j\omega t}$, we write the governing equation in the form of an eigenvalue problem:

$$\left(-\omega^2 \begin{bmatrix} M & 0 \\ 0 & \epsilon^2 m \end{bmatrix} + \epsilon^2 j\omega \begin{bmatrix} GcG' & -Gc \\ -cG' & c \end{bmatrix} + \begin{bmatrix} K + \epsilon^2 GkG' & -\epsilon^2 Gk \\ -\epsilon^2 kG' & \epsilon^2 k \end{bmatrix} \right) \begin{pmatrix} x_1 \\ x_2 \end{pmatrix} = \begin{pmatrix} 0 \\ 0 \end{pmatrix} \quad (3.3)$$

In the following, we develop approximations of ω, x_1, and x_2 by means of a perturbation expansion in the small parameter ϵ.

3.1.1 Scaling

We begin by scaling the parameters and response of the system in accordance with insights gained from the classical Den Hartog tuning rules [8]: (1) The absorber natural frequencies (when decoupled from the primary system) should be close to those of the primary system without the absorber. (2) The absorber damping should be light. We therefore write the absorber stiffness matrix as

$$k = k_0 + \epsilon k_1 + \epsilon^2 k_2 + \dots \quad (3.4)$$

where k_0 is chosen so that the natural frequencies (eigenvalues) of the absorber and primary system would be equal if $k = k_0$, and the damping matrix of the absorber as

$$c = \epsilon(c_0 + \epsilon c_1 + \epsilon^2 c_2 + \dots) \quad (3.5)$$

We also expect the eigenvalues of the coupled system to be in the neighborhood of the eigenvalues of the primary system. Based on the eigenvalue expansion of the SDOF TMD, we expect that the eigenvalues can be expressed in terms of integer powers of ϵ unless two eigenvalues come close together. In that case, their sensitivities to parameter changes become large, and half-power terms in ϵ are required. Hence, we expand the eigenvalues in the form

$$\omega_p = \omega_{p0} + \epsilon\omega_{p2} + \epsilon^{3/2}\omega_{p3} + \epsilon^2\omega_{p4} + \dots \tag{3.6}$$

where ω_{p0} is the p-th natural frequency of the decoupled systems. The $O(\epsilon^{3/2})$ term in this expansion is zero when the eigenvalues are well separated.

To be effective, a vibration absorber must undergo a large amplitude of vibration relative to that of the primary system. Based again on the SDOF absorber or the distinguished limits in a perturbation expansion, we write the system eigenvectors in the form

$$\begin{pmatrix} x_1 \\ x_2 \end{pmatrix} = \begin{pmatrix} \epsilon x_{10} \\ x_{20} \end{pmatrix} + \begin{pmatrix} \epsilon^{3/2} x_{11} \\ \epsilon^{1/2} x_{21} \end{pmatrix} + \begin{pmatrix} \epsilon^2 x_{12} \\ \epsilon x_{22} \end{pmatrix} + \dots \tag{3.7}$$

where the terms with half powers of ϵ go to zero if the eigenvalues are well separated.

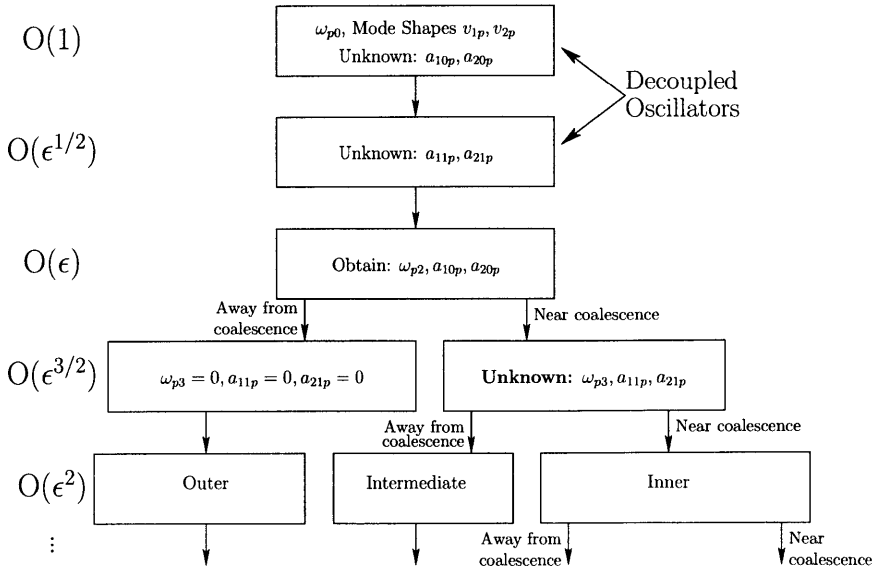

Figure 3-2: Diagram indicating the various steps in the perturbation expansion.

3.2 Perturbation Expansion

The primary system has $N \leq 6$ modes ($p = 1 \ldots N$), and the coupled system has $2N$ modes. The objective of the perturbation expansion is to obtain the approximate eigenvalues ω_p (two for each value of p) and the corresponding eigenvectors.

3.2.1 The Expansion to O(1)

At this order, we obtain

$$(K_c - \omega_{p0}^2 M_c) \begin{pmatrix} x_{10} \\ x_{20} \end{pmatrix} = \begin{pmatrix} 0 \\ 0 \end{pmatrix} \tag{3.8}$$

where ω_{p0} is the p-th natural frequency and

$$K_c = \begin{bmatrix} K & 0 \\ 0 & k_0 \end{bmatrix} \text{ and } M_c = \begin{bmatrix} M & 0 \\ 0 & m \end{bmatrix}$$

These are simply the decoupled equations governing the primary system and absorber. The corresponding eigenvectors (i.e., solutions to this singular, homogeneous system of linear equations) can be written as

$$x_{10} = a_{10p} v_{1p} \tag{3.9}$$

$$x_{20} = a_{20p} v_{2p} \tag{3.10}$$

where a_{10p} and a_{20p} are scalars (unknown to this order) and v_{1p} and v_{2p} are the eigenvectors of the primary and secondary decoupled systems, respectively. The eigenvectors are scaled to be orthonormal. That is $v_{1p}' M v_{1p} = 1$ and $v_{2p}' m v_{2p} = 1$.

3.2.2 The Expansion to $O(\epsilon^{1/2})$

The equations at this order are of the same form as at O(1):

$$(K_c - \omega_{p0}^2 M_c) \begin{pmatrix} x_{11} \\ x_{21} \end{pmatrix} = \begin{pmatrix} 0 \\ 0 \end{pmatrix} \tag{3.11}$$

Hence we obtain corrections to the eigenvectors in the form

$$x_{11} = a_{11p} v_{1p} \tag{3.12}$$

$$x_{21} = a_{21p} v_{2p} \tag{3.13}$$

where again the a_{11p} and a_{21p} are unknown at this order. These terms will be non-zero only when two eigenvalues are close to each other.

3.2.3 The Expansion to $O(\epsilon)$

At this order, the equations become coupled and are given by

$$(K_c - \omega_{p0}^2 M_c) \begin{pmatrix} x_{12} \\ x_{22} \end{pmatrix} = Q \begin{pmatrix} x_{10} \\ x_{20} \end{pmatrix} \tag{3.14}$$

where

$$Q = \begin{bmatrix} 2\omega_{p0}\omega_{p2} M & Gk_0 \\ k_0 G' & 2\omega_{p0}\omega_{p2} m - (k_1 + j\omega_{p0} c_0) \end{bmatrix}$$

The coefficient matrix on the left-hand side of this equation is singular; therefore, solutions of this non-homogeneous problem exist if and only if the non-homogeneous terms in the equation are orthogonal to each solution of the adjoint of the homogeneous problem. Making use of (3.9) and (3.10), and noting that the homogeneous problem is self-adjoint and of the same form as (3.8), we write the solvability condition as

$$S \begin{pmatrix} a_{10p} \\ a_{20p} \end{pmatrix} = \begin{pmatrix} 0 \\ 0 \end{pmatrix} \tag{3.15}$$

where

$$S = \begin{bmatrix} 2\omega_{p0}\omega_{p2} & v'_{1p}Gk_0v_{2p} \\ v'_{2p}k_0G'v_{1p} & 2\omega_{p0}\omega_{p2} - v'_{2p}(k_1 + j\omega_{p0}c_0)v_{2p} \end{bmatrix} \tag{3.16}$$

In order to obtain non-zero a_{10p} and a_{20p}, the determinant of S must be zero. This results in an equation for the first correction to the eigenvalue in the form

$$\omega_{p2} = \frac{v'_{2p}(k_1 + j\omega_{p0}c_0)v_{2p} \pm \sqrt{(v'_{2p}(k_1 + j\omega_{p0}c_0)v_{2p})^2 + 4(v'_{1p}Gk_0v_{2p})^2}}{4\omega_{p0}} \tag{3.17}$$

As expected, for each value of p (or each mode of the primary system), we obtain two eigenvalues in the coupled system. Equation (3.15) further yields a relation between the scalars a_{10p} and a_{20p}

$$\frac{a_{20p}}{a_{10p}} = -\frac{2\omega_{p0}\omega_{p2}}{v'_{1p}Gk_0v_{2p}} \tag{3.18}$$

Either a_{10p} or a_{20p} may be set arbitrarily.

The total solution of (3.14) can be written in the form

$$\begin{pmatrix} x_{12} \\ x_{22} \end{pmatrix} = \begin{pmatrix} a_{12p}v_{1p} + w_{12p} \\ a_{22p}v_{2p} + w_{22p} \end{pmatrix} \tag{3.19}$$

where a_{12p} and a_{22p} are unknown scalars at this order and w_{12p} and w_{22p} are particular solutions. To render the particular solution unique, we choose them to be mass-orthogonal to the homogeneous solution. That is

$$v'_{1p}Mw_{12p} = 0 \tag{3.20}$$

$$v'_{2p}mw_{22p} = 0 \tag{3.21}$$

Figure 3-3 shows a plot of the exact and approximate eigenvalues ω for a SDOF TMD on a SDOF primary system as the damping is varied and k is held fixed. (Only the upper half of the plot is shown because the eigenvalues form complex-conjugate pairs.) From the figure, we see that the $O(\epsilon)$ approximation is not accurate enough for use in design, and we therefore proceed to a higher order.

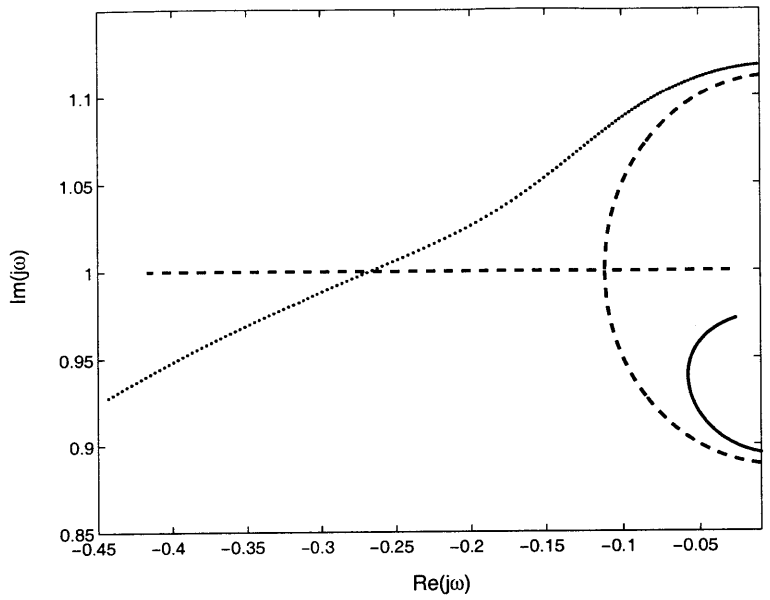

Figure 3-3: Comparison of the actual eigenvalues (dots) and $O(\epsilon)$ approximations to the eigenvalues (dashed) for a perfectly tuned ($k_1 = 0$) SDOF TMD with a mass ratio of 5% ($\epsilon = 0.22$) as the damping (c_0) is varied.

3.2.4 The Expansion to $O(\epsilon^{3/2})$

At this order, we obtain

$$(K_c - \omega_{p0}^2 M_c) \begin{pmatrix} x_{13} \\ x_{23} \end{pmatrix} = 2\omega_{p0}\omega_{p3} M_c \begin{pmatrix} x_{10} \\ x_{20} \end{pmatrix} + Q \begin{pmatrix} x_{11} \\ x_{21} \end{pmatrix} \tag{3.22}$$

The coefficient matrix on the left-hand side is the same as at $O(\epsilon)$. Therefore, a solvability condition must be imposed in order for a solution $(x_{13} \;\; x_{23})^T$ to exist. The solvability condition is

$$S \begin{pmatrix} a_{11p} \\ a_{21p} \end{pmatrix} + 2\omega_{p0}\omega_{p3} \begin{bmatrix} 1 & 0 \\ 0 & 1 \end{bmatrix} \begin{pmatrix} a_{10p} \\ a_{20p} \end{pmatrix} = \begin{pmatrix} 0 \\ 0 \end{pmatrix} \tag{3.23}$$

where S is the matrix given by (3.16). The scalars a_{11p} and a_{21p} are unknown and their coefficient matrix S was required to be singular in order to obtain non-zero a_{10p} and a_{20p} from (3.15). Imposing in turn a solvability condition on (3.23), we obtain

an equation for the second correction ω_{p3} to the eigenvalue in the form

$$2\omega_{p0}\omega_{p3}(a_{10p}^2 + a_{20p}^2) = 0 \tag{3.24}$$

This equation leads to the different solution regions shown in Figure 3-2. Usually, (3.24) requires that $\omega_{p3} = 0$. However, if the eigenvalues come close together (i.e., if the two values of ω_{p2} obtained from (3.17) are identical), then $a_{10p}^2 + a_{20p}^2 = 0$ and ω_{p3} remains unknown at this order.

If the eigenvalues of the coupled system come close together, the perturbation expansion becomes singular. This singularity leads to different solution regions (see Figure 3-2) depending on the closeness of the eigenvalues. First, we perform an "outer expansion" for the case where the TMD is sufficiently detuned that the expansion never becomes singular.

3.2.5 Outer Expansion

In this case, the TMD is detuned and hence $\omega_{p3} = 0$ and we proceed to solve for ω_{p4} at $O(\epsilon^2)$. The equations at this order are

$$(K_c - \omega_{p0}^2 M_c)\begin{pmatrix} x_{14} \\ x_{24} \end{pmatrix} = Q\begin{pmatrix} x_{12} \\ x_{22} \end{pmatrix} + 2\omega_{p0}\omega_{p3}M_c\begin{pmatrix} x_{11} \\ x_{21} \end{pmatrix} + \begin{bmatrix} P_{11} & P_{12} \\ P_{12}' & P_{22} \end{bmatrix}\begin{pmatrix} x_{10} \\ x_{20} \end{pmatrix} \tag{3.25}$$

where

$$P_{11} = (2\omega_{p0}\omega_{p4} + \omega_{p2}^2)M - Gk_0G' \tag{3.26}$$

$$P_{12} = G(k_1 + j\omega_{p0}c_0) \tag{3.27}$$

$$P_{22} = (2\omega_{p0}\omega_{p4} + \omega_{p2}^2)m - (k_2 + j\omega_{p0}c_1 + j\omega_{p2}c_0) \tag{3.28}$$

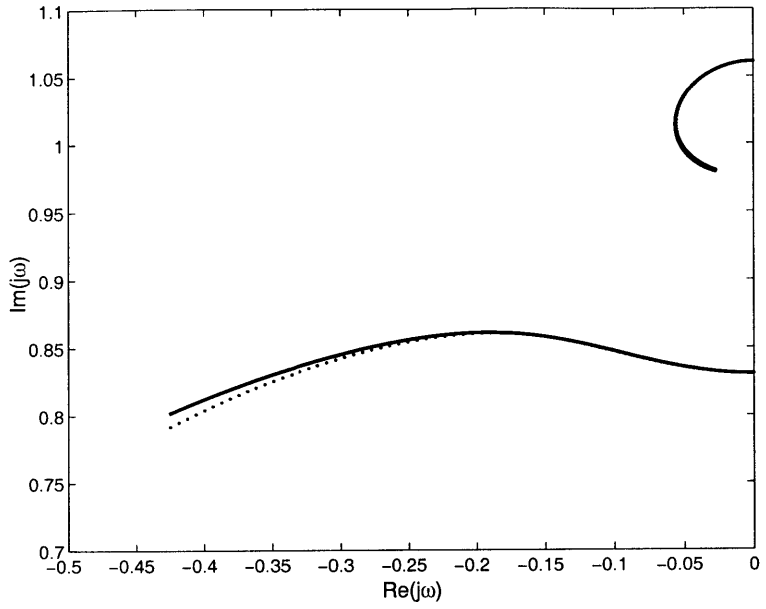

Figure 3-4: Outer expansion: Comparison of actual eigenvalues (dots) and $O(\epsilon^2)$ approximations to the eigenvalues (solid) for a SDOF TMD with a mass ratio of 5% with $k_1 = -1$, $k_2 = 0$, and $c_1 = 0$ as the damping (c_0) is varied.

Following a procedure similar to that at $O(\epsilon^{3/2})$, we obtain

$$\omega_{p4} = \frac{F}{2\omega_{p0}(a_{10p}^2 + a_{20p}^2)} \tag{3.29}$$

where

$$\begin{aligned} F = {} & a_{10p}^2 v_{1p}' G k_0 G' v_{1p} - (a_{10p}^2 + a_{20p}^2)\omega_{p2}^2 \\ & + a_{20p}^2 v_{2p}'(k_2 + j\omega_{p0}c_1 + j\omega_{p2}c0)v_{2p} \\ & + a_{20p} v_{2p}'(k_1 + j\omega_{p0}c_0)w_{22p} - a_{20p} v_{2p}' k_0 G' w_{12p} \\ & - a_{10p} v_{1p}' G k_0 w_{22p} - 2a_{10p}a_{20p} v_{1p}' G(k_1 + j\omega_{p0}c_0)v_{2p} \end{aligned} \tag{3.30}$$

Figure 3-4 shows a comparison of the exact and approximate eigenvalues (to $O(\epsilon^2)$) as the damping is varied for a SDOF TMD with $\epsilon = 0.22$. Based on this figure, we conclude that the approximation to this order is of sufficient accuracy for practical design. In the example shown in Figure 3-4, the stiffness is sufficiently detuned, and

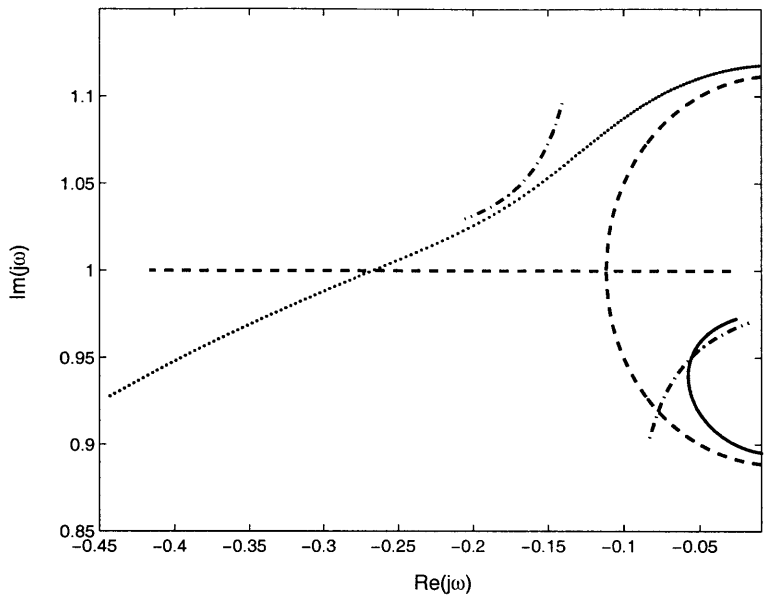

Figure 3-5: Comparison of actual and approximate eigenvalues including ω_{p3} for a perfectly tuned ($k_1 = 0$) SDOF TMD with a mass ratio of 5% as the damping (c_0) is varied: outer expansion (dashed), intermediate expansion (dashdot), exact (dots).

the expansion remains uniform. We observe that the expansion becomes nonuniform when the denominator $a_{10p}^2 + a_{20p}^2$ becomes small, which occurs as two eigenvalues come close together.

3.2.6 Intermediate Expansion

In this case, the eigenvalues are relatively close together, the two solutions for ω_{p2} obtained from (3.17) are identical, and ω_{p3} is non-zero and cannot be found using (3.24). Instead ω_{p3} is obtained by imposing a solvability condition at $O(\epsilon^2)$.

Following the same procedure as before, we obtain an expression for ω_{p3} of the form

$$\omega_{p3} = \pm\sqrt{\frac{A}{B}} \tag{3.31}$$

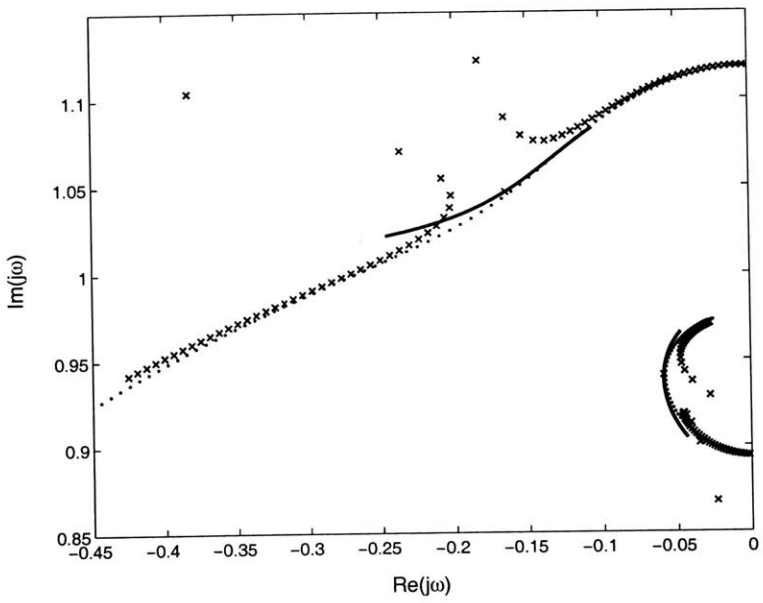

Figure 3-6: Comparison of actual and approximate eigenvalues including ω_{p4} for a SDOF TMD with a mass ratio of 5%, $k_1 = 0$, $c_1 = 0$, and $k_2 = 0$ as the damping (c_0) is varied: outer expansion ($\times$), intermediate expansion (solid), exact (dots).

where

$$\begin{aligned} A = {} & a_{10p}^2 v'_{1p} G k_0 G' v_{1p} - a_{20p} v'_{2p} k_0 G' w_{12p} \\ & + a_{20p}^2 v'_{2p} (k_2 + j\omega_{p0} c_1 + j\omega_{p2} c_0) v_{2p} \\ & + a_{20p} v'_{2p} (k_1 + j\omega_{p0} c_0) w_{22p} - a_{10p} v'_{1p} G k_0 w_{22p} \\ & - 2a_{10p} a_{20p} v'_{1p} G (k_1 + j\omega_{p0} c_0) v_{2p} \end{aligned} \tag{3.32}$$

and

$$B = \frac{8\omega_{p0}^3 \omega_{p2}}{\left(v'_{1p} G k_0 v_{2p}\right)^2} \tag{3.33}$$

Figure 3-5 shows the variation of the eigenvalues for a SDOF TMD on a SDOF primary system, where the approximation includes ω_{p3}. The exact and approximate solutions are not in close agreement; hence we proceed to solve for ω_{p4} by imposing solvability conditions (as before) at $O(\epsilon^{5/2})$. Figure 3-6 shows the combination of the outer and intermediate approximations to the eigenvalues for the SDOF TMD as the damping is varied. The intermediate expansion closely approximates the eigenvalue

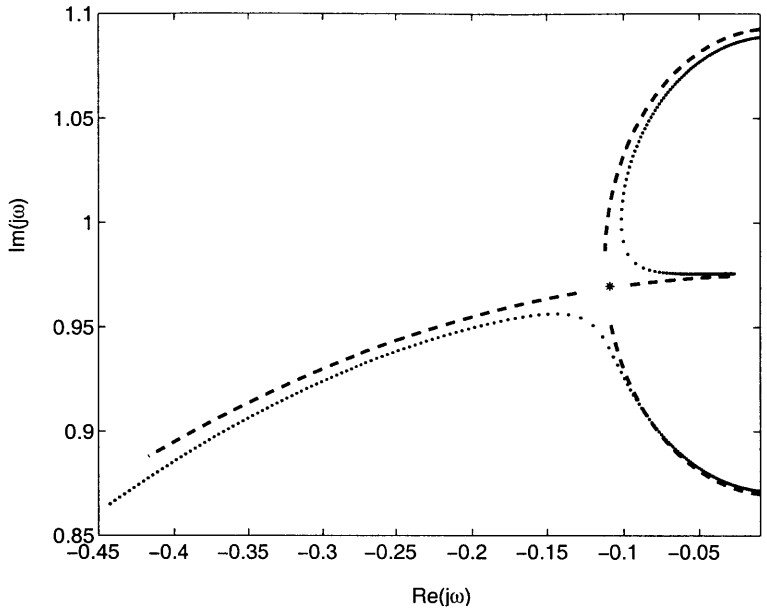

Figure 3-7: Outer expansion for a SDOF TMD when the eigenvalues are close to coalescence ($k_0 = 1$, $k_1 = 0$, $k_2 = -2$, $c_1 = 0$) as the damping (c_0) is varied: $O(\epsilon^2)$ approximate eigenvalue location (dashed), exact eigenvalue locations (dots).

locations in the region of non-uniformity where the outer expansion becomes singular.

3.2.7 Inner Expansion

If the numerator of the expression for ω_{p3} given by (3.31) is zero, the eigenvalues are very close together. In this case, we can determine ω_{p4} from a solvability condition at $O(\epsilon^3)$. The resulting expression is valid only in a small region where the distance between the eigenvalues is smaller than $O(\epsilon^{3/2})$.

A case of particular interest is that in which the numerator and denominator in the expression for ω_{p4} given by (3.29) are both zero. As c_0 (or k_1) is varied, the numerator F and the denominator $2\omega_{p0}(a_{10p}^2 + a_{20p}^2)$ approach zero at the same rate and the limit remains finite. Thus, the outer expansion remains valid even as the denominator goes to zero. For example, let us again consider the SDOF absorber coupled to a SDOF primary system with a mass ratio of 0.05. In the limit as we approach $k_1 = 0$, $k_2 = -2$, $c_0 = 2$, and $c_1 = 0$, the expression for ω_{p4} given in (3.29) approaches $-5/8$. If we hold $k_1 = 0$, $k_2 = -2$, and $c_1 = 0$ as we vary c_0, we obtain

Figure 3-7, where the expansion agrees closely with the exact solution even as the eigenvalues come very close together.

As shown by Figures 3-4, 3-6, and 3-7, the outer, intermediate, and inner expansions approximate well the eigenvalues and eigenvectors of the coupled systems despite a relatively large perturbation parameter ($\epsilon = 0.22$).

3.3 Approximate Minimax Design

Based on the perturbation expansion developed in the foregoing, we develop an approximate method for maximization of the minimal damping of all of the modes in the coupled primary and absorber system.

Consider first maximization of the minimal damping of the two modes of the coupled system that correspond to a given value of p, which is achieved by forcing the eigenvalues to coalesce. We impose this condition in turn for each term of the expansion for ω_p. For the eigenvalues to coalesce to $O(\epsilon)$, we set the radicand in the expression for ω_{p2} given by (3.17) to zero. The imaginary part is guaranteed to be zero if $k_1 = 0$. Setting the real part of the radicand to zero, we obtain

$$(\omega_{p0} v'_{2p} c_0 v_{2p})^2 = 4(v'_{1p} G k_0 v_{2p})^2 \tag{3.34}$$

The approximate damping ratio (associated with each of the two modes) becomes

$$\zeta_p \approx \frac{\epsilon}{2\omega_{p0}^2} v'_{1p} G k_0 v_{2p} \tag{3.35}$$

Thus, to maximize the damping in the p-th mode, we must choose $k_0 v_{2p}$ to have as large a projection as possible onto $G' v_{1p}$. Therefore, we make the two vectors parallel by setting

$$k_0 v_{2p} = \beta_p G' v_{1p} \tag{3.36}$$

where β_p is a scalar chosen such that $v'_{2p} m v_{2p} = 1$. In order for the eigenvalues of the decoupled systems to match, we must have $k_0 v_{2p} = \omega_{p0}^2 m v_{2p}$. Making use of this

expression, we write the optimal eigenvector v_{2p} as

$$v_{2p}^{*} = \frac{m^{-1}G'v_{1p}}{\left(v_{1p}'Gm^{-1}G'v_{1p}\right)^{1/2}} \tag{3.37}$$

which yields the approximate maximum damping damping in the p-th mode

$$\zeta_p^{*} \approx \frac{\epsilon}{2}\left(\frac{v_{1p}'GG'v_{1p}}{\left(v_{1p}'Gm^{-1}G'v_{1p}\right)^{1/2}}\right) \tag{3.38}$$

This expression for the approximate maximum achievable damping is a function only of the original eigenvectors of the primary system, the inertia matrix of the absorber, and the relative location of the center of mass of the absorber.

To be physically realizable, the v_{2p} must form a "mass orthogonal" set. That is, $v_{2p}'mv_{2n} = 0$ if $p \neq n$. In general, the set of eigenvectors chosen according to (3.37) will not satisfy this orthogonality condition. Because our goal is to maximize the minimal damping, we assign the v_{2p} using the following procedure: First, we compute the ζ_p^{*} and rank them from smallest to largest. For the mode with the smallest ζ_p^{*}, we use (3.37) and assign the eigenvector $v_{2p} = v_{2p}^{*}$. Then, in turn, we assign the eigenvector corresponding to the next higher value of ζ_p^{*} by maximizing the projection of v_{2p} onto the optimum vector v_{2p}^{*} subject to the constraint that $v_{2p}mv_{2n} = 0$, where n takes on the values corresponding to each of the previously assigned eigenvectors.

Assembling the desired eigenvectors v_{2p} into a matrix $V_2 = [v_{21}, v_{22}, \ldots]$ and the squares of the natural frequencies ω_{p0}^2 into a diagonal matrix Λ, we construct k_0 according to

$$k_0 = mV_2\Lambda V_2'm \tag{3.39}$$

If the TMD is to be constructed using N discrete springs, the locations and stiffnesses of the springs can be set to achieve the desired matrix k_0. The damping matrix c_0 must satisfy the N scalar equations given by (3.34). If, for example, the TMD is constructed using N discrete dashpots collocated with the N discrete springs (whose locations are already set), then (3.34) forms a set of N linear equations in the damping coefficients of the individual dash-pots.

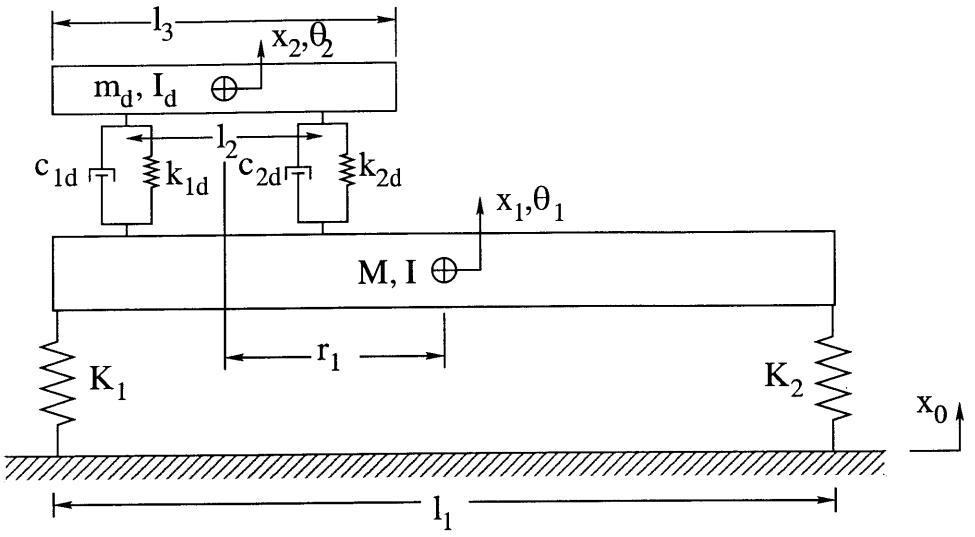

Figure 3-8: Diagram of the two-DOF system with tuned-mass damper: $l_1 = 1$, $M = 1$, $I = 0.0833$, $K_1 = 3$, $K_2 = 5$, $r_1 = 0.333$, $m = 0.05M$, $I_d = 0.0056I$, $l_3 = 0.333$.

This design based on the $O(\epsilon)$ expansion is perfectly tuned (i.e, the decoupled natural frequencies of the absorber and primary system match exactly), but based on Den Hartog's tuning rules [8] we expect that a slight detuning will improve performance. To determine further corrections to the stiffness and damping (k_2 and c_1), we force the two values of ω_{p3} given by (3.31) to coalesce, which can only happen when ω_{p3} is zero. The procedure is similar to that described above for ω_{p2}, and we obtain the condition that $c_1 = 0$ in addition to N equations for k_2, which can be used to solve for a correction to the stiffness of each of the N springs whose locations are already fixed.

3.4 Design Examples

3.4.1 Two-DOF System

To illustrate application of the methods developed in this paper, we consider the design of the two-DOF TMD for the two-DOF primary system shown in Figure 3-8. Taking the mass m and location r_1 as given, our goal is to determine k_{1d}, k_{2d}, c_{1d}, c_{2d}, and the distance l_2 so that the minimal damping is maximized.

Table 3.1: Results of the perturbation-based design: The perturbation method to $O(\epsilon)$ returns a distance between the springs of $l_2 = 0.1088$, which is used as a fixed parameter for the $O(\epsilon^2)$ design.

	Perturbation $O(\epsilon)$		Perturbation $O(\epsilon^2)$	
Mode	ω_n [rad/s]	ζ_n [%]	ω_n [rad/s]	ζ_n [%]
1	2.54	0.419	2.44	3.25
2	2.75	5.80	2.61	2.71
3	4.83	4.36	4.90	16.7
4	5.32	15.5	4.94	4.74

We begin by computing the approximate maximum achievable damping ζ_p^* for each mode using (3.38). For this system, we find that $\zeta_1^* = 2.97\%$ and $\zeta_2^* = 3.92\%$. Because the first mode has the lower ζ_p^*, we set $v_{21} = v_{21}^*$. Then, the other eigenvector is uniquely determined by requiring $v_{21}' m v_{22} = 0$ and $v_{21}' m v_{21} = 1$. Having determined the eigenvalues and eigenvectors of the absorber, we use (3.39) to calculate k_0. After calculating k_0, the individual spring stiffnesses k_{1d} and k_{2d} and location l_2 are calculated.

It is often practical to place the dampers in the same locations as the springs as shown in Figure 3-8. With the locations of the dampers known, the damping coefficients c_{1d} and c_{2d} are calculated from (3.34). The resulting parameter values are shown in the first row of Table 3.3.

To improve upon this initial design, we determine the first detuning k_2 so that ω_{p3} goes to zero, using the value of l_2 determined above. The parameter values obtained in this manner are shown in Table 3.3. The resonant frequencies and damping ratios for the "$O(\epsilon)$" and "$O(\epsilon^2)$" designs are shown in Table 3.1. The design based on the higher-order approximation provides substantially improved performance, increasing the lowest damping coefficient from 0.419% to 2.71%. These improvements are easily seen from the frequency response (Figure 3-9) and the eigenvalue locations (Figures 3-10 and 3-11). Table 3.2 provides for comparison of the performance to results obtained from the numerical methods developed by Zuo and Nayfeh [46].

Table 3.2: Optimization results from Verdirame *et al* [39]. The perturbation method to $O(\epsilon)$ returns a distance between the springs of $l_2 = 0.1088$, which is used as a fixed parameter in the optimization algorithm. In a second numerical optimization, the distance between the springs is taken as an additional design variable to be optimized.

	l_2 Fixed		l_2 Optimized	
Mode	ω_n [rad/s]	ζ_n [%]	ω_n [rad/s]	ζ_n [%]
1	2.56	4.11	2.58	9.54
2	2.56	4.11	2.58	9.54
3	4.86	4.11	4.89	9.54
4	5.19	17.3	4.89	9.54

Table 3.3: Various optimal designs: The perturbation method to $O(\epsilon)$ returns a distance between the springs of $l_2 = 0.1088$, which is used as a fixed parameter in the optimization algorithm. In a second numerical optimization, the distance between the springs is taken as an additional design variable to be optimized.

	k_{1d}	k_{2d}	c_{1d}	c_{2d}	l_2
Perturbation $O(\epsilon)$	0.4816	0.7309	0.0079	0.0769	0.1088
Perturbation $O(\epsilon^2)$	0.3838	0.6722	0.0079	0.0769	(0.1088)
Numerical, l_2 Fixed	0.40771	0.72652	0.02005	0.071675	(0.1088)
Numerical, l_2 Optimized	0.51604	0.15295	0.04096	0.02243	0.203147

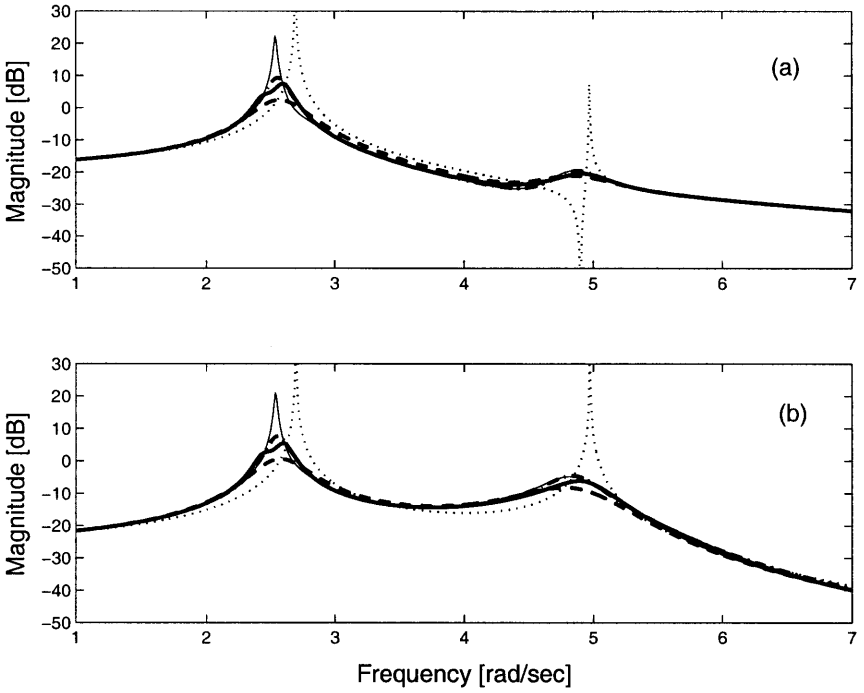

Figure 3-9: Frequency Responses: (a) shows the displacement x_1 of the center of main mass. (b) shows the rotation θ_1 of the center of main mass. Original system without TMD (dots), $O(\epsilon)$ perturbation design (thin solid), $O(\epsilon^2)$ perturbation design (thick solid), numerically optimal design with fixed l_2 (dashdot), and numerically optimal design with optimized l_2 (dashed).

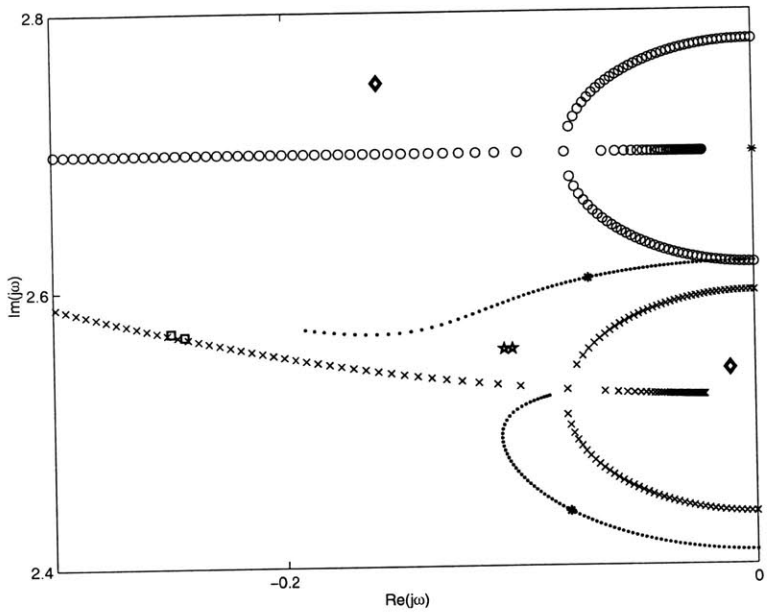

Figure 3-10: Eigenvalue Locations for Mode 1 of the two-DOF example: $O(\epsilon)$ approximation as the damping is varied ($\circ$), $O(\epsilon^2)$ approximate as the damping is varied ($\times$), $O(\epsilon)$ perturbation design ($\diamond$), $O(\epsilon^2)$ perturbation design ($*$), numerically optimal design with fixed l_2 ($\star$), and numerically optimal design with optimized l_2 ($\square$).

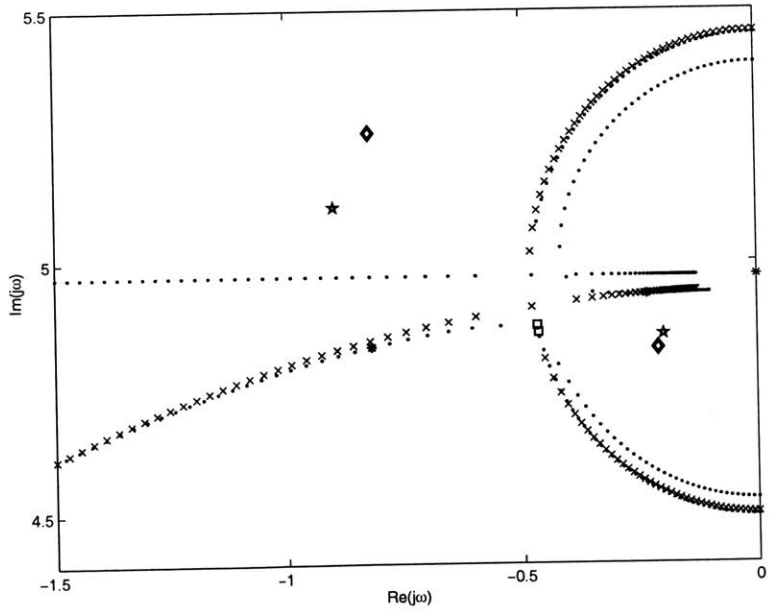

Figure 3-11: Eigenvalue Locations for Mode 2 of the two-DOF example: $O(\epsilon)$ approximation as the damping is varied ($\circ$), $O(\epsilon^2)$ approximate as the damning is varied ($\times$), $O(\epsilon)$ perturbation design ($\diamond$), $O(\epsilon^2)$ perturbation design ($*$), numerically optimal design with fixed l_2 ($\star$), and numerically optimal design with optimized l_2 ($\square$).

Table 3.4: Results of the perturbation-based design: The perturbation method to $O(\epsilon)$ returns the spring and damper locations and the angle ϕ, which is used as a fixed parameter for the $O(\epsilon^2)$ design.

	Perturbation $O(\epsilon)$		Perturbation $O(\epsilon^2)$	
Mode	ω_n [rad/s]	ζ_n [%]	ω_n [rad/s]	ζ_n [%]
1	0.725	1.27	0.719	7.69
2	0.757	4.86	0.733	1.27
3	1.48	3.81	1.50	10.7
4	1.60	11.9	1.51	5.71
5	2.00	5.76	2.02	19.8
6	2.26	20.4	2.06	7.63

3.4.2 Three-DOF System

As a second example of the design method, we consider the design of a three-DOF TMD for the three-DOF primary system shown in Figure 3-12. Taking the mass m, moment of inertia I_a, and location coordinates r_x and r_y as given, our goal is to determine k_{1d}, k_{2d}, k_{3d}, c_{1d}, c_{2d}, c_{3d}, ϕ, ℓ_x, and ℓ_y. The reason we need to determine angle ϕ is because the optimal stiffness matrix may be a full matrix, and the stiffness matrix will not be full if the springs are all parallel to the coordinate axes.

We again calculate the maximum achievable damping coefficient for each mode and find $\zeta_1^* = 3.07\%$, $\zeta_2^* = 3.33\%$, and $\zeta_3^* = 5.36\%$. Thus, we set $v_{21} = v_{21}^*$. Then, v_{22} and v_{23} are determined in turn using the methods outlined before and detailed in Appendix D. Then, k_0 is calculated. Once k_0 is determined, the location and orientation ϕ of the springs and dashpots are known. Then, the values of the damping coefficients c_{1d}, c_{2d}, and c_{3d} are determined. Finally, the stiffnesses are corrected at $O(\epsilon^2)$. The resulting parameter values are given Table 3.5. The performance of the $O(\epsilon)$ and $O(\epsilon^2)$ designs are given in Table 3.4. A typical frequency response, from x-direction ground displacement to x-direction displacement of the main mass) is given in Figure 3-13. The eigenvalue approximations and actual locations as the damping is varied for modes 1, 2, and 3 are shown in Figure 3-14, 3-15, and 3-16, respectively.

From Table 3.4 and Figure 3-13 we notice that the performance of the $O(\epsilon^2)$ design does not improve over the $O(\epsilon)$ design as happened with the two-DOF example. In

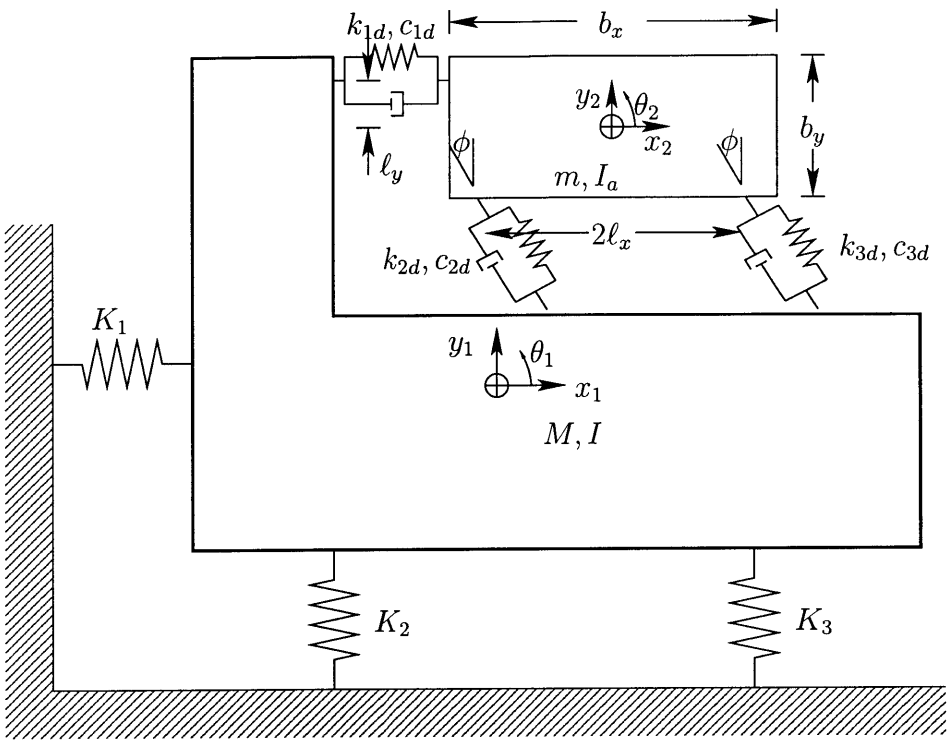

Figure 3-12: Diagram of a three-DOF system with a tuned-mass damper. $M = 1$, $K_1 = 1$, $K_2 = 1$, $K_3 = 2$, $I = 0.0853$, $m = 0.05M$, $I_a = 0.001157$, $r_x = 0.1667$, $r_y = 0.0833$, $b_x = 0.5$. $b_y = 0.1667$

Table 3.5: Three-DOF absorber parameters determined by the perturbation methods.

Parameter	Perturbation O(ϵ)	Perturbation O(ϵ^2)
$k_1 d$	0.1244	0.1142
$k_2 d$	0.0777	0.0830
$k_3 d$	0.1391	0.1018
$c_1 d$	0.0247	0.0247
$c_2 d$	0.0054	0.0054
$c_3 d$	0.0464	0.0464
ℓ_x	0.1158	0.1158
ℓ_y	0.0105	0.0105
ϕ	0.1746	0.1746

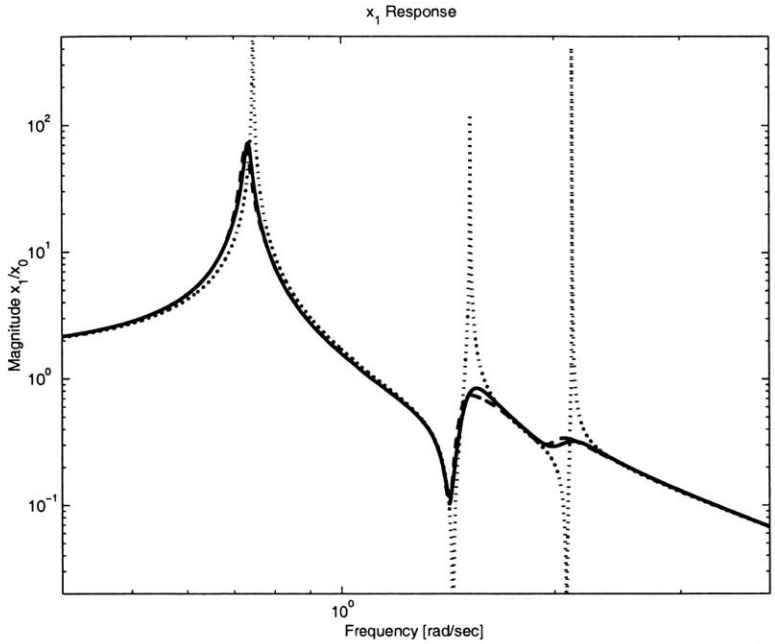

Figure 3-13: Frequency response showing the response of M in the x-direction due to ground displacement in the x-direction. Original system without TMD (dots), $O(\epsilon)$ perturbation design (dashed), $O(\epsilon^2)$ perturbation design (solid).

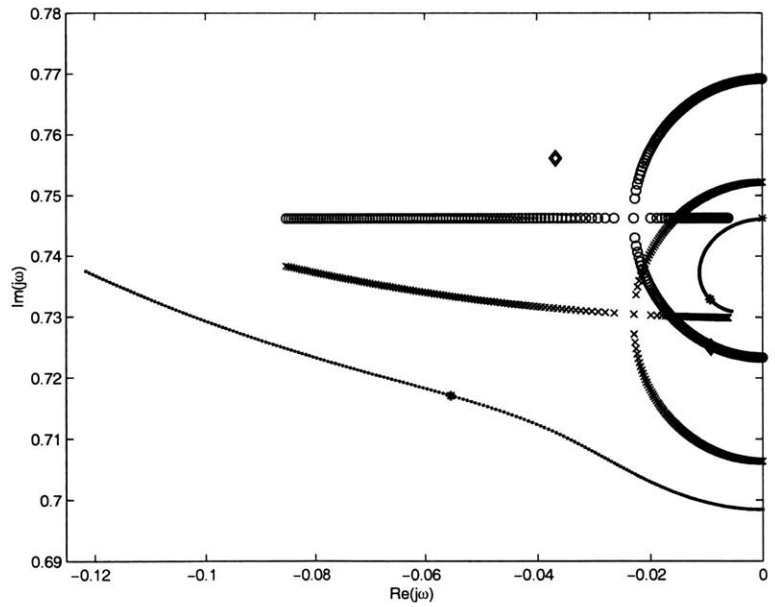

Figure 3-14: Comparison of actual and approximate eigenvalues for mode 1 of the three-DOF example as the damping is varied: $O(\epsilon)$ approximation (circles), $O(\epsilon^2)$ approximation ($\times$), exact (dots), $O(\epsilon)$ design (diamond), $O(\epsilon^2)$ design ($*$).

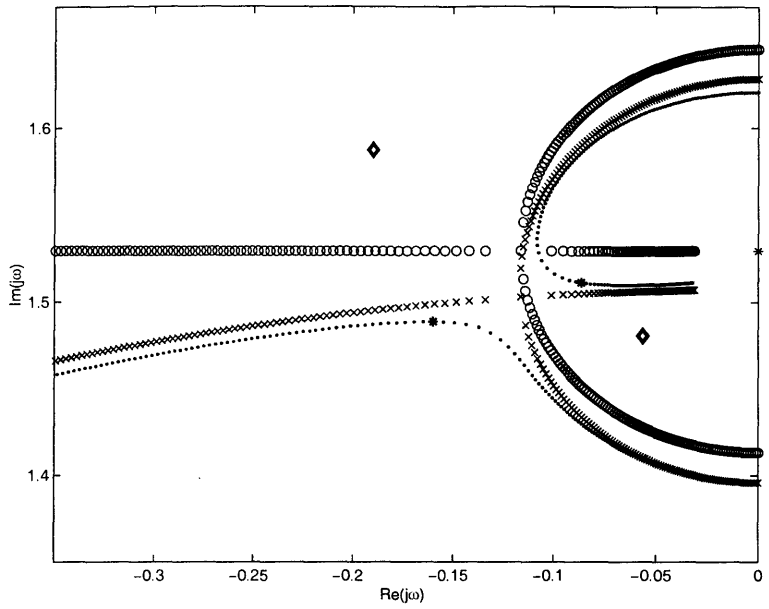

Figure 3-15: Comparison of actual and approximate eigenvalues for mode 2 of the three-DOF example as the damping is varied: $O(\epsilon)$ approximation (circles), $O(\epsilon^2)$ approximation ($\times$), exact (dots), $O(\epsilon)$ design (diamond), $O(\epsilon^2)$ design ($*$).

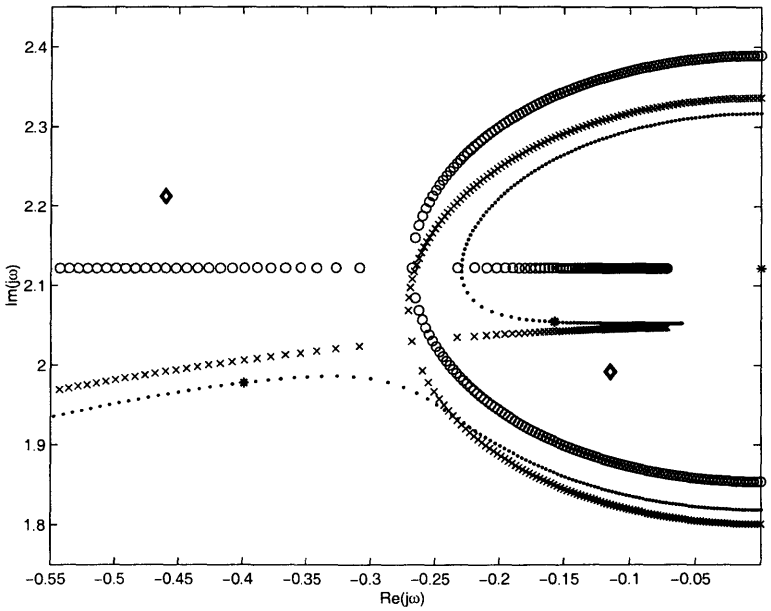

Figure 3-16: Comparison of actual and approximate eigenvalues for mode 3 of the three-DOF example as the damping is varied: $O(\epsilon)$ approximation (circles), $O(\epsilon^2)$ approximation ($\times$), exact (dots), $O(\epsilon)$ design (diamond), $O(\epsilon^2)$ design ($*$).

fact, the smallest damping coefficient has actually decreased. However, the eigenvalue plots seem to indicate that the poles for the $O(\epsilon^2)$ design are marginally closer to coalescing than the $O(\epsilon)$ design poles. There are a couple of reasons for the lack of improvement.

First, the perturbation design method for MDOF systems does not generally converge to the true minimax optimal design as it does in the SDOF case. The error should become small, but convergence is not guaranteed.

The second, and more important, factor is the scaling of the rotational terms. In scaling the equations, we assumed the characteristic lengths, such as the radii of gyration, of the primary system and the absorber were the same. For this example, the two-DOF example, and many examples the characteristic length of the primary system is much greater than the characteristic length of the absorber. Thus, the ratio of the rotational inertias of the absorber to those of the primary system is much smaller than the mass ratio. Then modes in which rotary inertia plays a significant role are not as well damped as desired. In the three-DOF example, the mode shape of the absorber is

$$v_{21} = \begin{pmatrix} 0.3987 \\ 0.0238 \\ 29.2764 \end{pmatrix} \tag{3.40}$$

but the rotational inertia ratio is 0.0136, and the distance between the center of masses is of the same order as the absorber's radius of gyration.

To test this hypothesis, we examine the three-DOF example but increase the rotational inertia of the absorber so that the inertia ratio is 0.492 while the mass ratio is still 0.05. (The distance between the centers of mass is kept the same as before). Table 3.6 compares the damping ratios and natural frequencies for the $O(\epsilon)$ and $O(\epsilon^2)$ designs. The smallest damping ratio improves from 2.95% for the $O(\epsilon)$ design to 4.42% for the $O(\epsilon^2)$ design. Qualitatively, the improvement is seen by examining the eigenvalue plots (see Figures 3-17 through 3-19). The design poles obviously provide better performance in the case $O(\epsilon^2)$ case. Additionally, the error between the approximate and exact solutions as the damping is varied is now smaller

Table 3.6: Results of the perturbation-based design for $I_a/I = 0.492$: The perturbation method to $O(\epsilon)$ returns the spring and damper locations and the angle ϕ, which is used as a fixed parameter for the $O(\epsilon^2)$ design.

	Perturbation $O(\epsilon)$		Perturbation $O(\epsilon^2)$	
Mode	ω_n [rad/s]	ζ_n [%]	ω_n [rad/s]	ζ_n [%]
1	0.719	2.95	0.722	7.33
2	0.760	8.64	0.733	4.42
3	1.48	3.97	1.50	11.9
4	1.60	12.6	1.51	5.54
5	2.01	6.85	2.05	20.8
6	2.26	20.2	2.07	7.98

than in the case where the inertia ratio was much smaller than the mass ratio.

One approach to understanding the scaling is to reexamine the SDOF TMD. In the case of a translational system, the small parameter is the square root of the mass ratio. In the case of a rotational system, the small parameter is the square root of the rotational inertia ratio.

In the MDOF case, both translation and rotation occur so we expect both the mass ratio and the inertia ratio to be important. Furthermore, the distance between the centers of mass matters because the mass contributes an rotary inertia about that point. The modal mass ratio is the important ratio, but we are trying to determine the mode shapes so we are unable to determine this ratio.

We conclude that to obtain a more accurate expansion we must consider two small parameters, the mass ratio as before and either a characteristic length ratio or the inertia ratio.

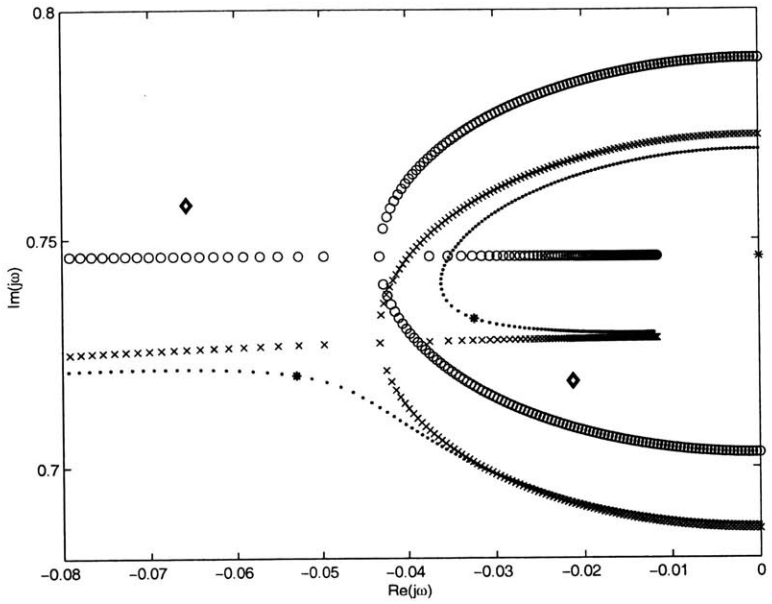

Figure 3-17: Comparison of actual and approximate eigenvalues for mode 1 of the three-DOF example as the damping is varied for $I_d = 0.0492I$: $O(\epsilon)$ approximation (circles), $O(\epsilon^2)$ approximation ($\times$), exact (dots), $O(\epsilon)$ design (diamond), $O(\epsilon^2)$ design ($*$).

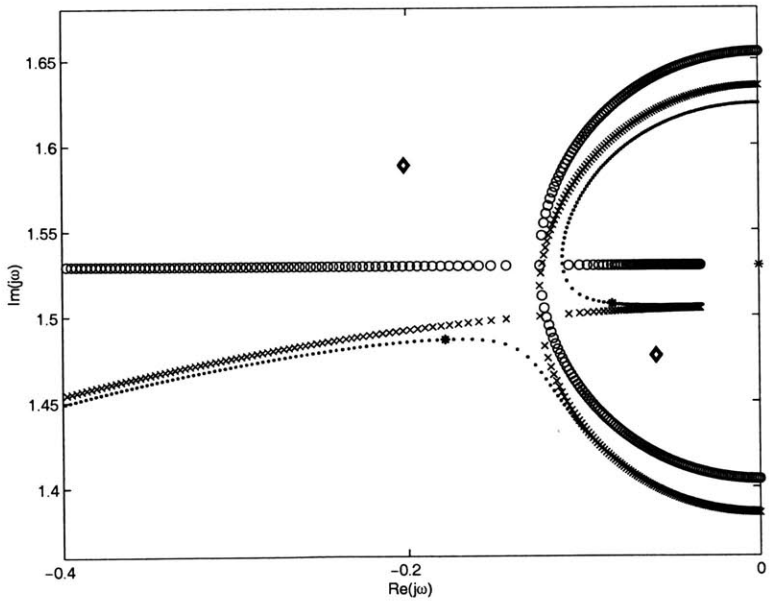

Figure 3-18: Comparison of actual and approximate eigenvalues for mode 2 of the three-DOF example as the damping is varied for $I_d = 0.0492I$: $O(\epsilon)$ approximation (circles), $O(\epsilon^2)$ approximation ($\times$), exact (dots), $O(\epsilon)$ design (diamond), $O(\epsilon^2)$ design ($*$).

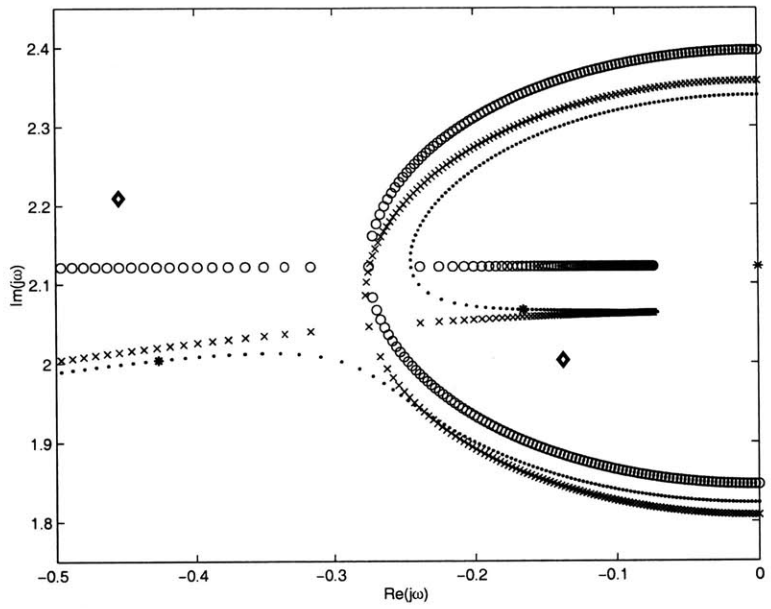

Figure 3-19: Comparison of actual and approximate eigenvalues for mode 3 of the three-DOF example as the damping is varied for $I_d = 0.0492I$: $O(\epsilon)$ approximation (circles), $O(\epsilon^2)$ approximation ($\times$), exact (dots), $O(\epsilon)$ design (diamond), $O(\epsilon^2)$ design ($*$).

Chapter 4

Conclusions and Future Work

4.1 Findings

The goal of this thesis is to provide insight for the design of multi-degree-of-freedom tuned-mass dampers. Zuo and Nayfeh [50] have shown that in many cases the MDOF TMD is better than multiple SDOF TMDs and developed efficient numerical methods for optimizing the values of the springs and dampers. In design, however, analytical formulas for the performance and design of the system are desirable. Furthermore, the methods of Zuo and Nayfeh are unable to determine the optimal locations of the springs and dampers. To address these limitations in this thesis, we have developed approximate formulas for the response, performance, and design (including the spring and damper locations) of multi-degree-of-freedom tuned-mass dampers using eigenvalue perturbation.

First, the SDOF TMD was analyzed to provide insight for the MDOF case. Then, the MDOF TMD was analyzed. Analytical formulas for the approximate eigenvectors and eigenvalues were developed. As an example of how these approximations may be used for design, we developed an approximate minimax design, which maximizes the minimum damping coefficient. The minimax design is an eigenvalue shifting procedure which makes it relatively simple to perform based on the approximate eigenvalues and eigenvectors. Input-output design methods (such as $H2$ and H_∞ optimization [47]) can be developed based on the approximate eigenvalues and eigen-

vectors. In the approximate minimax design, we first determine the approximate performance (damping coefficient) and try to maximize it. This process determines the stiffness and damping matrices for the absorber, which allow us to calculate the stiffness and damping values as well as their locations.

Although we have formulated this perturbation approach for the design of a damper attached to a single body and both the main mass and the absorber have N degrees of freedom, the approach is easily adaptable for multiple dampers or other systems with multiple degrees of freedom.

4.2 Future Work

4.2.1 Two Parameter Expansion

In Chapter 3, we concluded from the three-DOF example that a ratio of characteristic rotational inertias is another important small parameter. Based on that example, we expect that a two-parameter expansion will be useful when the ratio of rotational inertias is much smaller than the mass ratio and/or the distance between the centers of mass is small.

If the primary structure has a characteristic length ρ_1 (an average radius of gyration, say) and the absorber has a characteristic length ρ_2, then we define

$$\eta = \frac{\rho_2}{\rho_1} \tag{4.1}$$

When η is small, then the ratio of radii of inertia $\lambda = \epsilon\eta$ is small. This λ is the second small parameter and is given by

$$\lambda = \sqrt{\frac{m\rho_2^2}{M\rho_1^2}} \tag{4.2}$$

Consider again the system consisting of a MDOF primary system to which a MDOF tuned-mass damper is attached as shown in Figure 3-1. Nondimensionalizing lengths by ρ_1, scaling the displacements and rotations of the primary mass by ϵ and the

rotations of the absorber by η^{-1}, and making use of both ϵ and λ, the nondimensional equations of motion may be written as

$$\begin{bmatrix} M & 0 \\ 0 & m \end{bmatrix} \begin{pmatrix} D^2x_1 \\ D^2x_2 \end{pmatrix} + \begin{bmatrix} (\epsilon G_0 + \lambda\hat{G})c(\epsilon G_0 + \lambda\hat{G})' & -(\epsilon G_0 + \lambda\hat{G})c \\ -c(\epsilon G_0 + \lambda\hat{G})' & c \end{bmatrix} \begin{pmatrix} Dx_1 \\ Dx_2 \end{pmatrix}$$
$$+ \begin{bmatrix} K + (\epsilon G_0 + \lambda\hat{G})k(\epsilon G_0 + \lambda\hat{G})' & -(\epsilon G_0 + \lambda\hat{G})k \\ -k(\epsilon G_0 + \lambda\hat{G})' & k \end{bmatrix} \begin{pmatrix} x_1 \\ x_2 \end{pmatrix} = \begin{pmatrix} f(T) \\ 0 \end{pmatrix} \tag{4.3}$$

where the D is the operator denoting differentiation with respect to nondimensional time T, G_0 is given by

$$G_0 = \begin{bmatrix} I & 0 \\ R & 0 \end{bmatrix} \tag{4.4}$$

where R is an O(1) skew-symmetric cross-product matrix representing the nondimensional vector from the center of mass of the primary structure to the center of mass of the absorber, and $\hat{G}$ is given by

$$\hat{G} = \begin{bmatrix} 0 & 0 \\ 0 & I \end{bmatrix} \tag{4.5}$$

If the distance between the centers of mass is small (of the same order as the characteristic length of the absorber instead of the primary mass), then it may be necessary to change G_0 to have the form

$$G_0 = \begin{bmatrix} I & 0 \\ 0 & 0 \end{bmatrix} \tag{4.6}$$

and $\hat{G}$ to have the form

$$\hat{G} = \begin{bmatrix} 0 & 0 \\ R & I \end{bmatrix} \tag{4.7}$$

The absorber stiffness must be expanded in a similar manner as before, but now two small parameters are used to obtain

$$k = k_0 + \epsilon k_1 + \epsilon^{1/2}\lambda^{1/2}\tilde{k}_1 + \lambda\hat{k}_1 + \epsilon^2 k_2 + \epsilon\lambda\tilde{k}_2 + \lambda^2\hat{k}_2 + \ldots \tag{4.8}$$

where k_0 is a stiffness matrix chosen so that the natural frequencies of the absorber exactly match the absorber of the undamped primary structure. The damping must be light so c is expanded in the form

$$c = \epsilon c_0 + \epsilon^{1/2}\lambda^{1/2}\tilde{c}_0 + \lambda\hat{c}_0 + \epsilon^2 c_1 + \epsilon\lambda\tilde{c}_1 + \lambda^2\hat{c}_1 + \ldots \tag{4.9}$$

The eigenvalues should be expanded as

$$\begin{aligned}\omega_p = \omega_{p0} + \epsilon\omega_{p2} + \epsilon^{1/2}\lambda^{1/2}\tilde{\omega}_{p2} + \lambda\hat{\omega}_{p2} + \epsilon^{3/2}\omega_{p3} + \epsilon\lambda^{1/2}\tilde{\omega}_{p3} \\ + \epsilon^{1/2}\lambda\overline{\omega}_{p3} + \lambda^{3/2}\hat{\omega}_{p3} + \epsilon^2\omega_{p4} + \epsilon\lambda\tilde{\omega}_{p4} + \lambda^2\hat{\omega}_{p4} + \ldots\end{aligned} \tag{4.10}$$

where ω_{p0} is the p-th natural frequency of the undamped primary system. The eigenvectors should be expanded as

$$\begin{aligned}\begin{pmatrix} x_1 \\ x_2 \end{pmatrix} = \begin{pmatrix} x_{10} \\ x_{20} \end{pmatrix} + \epsilon^{1/2}\begin{pmatrix} x_{11} \\ x_{21} \end{pmatrix} + \lambda^{1/2}\begin{pmatrix} \hat{x}_{11} \\ \hat{x}_{21} \end{pmatrix} \\ + \epsilon\begin{pmatrix} x_{12} \\ x_{22} \end{pmatrix} + \epsilon^{1/2}\lambda^{1/2}\begin{pmatrix} \tilde{x}_{12} \\ \tilde{x}_{22} \end{pmatrix} + \lambda\begin{pmatrix} \hat{x}_{12} \\ \hat{x}_{22} \end{pmatrix} + \ldots\end{aligned} \tag{4.11}$$

4.2.2 Tuning Multiple Modes of the Absorber to One Mode of the Primary Structure

Zuo and Nayfeh [48] showed that a MDOF TMD can achieve better performance than a single SDOF TMD or multiple SDOF TMDs for suppression of a single mode of vibration. They reached this conclusion by comparing the performance of a two-DOF absorber, two SDOF absorbers, and a single SDOF absorber for a SDOF primary system. The two-DOF absorber achieves better performance provided that the ratio of the radius of gyration of the absorber to the distance between the springs is properly chosen. Numerical methods are sufficient for a two-DOF system because a simple search can be used to find the optimal ratio. However, the same problem arises that occurred for MDOF absorbers on MDOF systems: the numerical method

cannot determine the optimal location of the springs and dampers. Therefore, we should use perturbation methods to determine approximate optimal locations of the springs and dampers. Furthermore, the perturbation expansion will again result in analytical formulas for the approximate performance and design which are useful in the preliminary design stages. Before performing the perturbation expansion, we expect that the equations of motion must be rescaled because more than three or more poles will be close to coalescence.

4.2.3 Other Work

To improve on the perturbation design, a better estimate of the optimal location for the springs and dampers should be found. In the current procedure, an $O(\epsilon)$ estimate of the achievable damping ratio is used. To improve on the design, we should try to maximize the $O(\epsilon^2)$ estimate of the damping ratio, which may be written as

$$\zeta_p = \epsilon \frac{\omega_{p2} + \epsilon \mathrm{Im}(\omega_{p4})}{\omega_{p0} + \epsilon^2 \mathrm{Re}(\omega_{p4})} \tag{4.12}$$

However, forcing the poles to coalesce causes the imaginary part of ω_{p4} to be zero. Therefore, we must make ω_{p4} as large and negative as possible.

To give a more complete picture of the design of MDOF TMDs for MDOF structures, we must develop approaches for the approximate $H2$ and H_∞ optimal designs. This should be an extension of the work in Appendices A and B, which examine these designs for SDOF structures.

To truly verify the usefulness of MDOF TMDs, we must implement them on physical systems such as shown in Figure 1-1. This work will involve the use of the design methods of this thesis and the methods of Zuo and Nayfeh [50] and the development of adjustable springs and dampers. Zuo [45] has developed some flexures with both adjustable stiffness and damping. Viscoelastic materials are inexpensive and convenient materials to construct tuned-mass dampers. To facilitate the construction of TMDs using viscoelastic materials, the perturbation methods of this thesis must be adapted to reflect the viscoelastic damping model.

Appendix A

Single-Degree-of-Freedom Tuned-Mass Damper Subject to Harmonic Forcing

In this appendix, we examine the behavior of a SDOF TMD subject to light, harmonic forcing using the method of multiple scales. (An alternative method is to project the forcing in to modal coordinates using the approximate mode shapes determined in Chapter 2.) Then, we use the expansion for design. Specifically, we determine the approximate tuning and damping for the H_∞ optimal design, which minimizes the peak value of the frequency response of the primary mass.

A.1 Method of Multiple Scales

The nondimensionalization procedure is the same as for the unforced SDOF TMD examined in Chapter 2 with the exception of the forcing. We assume the forcing is light (scales with ϵ) and that its frequency is near the natural frequency of the

primary system. The nondimensional equations of motion are

$$\begin{bmatrix} 1 & 0 \\ 0 & 1 \end{bmatrix} \begin{pmatrix} D^2 x_1 \\ D^2 x_2 \end{pmatrix} + \begin{bmatrix} \epsilon^3 c & -\epsilon^2 c \\ -\epsilon^2 c & \epsilon c \end{bmatrix} \begin{pmatrix} Dx_1 \\ Dx_2 \end{pmatrix} + \begin{bmatrix} 1+\epsilon^2 k & -\epsilon k \\ -\epsilon k & k \end{bmatrix} \begin{pmatrix} x_1 \\ x_2 \end{pmatrix} = \begin{pmatrix} \epsilon f e^{i\omega T} \\ 0 \end{pmatrix} \quad \text{(A.1)}$$

where D is the operator denoting differtiation with respect to nondimensional time, $T = \Omega_n t$. Because the tuning and damping will not be chosen to make that the eigenvalues are close to coalescence, as will become evident in the expansion to $O(\epsilon)$, the expansions for the eigenvalues and eigenvectors do not need to include the terms with $\epsilon^{1/2}$ powers. Thus, we write the displacements as

$$\begin{pmatrix} x_1 \\ x_2 \end{pmatrix} = \begin{pmatrix} x_{10} \\ x_{20} \end{pmatrix} + \epsilon \begin{pmatrix} x_{11} \\ x_{21} \end{pmatrix} + \epsilon^2 \begin{pmatrix} x_{12} \\ x_{22} \end{pmatrix} + \ldots \quad \text{(A.2)}$$

The frequency of excitation is expanded as

$$\omega = 1 + \epsilon\sigma \quad \text{(A.3)}$$

where σ is O(1). We introduce nondimensional time scales

$$T_0 = T \qquad T_1 = \epsilon T \qquad T_2 = \epsilon^2 T, \ldots \quad \text{(A.4)}$$

The derivative operator D is expanded as

$$D = D_0 + \epsilon D_1 + \epsilon^2 D_2 + \ldots \quad \text{(A.5)}$$

where D_0 is the derivative operator with respect to T_0, D_1 is the derivative operator with respect to T_1, and so on. The stiffness of the absorber is written as

$$k = 1 + \epsilon k_1 + \epsilon^2 k_2 + \ldots \quad \text{(A.6)}$$

The damping of the absorber is written as

$$c = c_0 + \epsilon c_1 + \epsilon^2 c_2 + \dots \tag{A.7}$$

A.1.1 Expansion to O(1)

The equations at this order are

$$\begin{bmatrix} 1 & 0 \\ 0 & 1 \end{bmatrix} \begin{pmatrix} D_0^2 x_{10} \\ D_0^2 x_{20} \end{pmatrix} + \begin{bmatrix} 1 & 0 \\ 0 & 1 \end{bmatrix} \begin{pmatrix} x_{10} \\ x_{20} \end{pmatrix} = \begin{pmatrix} 0 \\ 0 \end{pmatrix} \tag{A.8}$$

The response is

$$x_{10} = A_0 e^{iT_0} + \text{cc} \tag{A.9}$$

$$x_{20} = B_0 e^{iT_0} + \text{cc} \tag{A.10}$$

where cc denotes complex conjugate. We may ignore the complex conjugate because this problem is linear.

A.1.2 Expansion to O(ϵ)

At this order, the equations are

$$\begin{bmatrix} 1 & 0 \\ 0 & 1 \end{bmatrix} \begin{pmatrix} D_0^2 x_{11} \\ D_0^2 x_{21} \end{pmatrix} + \begin{bmatrix} 1 & 0 \\ 0 & 1 \end{bmatrix} \begin{pmatrix} x_{11} \\ x_{21} \end{pmatrix} = \begin{pmatrix} -2iD_1A_0 + B_0 + fe^{i\sigma T_1} \\ A_0 - 2iD_1B_0 - (k_1 + ic_0)B_0 \end{pmatrix} e^{iT_0} \tag{A.11}$$

To suppress secular terms, we require that the RHS be zero. Rearranging terms, we obtain

$$\begin{pmatrix} D_1A_0 \\ D_1B_0 \end{pmatrix} = \begin{bmatrix} 0 & -\frac{i}{2} \\ -\frac{i}{2} & \frac{k_1 i - c_0}{2} \end{bmatrix} \begin{pmatrix} A_0 \\ B_0 \end{pmatrix} + \begin{pmatrix} f_0 e^{i\sigma T_1} \\ 0 \end{pmatrix} \tag{A.12}$$

The solution for A_0 and B_0 may be separated into homogeneous and particular parts. We are concerned with the forced response and thus only care about the

particular solution, which we write as

$$\begin{pmatrix} A_{0p} \\ B_{0p} \end{pmatrix} = \begin{pmatrix} a_{0p} \\ b_{0p} \end{pmatrix} e^{i\sigma T_1} \tag{A.13}$$

Substituting this solution form into (A.12), we obtain

$$\begin{bmatrix} 2\sigma & 1 \\ 1 & 2\sigma - (k_1 + ic_0) \end{bmatrix} \begin{pmatrix} a_{0p} \\ b_{0p} \end{pmatrix} = \begin{pmatrix} -f \\ 0 \end{pmatrix} \tag{A.14}$$

For convenience, we define

$$P = \begin{bmatrix} 2\sigma & 1 \\ 1 & 2\sigma - (k_1 + ic_0) \end{bmatrix} \tag{A.15}$$

Solving for a_{0p} and b_{0p}, we obtain transfer functions

$$\frac{a_{0p}}{f} = \frac{\frac{\sigma}{2} - \frac{k_1 + ic_0}{4}}{-\sigma^2 + \frac{\sigma}{2}(k_1 + ic_0) + \frac{1}{4}} \tag{A.16}$$

$$\frac{b_{0p}}{f} = \frac{-\frac{1}{4}}{-\sigma^2 + \frac{\sigma}{2}(k_1 + ic_0) + \frac{1}{4}} \tag{A.17}$$

The response at this order x_{12} and x_{22} maybe written as

$$x_{11} = A_1 e^{iT_0} + \text{cc} \tag{A.18}$$

$$x_{21} = B_1 e^{iT_0} + \text{cc} \tag{A.19}$$

A.1.3 Expansion to $O(\epsilon^2)$

The equations at this order are

$$\begin{bmatrix} 1 & 0 \\ 0 & 1 \end{bmatrix} \begin{pmatrix} D_0^2 x_{12} \\ D_0^2 x_{22} \end{pmatrix} + \begin{bmatrix} 1 & 0 \\ 0 & 1 \end{bmatrix} \begin{pmatrix} x_{12} \\ x_{22} \end{pmatrix} = \begin{bmatrix} -2D_0D_1 & 1 \\ 1 & -2D_0D_1 - (k_1 + c_0D_0) \end{bmatrix} \begin{pmatrix} x_{11} \\ x_{21} \end{pmatrix} + \begin{bmatrix} -2D_0D_2 - D_1^2 - 1 & k_1 + c_0D_0 \\ k_1 + c_0D_0 & -2D_0D_2 - D_1^2 - (k_2 + c_1D_0 + c_0D_1) \end{bmatrix} \begin{pmatrix} x_{10} \\ x_{20} \end{pmatrix} \quad \text{(A.20)}$$

We substitute for x_{10}, x_{20}, x_{11}, and x_{21} and suppress secular terms by setting the RHS to zero. We obtain

$$\begin{bmatrix} -2iD_2 - D_1^2 - 1 & k_1 + ic_0 \\ k_1 + ic_0 & -2iD_2 - D_1^2 - (k_2 + ic_1 + c_0D_1) \end{bmatrix} \begin{pmatrix} A_0 \\ B_0 \end{pmatrix} + \begin{bmatrix} -2iD_1 & 1 \\ 1 & -2iD_1 - (k_1 + ic_0) \end{bmatrix} \begin{pmatrix} A_1 \\ B_1 \end{pmatrix} = \begin{pmatrix} 0 \\ 0 \end{pmatrix} \quad \text{(A.21)}$$

where A_0 and B_0 are functions of f and T_1 only; therefore, the derivative with respect to T_2 is zero. Because A_0 and B_0 are harmonic functions of the form $e^{i\sigma T_1}$, we assume particular solutions for A_1 and B_1 have the form the form

$$\begin{pmatrix} A_{1p} \\ B_{1p} \end{pmatrix} = \begin{pmatrix} a_{1p} \\ b_{1p} \end{pmatrix} e^{i\sigma T_1} \quad \text{(A.22)}$$

Substituting into (A.21), we obtain

$$P \begin{pmatrix} a_{1p} \\ b_{1p} \end{pmatrix} = -Q \begin{pmatrix} a_{0p} \\ b_{0p} \end{pmatrix} \quad \text{(A.23)}$$

where Q is given by

$$Q = \begin{bmatrix} \sigma^2 - 1 & k_1 + ic_0 \\ k_1 + ic_0 & \sigma^2 - (k_2 + ic_1 + ic_0\sigma) \end{bmatrix} \quad \text{(A.24)}$$

The unknowns a_{0p} and b_{0p} are linear functions of f as given by (A.16) and (A.17). Substituting the transfer function for a_{0p} and b_{0p}, we find

$$\begin{pmatrix} \frac{a_{1p}}{f_0} \\ \frac{b_{1p}}{f_0} \end{pmatrix} = P^{-1}QP^{-1} \begin{pmatrix} 1 \\ 0 \end{pmatrix} \tag{A.25}$$

The transfer functions are

$$\frac{a_{1p}}{f_0} = \frac{4\sigma^4 - 4(k_1 + jc_0)\sigma^3 + \sigma^2((k_1 + jc_0)^2 - 3) - j\sigma c_0 + (k_1 + jc_0)^2 - (k_2 + jc_1)}{(4\sigma^2 - 2\sigma(k_1 + jc_0) - 1)^2} \tag{A.26}$$

$$\frac{b_{1p}}{f_0} = \frac{-\sigma\left(4\sigma^2 - \sigma(5k_1 + 7jc_0) + 2(k_1 + jc_0)^2 - 2(k_2 + jc_1 + 1)\right)}{(4\sigma^2 - 2\sigma(k_1 + jc_0) - 1)^2} \tag{A.27}$$

The resulting response for x_{12} and x_{22} is

$$x_{12} = A_2 e^{iT_0} + \text{cc} \tag{A.28}$$

$$x_{22} = B_2 e^{iT_0} + \text{cc} \tag{A.29}$$

A.1.4 Expansion to $O(\epsilon^3)$

The equations at this order are

$$\begin{aligned} \begin{bmatrix} 1 & 0 \\ 0 & 1 \end{bmatrix} \begin{pmatrix} D_0^2 x_{13} \\ D_0^2 x_{23} \end{pmatrix} + \begin{bmatrix} 1 & 0 \\ 0 & 1 \end{bmatrix} \begin{pmatrix} x_{13} \\ x_{23} \end{pmatrix} &= \begin{bmatrix} \delta_{11} & \delta_{12} \\ \delta_{12} & \delta_{22} \end{bmatrix} \begin{pmatrix} x_{10} \\ x_{20} \end{pmatrix} \\ &+ \begin{bmatrix} -2D_0D_2 - D_1^2 - 1 & k_1 + c_0D_0 \\ k_1 + c_0D_0 & -2D_0D_2 - D_1^2 - (k_2 + c_1D_0 + c_0D_1) \end{bmatrix} \begin{pmatrix} x_{11} \\ x_{21} \end{pmatrix} \\ &+ \begin{bmatrix} -2D_0D_1 & 1 \\ 1 & -2D_0D_1 - (k_1 + c_0D_0) \end{bmatrix} \begin{pmatrix} x_{12} \\ x_{22} \end{pmatrix} \end{aligned} \tag{A.30}$$

where

$$\delta_{11} = -2D_0D_3 - 2D_1D_2 - (k_1 + c_0D_0) \tag{A.31}$$

$$\delta_{12} = k_2 + c_1D_0 + c_0D_1 \tag{A.32}$$

$$\delta_{22} = -2D_0D_3 - 2D_1D_2 - (k_3 + c_1D_1 + c_2D_0 + c_0D_2) \tag{A.33}$$

We suppress secular terms in the same manner by setting the RHS equal to zero. All variables are only a function of T_1 so higher derivatives (D_2, D_3, ...) are zero. We assume a particular solution for A_2, B_2 of the form

$$\begin{pmatrix} A_{2p} \\ B_{2p} \end{pmatrix} = \begin{pmatrix} a_{2p} \\ b_{2p} \end{pmatrix} e^{i\sigma T_1} \tag{A.34}$$

The resulting equation is

$$P \begin{pmatrix} a_{2p} \\ b_{2p} \end{pmatrix} + Q \begin{pmatrix} a_{1p} \\ b_{1p} \end{pmatrix} + R \begin{pmatrix} a_{0p} \\ b_{0p} \end{pmatrix} = \begin{pmatrix} 0 \\ 0 \end{pmatrix} \tag{A.35}$$

where R is given by

$$R = \begin{bmatrix} -(k_1 + ic_0) & k_2 + i\sigma c_0 + ic_1 \\ k_2 + i\sigma c_0 + ic_1 & -(k_3 + i\sigma c_1 + ic_2) \end{bmatrix} \tag{A.36}$$

Making use of (A.14) and (A.25), we obtain

$$\begin{pmatrix} \frac{a_{2p}}{f_0} \\ \frac{b_{2p}}{f_0} \end{pmatrix} = P^{-1} \left(-QP^{-1}Q + R \right) P^{-1} \begin{pmatrix} 1 \\ 0 \end{pmatrix} \tag{A.37}$$

A.2 Approximate H_∞ Optimal Design

To determine the approximate design, we examine the total response at each order and try to minimize the peak height(s) of the transfer function by varying the parameters. Ormondroyd and Den Hartog [26] and Brock [4] used the ideal of "equal peaks" to find a very good approximation of the H_∞ optimal design. The idea is that the optimal design is the one which the two peaks are of equal height and that height is as small as possible. Furthermore, Ormondroyd and Den Hartog were able to simplify the calculations by recognizing that for fixed stiffness tuning, all frequency response curves pass through two points independent of damping. For the optimal design,

these points are the peaks. Ormondroyd and Den Hartog then found the optimal frequency tuning to be

$$\frac{\omega_a}{\Omega_n} = \frac{1}{1+\mu} \tag{A.38}$$

where μ is the mass ratio. Brock contributed a formula for the damping of the absorber by noting the slope of the frequency response curve is zero at the peak. The optimal damping coefficient of the absorber is

$$\hat{\zeta}_a = \sqrt{\frac{3\mu}{8(1+\mu)^3}} \tag{A.39}$$

where $\hat{\zeta}_a = 2m\Omega_n$. This definition of the damping ratio is not exactly correct because the natural frequency should be that of the absorber. Making use of the optimal frequency tuning, the damping coefficient of the absorber may be written as

$$\zeta_a = \sqrt{\frac{3\mu}{8(1+\mu)}} \tag{A.40}$$

where $\zeta = 2m\omega_a$. This design is not the true optimal because the peaks are not of equal height, as noted by Brock. However, the design is a very good approximation when compared to the formula for the exact optimum given by Asami *et al.* [3] through a Taylor series expansion, for example. The optimal tuning is

$$\frac{\omega_a}{\Omega_N} = \frac{2}{1+\epsilon^2}\sqrt{\frac{2\left(16+23\epsilon^2+9\epsilon^4+2(2+\epsilon^2)\sqrt{4+3\epsilon^2}\right)}{3\left(64+80\epsilon^2+27\epsilon^4\right)}} \tag{A.41}$$

and

$$2m\omega_a = \frac{1}{4}\sqrt{\frac{8+9\epsilon^2-4\sqrt{4+3\epsilon^2}}{1+\epsilon^2}} \tag{A.42}$$

The result of the $O(\epsilon)$ expansion is a transfer function for a_{0p} given by (A.16). We first may argue that the transfer function should be symmetric about $\sigma = 0$ to obtain $k_1 = 0$. Then, we follow a procedure analogous to that of Ormondroyd and Den Hartog [26] and Brock [4] to obtain $c_0 = \frac{\sqrt{6}}{2}$. Figure A-1 shows the tranfer function for various values of the damping with $k_1 = 0$. The bold curve is the

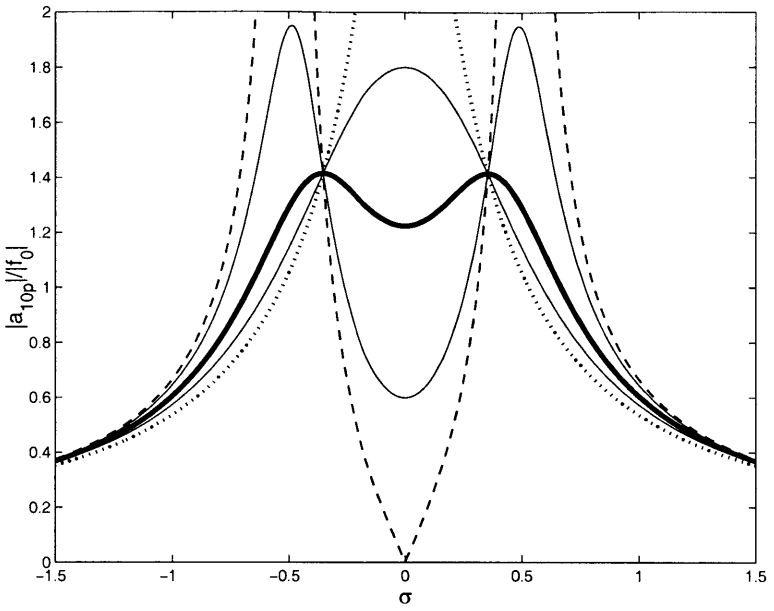

Figure A-1: Frequency response of a_{0p} for various damping c_0 with $k_1 = 0$: original system without TMD (dots), $c_0 = 0$ (dashed), O(ϵ) design (bold solid), various non-optimal designs (solid).

approximate behavior for the approximate design. (The curve with a single peak is the minimax design described in Chapter 2.)

At O(ϵ^2), we obtain a transfer function for a_{1p}. We again want to minimize the peak response of x_1, but now we have a better approximation of the behavior. First, we calculate the total transfer function $a_{0p} + \epsilon a_{1p}$. The value of ϵ does not effect the resulting design. We again would like to make the heights of the peaks equal, but there are no stationary points so the approach is more brute force. First, we find the locations of the peaks by setting the derivative of the transfer function with respect to σ equal to zero. Then, in order to minimize the height of the peaks, we differentiate with respect to the parameters k_2 anc c_1 and set the resulting equations equal to zero. The resulting design is $k_2 = -2$ and $c_1 = 0$. Figure A-2 shows the magnitude of the transfer function for various k_2.

At O(ϵ^3), the transfer function for a_{2p} is found. Similar methods to those used at O(ϵ^2) can be used to find the optimal k_3 and c_2.

Now, we compare the perturbation design to the Den Hartog [8] and exact designs.

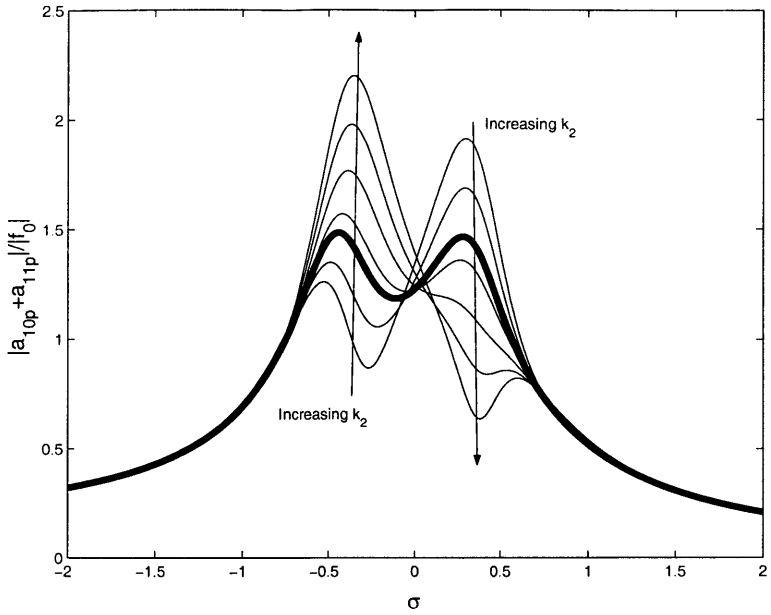

Figure A-2: Frequency response of $a_{0p} + a_{1p}$ for various tuning k_2 with $c_1 = 0$: $O(\epsilon^2)$ design $k_2 = -2$ (bold solid), various non-optimal designs (solid).

The transfer function for the dimensional equations is given by

$$\frac{X_1(s)}{F(s)} = \frac{ms^2 + cs + k}{Mms^4 + cs^3(m+M) + s^2(mK + k(m+M)) + Kcs + kK} \tag{A.43}$$

Figure A-3 shows the frequency responses of the various designs for $\epsilon = 0.22$ (i.e. mass ratio=0.05). The Den Hartog design is undiscernible from the exact H_∞ optimal design for this value of ϵ.

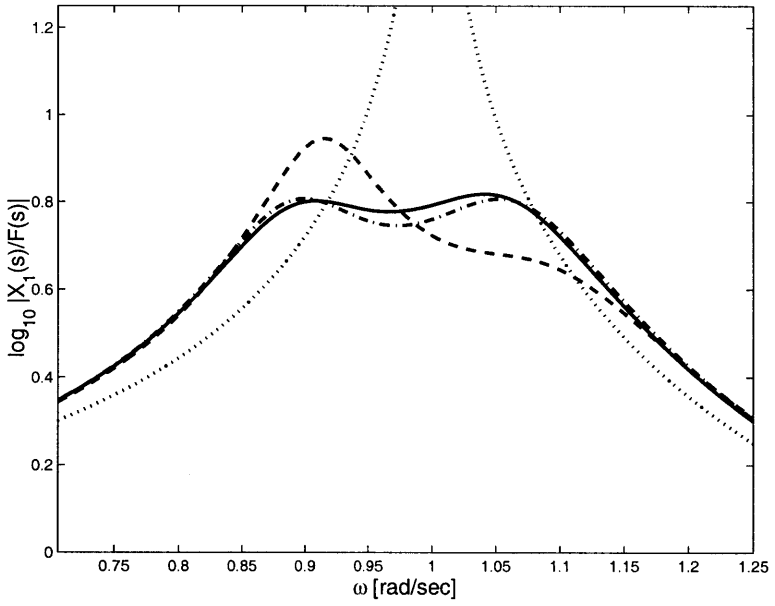

Figure A-3: Frequency response with mass ratio of 0.05: original system without TMD (dots), O(ϵ) design (dashed), O(ϵ^2) design (solid), optimal design (dashdot).

Appendix B

Single-Degree-of-Freedom Tuned-Mass Damper Subject to Random Excitation

In this appendix, we examine the behavior of a SDOF TMD subject to light, random excitation. Specifically, we determine the approximate tuning and damping for the $H2$ optimal design, which minimizes the variance to white noise excitation.

The nondimensionalization procedure is the same as for the harmonically excited system discussed in Appendix A. The nondimensional equations of motion are

$$\begin{bmatrix} 1 & 0 \\ 0 & 1 \end{bmatrix} \begin{pmatrix} D^2x_1 \\ D^2x_2 \end{pmatrix} + \begin{bmatrix} \epsilon^3 c & -\epsilon^2 c \\ -\epsilon^2 c & \epsilon c \end{bmatrix} \begin{pmatrix} Dx_1 \\ Dx_2 \end{pmatrix} + \begin{bmatrix} 1+\epsilon^2 k & -\epsilon k \\ -\epsilon k & k \end{bmatrix} \begin{pmatrix} x_1 \\ x_2 \end{pmatrix} = \begin{pmatrix} \epsilon f(T;\epsilon) \\ 0 \end{pmatrix} \quad \text{(B.1)}$$

where D is the operator denoting differentiation with respect to nondimensional time $T = \Omega_n t$. Because the tuning and damping will not be chosen to make the eigenvalues close to coalescence, the expansions for the eigenvalues and eigenvectors do not need

to include terms with $\epsilon^{1/2}$ powers. Thus, we write the displacements as

$$\begin{pmatrix} x_1 \\ x_2 \end{pmatrix} = \begin{pmatrix} x_{10} \\ x_{20} \end{pmatrix} + \epsilon \begin{pmatrix} x_{11} \\ x_{21} \end{pmatrix} + \epsilon^2 \begin{pmatrix} x_{12} \\ x_{22} \end{pmatrix} + \dots \tag{B.2}$$

We introduce nondimensional time scales

$$T_0 = T \quad T_1 = \epsilon T \quad T_2 = \epsilon^2 T, \dots \tag{B.3}$$

The derivative operator D is expanded as

$$D = D_0 + \epsilon D_1 + \epsilon^2 D_2 + \dots \tag{B.4}$$

where D_0 is the derivative operator with respect to T_0, D_1 is the derivative operator with respect to T_1, D_2 is the derivative operator with respect to T_2, and so on. The stiffness of the absorber is written as

$$k = 1 + \epsilon k_1 + \epsilon^2 k_2 + \dots \tag{B.5}$$

The damping of the absorber is written as

$$c = c_0 + \epsilon c_1 + \epsilon^2 c_2 + \dots \tag{B.6}$$

We expect that the dominant component behavior is due the components of the response in the neighborhood of resonance so we consider the forcing to be in the neighborhood of resonance. The frequency of excitation is expanded as

$$\omega = 1 + \epsilon\sigma \tag{B.7}$$

where σ is O(1). Therefore, the scaled forcing is given by

$$f(T;\epsilon) = f_0 e^{iT_0(1+\epsilon\sigma)} \tag{B.8}$$

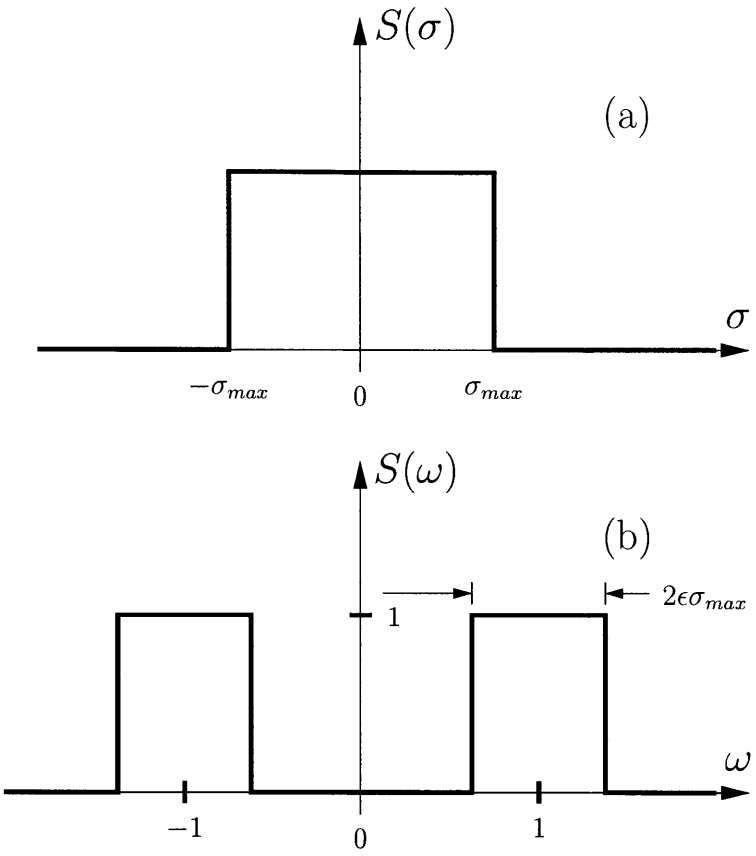

Figure B-1: Spectrum of excitation force: (a) Spectrum of σ, (b) Spectrum of ω.

The forcing is band-limited white noise (random) by requiring the specturm $S(\sigma)$ to be zero when $\sigma > O(1)$ (see Figure B-1). Now, we are ready to perform the perturbation expansion.

B.1 Method of Multiple Scales

B.1.1 Expansion to O(1)

At this order, the two subsystems are decoupled and the governing equation is

$$\begin{bmatrix} 1 & 0 \\ 0 & 1 \end{bmatrix} \begin{pmatrix} D_0^2 x_{10} \\ D_0^2 x_{20} \end{pmatrix} + \begin{bmatrix} 1 & 0 \\ 0 & 1 \end{bmatrix} \begin{pmatrix} x_{10} \\ x_{20} \end{pmatrix} = \begin{pmatrix} 0 \\ 0 \end{pmatrix} \tag{B.9}$$

The response is

$$x_{10} = A_0 e^{iT_0} + \text{cc} \tag{B.10}$$

$$x_{20} = B_0 e^{iT_0} + \text{cc} \tag{B.11}$$

where cc denotes complex conjugate. As before, we may ignore the complex conjugate because this problem is linear.

B.1.2 Expansion to O(ϵ)

The equations at this order are

$$\begin{bmatrix} 1 & 0 \\ 0 & 1 \end{bmatrix} \begin{pmatrix} D_0^2 x_{11} \\ D_0^2 x_{21} \end{pmatrix} + \begin{bmatrix} 1 & 0 \\ 0 & 1 \end{bmatrix} \begin{pmatrix} x_{11} \\ x_{21} \end{pmatrix} = \begin{pmatrix} -2iD_1A_0 + B_0 + f_0 e^{i\sigma T_1} \\ A_0 - 2iD_1B_0 - (k_1 + ic_0)B_0 \end{pmatrix} e^{iT_0} \tag{B.12}$$

To suppress secular terms, we require that the RHS be zero. Rearranging terms, we obtain

$$\begin{pmatrix} D_1A_0 \\ D_1B_0 \end{pmatrix} = \begin{bmatrix} 0 & -\frac{i}{2} \\ -\frac{i}{2} & \frac{k1i-c_0}{2} \end{bmatrix} \begin{pmatrix} A_0 \\ B_0 \end{pmatrix} + \begin{pmatrix} f_0 e^{i\sigma T_1} \\ 0 \end{pmatrix} \tag{B.13}$$

Now, we would like to find the variance of the response A_0 to the excitation $f_0 e^{i\sigma T_1}$ where the spectrum $S(\sigma)$ is constant band-limited. Therefore, we want to calculate

$$E[A_0^2] = \int_{-\sigma_{max}}^{\sigma_{max}} |H_0(\sigma)|^2 d\sigma \tag{B.14}$$

where $H_0(\sigma)$ is the transfer function from f_0 to A_0. This integral is difficult to calculate. Because we expect the contribution to the integral to be negligible for $|\sigma| > \sigma_{max}$, we extend the limits of integration to $\pm\infty$. Thus, the expected value becomes

$$E[A_0^2] = \int_{-\infty}^{\infty} |H_0(\sigma)|^2 d\sigma \tag{B.15}$$

The transfer function as given in Appendix A is

$$H_0(\sigma) = \frac{A_0}{f_0} = \frac{\frac{\sigma}{2} - \frac{k_1 + ic_0}{4}}{-\sigma^2 + \frac{\sigma}{2}(k_1 + ic_0) + \frac{1}{4}} \tag{B.16}$$

Then, $|H_0(\sigma)|^2$ is a rational function whose denominator is a fourth-order polynomial and whose numerator is a second-order polynomial. Its integral must be evaluated using contour integration. Tables of integrals of rational functions of the form

$$\int_{-\infty}^{\infty} \left| \frac{g(j\omega)}{h(j\omega)} \right|^2 d\omega \tag{B.17}$$

where g and h are polynomials with real coefficients are given in many references, such as [6] and [16]. For these formulas to be valid, the poles of the transfer function must not lie on the real axis. (Otherwise, an indented contour must be used and the resulting formulas will be different.) However for the transfer function in our problem, the coefficients of the polynomial in the denominator are complex, and these tables are not available.

To compute the integral, we make use of Cauchy's Residue Theorem [31]:

$$\oint f(z)dz = 2\pi i \sum_{m=1}^{n} \text{Res}(z_m) \tag{B.18}$$

where $\text{Res}(z_m)$ is the residue of the poles z_m inside the contour. We choose a "D"-shaped countour which extends from $-\infty$ to $+\infty$ along the real axis, and whose ends are connected by a semicircular arc in the counterclockwise direction in the upper half-plane (see Figure B-2). The contribution to the integral of the semi-circular arc is zero because the numerator of the integrand is two orders in σ smaller than the denominator.

Another requirement is that no poles exist on the real axis, otherwise we must complicate the procedure by using an indented contour. Through conformal mapping (e.g. [31]), we now show that if $c_0 > 0$, then both poles of $H_0(\sigma)$ will occur in the upper half plane, and if $c_0 < 0$, then both poles will occur in the lower half-plane. The transfer function has poles at

$$\sigma = \frac{1}{2}\left(\frac{k_1 + jc_0}{2} \pm \sqrt{\frac{(k_1 + jc_0)^2}{4} + 1} \right) \tag{B.19}$$

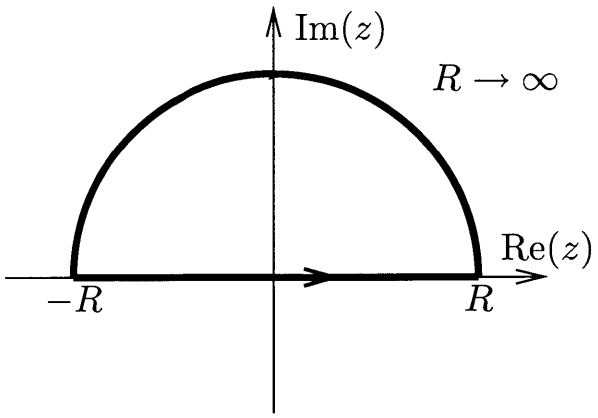

Figure B-2: Integration contour

We define a complex variable z of the form

$$z = \frac{k_1 + jc_0}{2} \tag{B.20}$$

and examine the mapping

$$w = \sigma(z) = \frac{1}{2}\left(z \pm \sqrt{z^2+1}\right) \tag{B.21}$$

The square root is a multi-valued function so we must define a branch cut. The branch point is a point at which the function is not analytic. For $w = \sigma(z)$, the branch points are $z = \pm i$. We may rewrite this function as

$$w = \sigma(z) = \frac{1}{2}\left(z \pm e^{\frac{1}{2}\ln|z^2+1| + \frac{i}{2}\arg(z^2+1)}\right) \tag{B.22}$$

or, equivalently, as

$$w = \sigma(z) = \frac{1}{2}\left(z \pm ze^{\frac{1}{2}\ln|1+\frac{1}{z^2}| + \frac{i}{2}\arg(1+\frac{1}{z^2})}\right) \tag{B.23}$$

where arg is the argument function $-\pi < \arg(z) \leq \pi$. The branch cuts are the places where $z^2 + 1$ is negative real. In the case of (B.22), we choose the branch cuts to go from $z = -i$ to $-i\infty$ along the imaginary axis and from $z = i$ to $i\infty$ along the

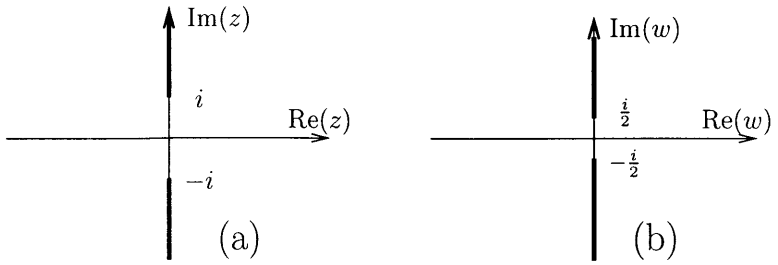

Figure B-3: Mapping of z-plane (a) to w-plane (b) for $w = \sigma(z)$ given by (B.22)

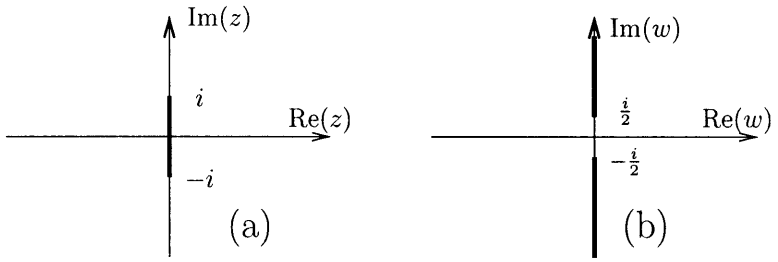

Figure B-4: Mapping of z-plane (a) to w-plane (b) for $w = \sigma(z)$ given by (B.23)

imaginary axis. In the case of (B.23), we choose the branch cuts to go from $z = -i$ to $z = i$. Under both mappings, (B.22) and (B.22), the branch cut is mapped to the imaginary axis (see Figures B-3 and B-4).

Conformal mapping of a grid in the upper half-plane (see Figure B-5) under the transformation $w = \sigma(z)$ given by (B.22) shows that as long as the damping is non-zero both poles of the transfer function are in the upper half-plane if $c_0 > 0$ and in the lower half-plane if $c_0 < 0$. Figure B-6 shows this for the case $c > 0$. The mapping breaks down near the branch cut because the grid is not properly spaced close to it. Thus, the poles of $|H(\sigma)|^2$ are the poles of the transfer function and their complex conjugates (see Figure B-7).

We are now ready to calculate the integral I, which involves quite tedious algebra. To be somewhat more general, we write the transfer function in the form

$$H(\sigma) = \frac{B_1\sigma + B_{0,R} + iB_{0,I}}{-A_2\sigma^2 + i\sigma(-iA_{1,I} + A_{1,R}) + A_0} \tag{B.24}$$

where B_1, $B_{0,R}$, $B_{0,I}$, A_2, $A_{1,I}$, $A_{1,R}$, and A_0 are real. Using Cauchy's Residue Theo-

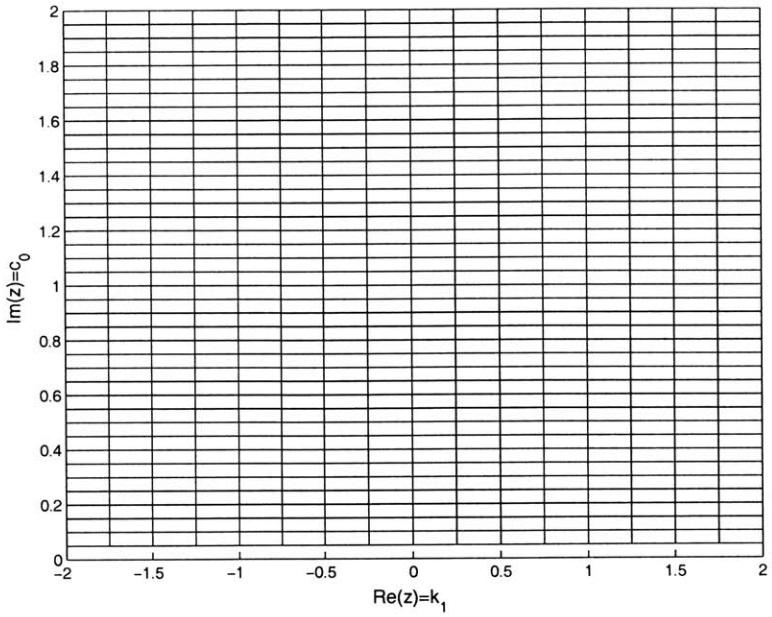

Figure B-5: Grid of points in the upper half of the z-plane.

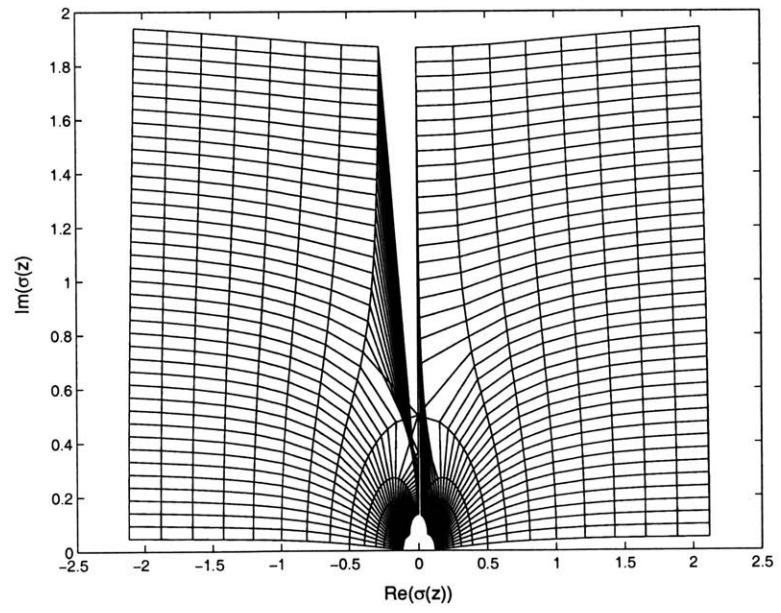

Figure B-6: Mapping of the z-plane grid shown in Figure B-5 under the mapping $w = \sigma(z)$ as given by (B.22).

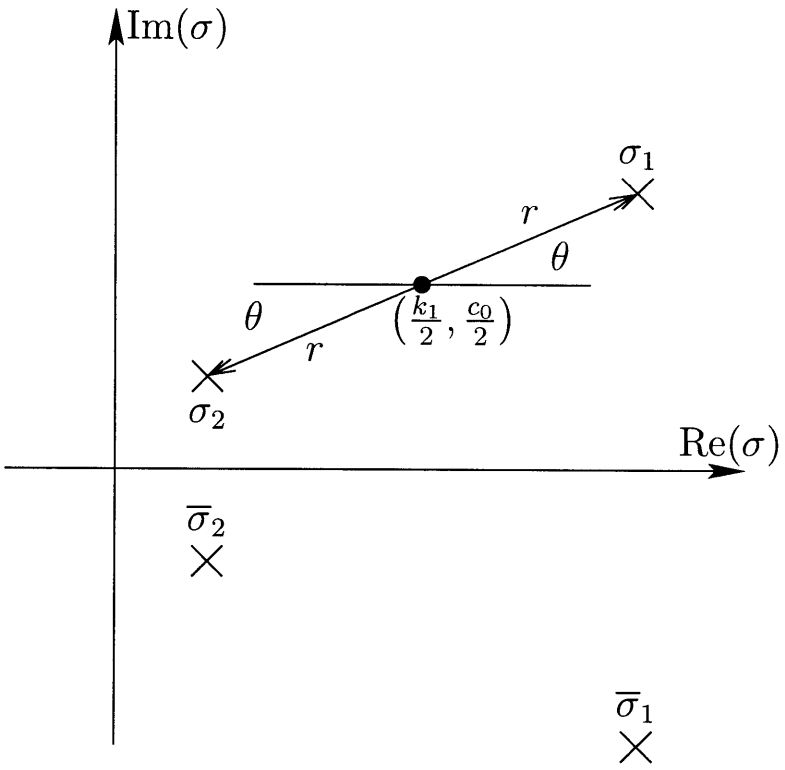

Figure B-7: Schematic of pole locations for $H(\sigma)$.

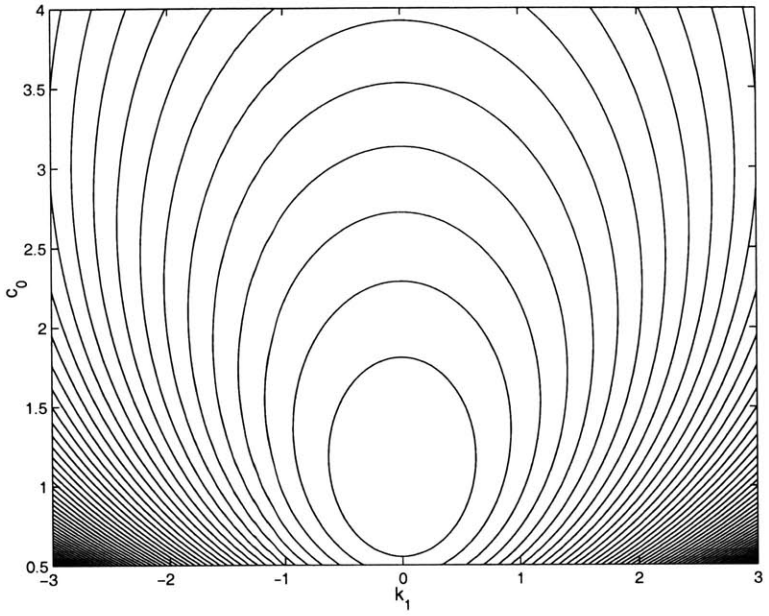

Figure B-8: Contour plot of the variance $E[A_0^2]$ as a function k_1 and c_0.

rem, we obtain

$$I = \frac{\pi}{A_2} \frac{\begin{bmatrix} 4(B_{0,R}^2 + B_{0,I}^2)A_2^2 A_{1,R} + B_1^2(A_{1,R}^3 + A_{1,R}A_{1,I}^2) \\ +4B_1 B_{0,R} A_{1,I} A_{1,R} A_2 + r^2 \left(B_1^2(A_{1,R}\cos 2\theta - A_{1,I}\sin 2\theta) - 2B_1 B_{0,R} A_2 \sin 2\theta\right) \end{bmatrix}}{A_{1,R}^4 + A_{1,R}^2 R^2 \cos 2\theta - r^4 \cos^2\theta \sin^2\theta} \tag{B.25}$$

where r is given by

$$r = \sqrt{\left|4A_2A_0 - A_{1,R}^2 + A_{1,I}^2 + 2iA_{1,R}A_{1,I}\right|} \tag{B.26}$$

and θ is given by

$$\theta = \frac{1}{2}\arg(4A_2A_0 - A_{1,R}^2 + A_{1,I}^2 + 2iA_{1,R}A_{1,I}) \tag{B.27}$$

We substitute for B_1, $B_{0,R}$, $B_{0,I}$, A_2, $A_{1,I}$, $A_{1,R}$, and A_0 obtain and an expression for $E[A_0^2]$. A contour plot as k_1 and c_0 are varied is given in Figure B-8.

After suppression of the secular terms, the response for x_{11} and x_{21} is given by

$$x_{11} = A_1 e^{iT_0} + \text{cc} \tag{B.28}$$

$$x_{21} = B_1 e^{iT_0} + \text{cc} \tag{B.29}$$

B.1.3 Expansion to O(ϵ^2)

As for the system with harmonic forcing, the governing equations at this order are

$$\begin{bmatrix} 1 & 0 \\ 0 & 1 \end{bmatrix} \begin{pmatrix} D_0^2 x_{12} \\ D_0^2 x_{22} \end{pmatrix} + \begin{bmatrix} 1 & 0 \\ 0 & 1 \end{bmatrix} \begin{pmatrix} x_{12} \\ x_{22} \end{pmatrix} = \begin{bmatrix} -2D_0D_1 & 1 \\ 1 & -2D_0D_1 - (k_1 + c_0D_0) \end{bmatrix} \begin{pmatrix} x_{11} \\ x_{21} \end{pmatrix}$$
$$+ \begin{bmatrix} -2D_0D_2 - D_1^2 - 1 & k_1 + c_0D_0 \\ k_1 + c_0D_0 & -2D_0D_2 - D_1^2 - (k_2 + c_1D_0 + c_0D_1) \end{bmatrix} \begin{pmatrix} x_{10} \\ x_{20} \end{pmatrix} \tag{B.30}$$

We substitute for x_{10}, x_{20}, x_{11}, and x_{21} and suppress secular terms by setting the RHS to zero. We obtain

$$\begin{bmatrix} -2iD_2 - D_1^2 - 1 & k_1 + ic_0 \\ k_1 + ic_0 & -2iD_2 - D_1^2 - (k_2 + ic_1 + c_0D_1) \end{bmatrix} \begin{pmatrix} A_0 \\ B_0 \end{pmatrix}$$
$$+ \begin{bmatrix} -2iD_1 & 1 \\ 1 & -2iD_1 - (k_1 + ic_0) \end{bmatrix} \begin{pmatrix} A_1 \\ B_1 \end{pmatrix} = \begin{pmatrix} 0 \\ 0 \end{pmatrix} \tag{B.31}$$

where A_0 and B_0 are functions of f and T_1 only. To obtain a transfer function from f_0 to a_1, we again assume a solution of the form

$$\begin{pmatrix} A_{1p} \\ B_{1p} \end{pmatrix} = \begin{pmatrix} a_{1p} \\ b_{1p} \end{pmatrix} e^{i\sigma T_1} \tag{B.32}$$

and obtain

$$\begin{pmatrix} \frac{a_{1p}}{f_0} \\ \frac{b_{1p}}{f_0} \end{pmatrix} = P^{-1}QP^{-1} \begin{pmatrix} 1 \\ 0 \end{pmatrix} \tag{B.33}$$

where

$$P = \begin{bmatrix} 2\sigma & 1 \\ 1 & 2\sigma - (k_1 + ic_0) \end{bmatrix} \tag{B.34}$$

and

$$Q = \begin{bmatrix} \sigma^2 - 1 & k_1 + ic_0 \\ k_1 + ic_0 & \sigma^2 - (k_2 + ic_1 + ic_0\sigma) \end{bmatrix} \tag{B.35}$$

The transfer function for a_{1p} is

$$\frac{a_{1p}}{f_0} = \frac{4\sigma^4 - 4(k_1 + jc_0)\sigma^3 + \sigma^2((k_1 + jc_0)^2 - 3) - j\sigma c_0 + (k_1 + jc_0)^2 - (k_2 + jc_1)}{(4\sigma^2 - 2\sigma(k_1 + jc_0) - 1)^2} \tag{B.36}$$

Because both the numerator and denominator are fourth-order, the integral to calculate the variance of a_{1p} will not converge in general. Thus, we leave this step and higher orders to future work.

B.2 Approximate $H2$ Optimal Design

The $H2$ optimal design minimizes the variance to white noise excitation. The approximate design must minimize the variance of A_0. To find the optimal values of c_0 and k_1, we set the partial derivative of the expression for the variance of A_0 with respect to c_0 and k_1 to zero and solve for c_0 and k_1 simultaneously. This step is very tedious because of the cumbersome nature of the expression for the variance of A_0. From the contour plot of the variance (see Figure B-8), we observe that the variance is symmetric about $k_1 = 0$. Therefore, we expect that $k_1 = 0$ is the optimal value. Another, perhaps more naive, approach is to examine the expression for $|H_0(\sigma)|^2$:

$$|H_0(\sigma)| = \frac{\left(\frac{\sigma}{2} - \frac{k_1}{4}\right)^2 + \left(\frac{c_0}{4}\right)^2}{\left(\frac{1}{4} - \sigma^2 + \frac{k_1}{2}\sigma\right)^2 + \left(\frac{c_0}{2}\sigma\right)^2} \tag{B.37}$$

Then, we may guess that the optimal value of k_1 is such that the maximum of $\frac{1}{4} - \sigma^2 + \frac{k_1}{2}\sigma$ occurs at $\sigma = 0$. Again, we find $k_1 = 0$.

The benefit of finding $k_1 = 0$ is that we may use the simpler expressions for the

variance found in textbooks, such as Crandall and Mark [6]. In that case the variance of A_0 is

$$E[A_0^2] = \pi \left(\frac{c_0}{8} + \frac{1}{8c_0} \right) \tag{B.38}$$

The value of c_0 which minimizes this expression is $c_0 = 1$. (We ignore $c_0 = -1$ because the damping should be positive.) This design matches the Maclaurin series expansion of the exact solution given below.

B.2.1 Comparison to the Exact $H2$ Optimal Design

To calculate the variance of the exact solution, we use Equation 2.38 from the text by Crandall and Mark [6]. (One may equivalently use their Equation 2.55.) For the transfer function

$$H(\omega) = \frac{-i\omega^3 B_3 - \omega^2 B_2 + i\omega B_1 + B_0}{\omega^4 A_4 - i\omega^3 A_3 - \omega^2 A_2 + i\omega A_1 + A_0} \tag{B.39}$$

the variance is

$$\int_{-\infty}^{\infty} |H(\omega)|^2 \, d\omega = \pi \frac{\left[\begin{array}{l} (B_0^2/A_0)(A_2A_3 - A_1A_4) + A_3(B_1^2 - 2B_0B_2) \\ +A_1(B_2^2 - 2B_1B_3) + (B_3^2/A_4)(A_1A_2 - A_0A_3) \end{array} \right]}{A_1(A_2A_3 - A_1A_4) - A_0A_3^2} \tag{B.40}$$

The exact solution for tuning the SDOF TMD given by Asami *et al* [3] is

$$k = \frac{\omega_a^2}{\Omega_n^2} = \frac{1}{(1+\epsilon^2)^2} \frac{2+\epsilon^2}{2} \tag{B.41}$$

$$\zeta = 2m\omega_a = \epsilon \sqrt{\frac{4+3\epsilon^2}{8(1+\epsilon^2)(2+\epsilon^2)}} \tag{B.42}$$

With mass M normalized to be 1, time normalized to give $\Omega_n = 1$, and a mass ratio of 0.05, the variance of the exact solution is 27.9315. (Sometimes this value is normalized by π.) The variance for the $O(\epsilon)$ design is 29.5042. The next correction in the Maclaurin series expansion of the exact solution results in a variance of 27.9803. The third correction (should agree with $O(\epsilon^3)$) results in a variance of 27.9389.

Appendix C

Derivation of the Coupled Equations of Motion

In this appendix, we derive the form of the coupled equations of motion for the small displacements of two rigid bodies connected by linear springs and dampers by using the principle of superposition.

Consider the diagram of a MDOF TMD shown in Figure C-1. The coordinate systems of the two bodies are parallel and centered at their respective centers of mass.

We consider only the stiffness matrix because the damping is easily extrapolated from the form of the coupled stiffness matrix. The force-displacement relationship for the primary mass without the absorber is given by

$$\begin{pmatrix} F_1 \\ \Gamma_1 \end{pmatrix} = \begin{bmatrix} k_{xx1} & k_{x\theta 1} \\ k'_{x\theta 1} & k_{\theta\theta 1} \end{bmatrix} \begin{pmatrix} x_1 \\ \theta_1 \end{pmatrix} = K_1 \begin{pmatrix} x_1 \\ \theta_1 \end{pmatrix} \tag{C.1}$$

where F_1 is the vector of forces at the center of mass, Γ_1 is the vector of moments about the center of mass, x_1 is the vector of translations of the center of mass, and θ_1 is the vector of rotations. Similarly, the force-displacement relationship of the

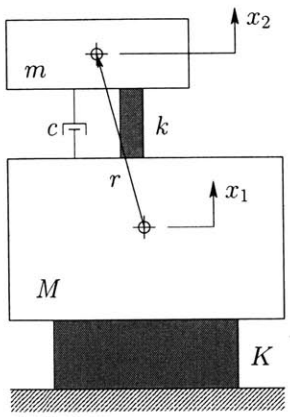

Figure C-1: Diagram of a vibratory system comprising a mass M to which a tuned-mass damper m is attached.

absorber is given by

$$\begin{pmatrix} F_2 \\ \Gamma_2 \end{pmatrix} = \begin{bmatrix} k_{xx2} & k_{x\theta 2} \\ k'_{x\theta 2} & k_{\theta\theta 2} \end{bmatrix} \begin{pmatrix} x_2 \\ \theta_2 \end{pmatrix} = K_2 \begin{pmatrix} x_2 \\ \theta_2 \end{pmatrix} \tag{C.2}$$

where x_2 is the vector of translations of the absorber's center of mass and θ_2 is the vector of rotations of the absorber.

First, we calculate the force and torque (applied at the center of mass) required to hold the primary mass in place with zero displacement while the absorber is given a general, static, non-zero displacement. The forces and torques on the two bodies are given by

$$\begin{pmatrix} F_1 \\ \Gamma_1 \\ F_2 \\ \Gamma_2 \end{pmatrix} = \begin{bmatrix} -k_{xx2} & -k_{x\theta 2} \\ -k'_{x\theta_2} - Rk_{xx2} & -k_{\theta\theta 2} - Rk_{x\theta 2} \\ k_{xx2} & k_{x\theta 2} \\ k'_{x\theta 2} & k_{\theta\theta 2} \end{bmatrix} \begin{pmatrix} x_2 \\ \theta_2 \end{pmatrix} \tag{C.3}$$

where the cross product has been written in matrix form using a skew-symmetric matrix representing the vector from the center of mass of the primary mass to the

center of mass of the absorber:

$$r \times F = \begin{bmatrix} 0 & -r_z & r_y \\ r_z & 0 & -r_x \\ -r_y & r_x & 0 \end{bmatrix} \begin{pmatrix} F_x \\ F_y \\ F_z \end{pmatrix} \tag{C.4}$$

Now, we hold the absorber fixed with zero displacement in the inertial reference frame while the primary mass is given a general, static, non-zero displacement. The resulting forces and torques on the bodies are

$$\begin{pmatrix} F_1 \\ \Gamma_1 \\ F_2 \\ \Gamma_2 \end{pmatrix} = \begin{bmatrix} k_{xx1} + k_{xx2} & k_{x\theta 2} - k_{xx2}R + k_{x\theta_2} \\ k_{x\theta 1} + Rk_{xx2} + k'_{x\theta 2} & k_{\theta\theta 1} + k_{\theta\theta 2} - Rk_{xx2}R + Rk_{x\theta 2} - k'_{x\theta 2}R \\ -k_{xx2} & -k_{x\theta_2} + k_{xx2}R \\ -k'_{x\theta_2} & -k_{\theta\theta 2} + k'_{x\theta_2}R \end{bmatrix} \begin{pmatrix} x_1 \\ \theta_1 \end{pmatrix} \tag{C.5}$$

Using the principle of superposition, we find the force-displacement relation for the coupled system to be

$$\begin{pmatrix} F_1 \\ \Gamma_1 \\ F_2 \\ \Gamma_2 \end{pmatrix} = \begin{bmatrix} K_1 + \tilde{G}K_2\tilde{G}' & -\tilde{G}K_2 \\ -K_2\tilde{G}' & K_2 \end{bmatrix} \begin{pmatrix} x_1 \\ \theta_1 \\ x_2 \\ \theta_2 \end{pmatrix} \tag{C.6}$$

where

$$G = \begin{bmatrix} I & 0 \\ R & I \end{bmatrix} \tag{C.7}$$

where R is given by and I is the $n \times n$ identity matrix (Each system, absorber and primary mass, has n degrees-of-freedom.).

Appendix D

Assignment of the Absorber Mode Shapes

In the approximate minimax design of the MDOF TMD (Section 3.3), we assign mode shapes of the absorber in a ranked order. In this appendix, we describe how this process works. This process is basically the Gram-Schmidt orthogonalization except that the vector must be mass-orthogonal instead of orthogonal.

The set of optimal eigenvectors v_{2p}^* are known, but they do not form a mass-orthogonal set. The mode shape with the least damping is assigned exactly its determined optimal v_{2p}^*. For simplicity and without loss of generality, we assume that the achievable damping increases with p (i.e, mode 1 has the least achievable damp-

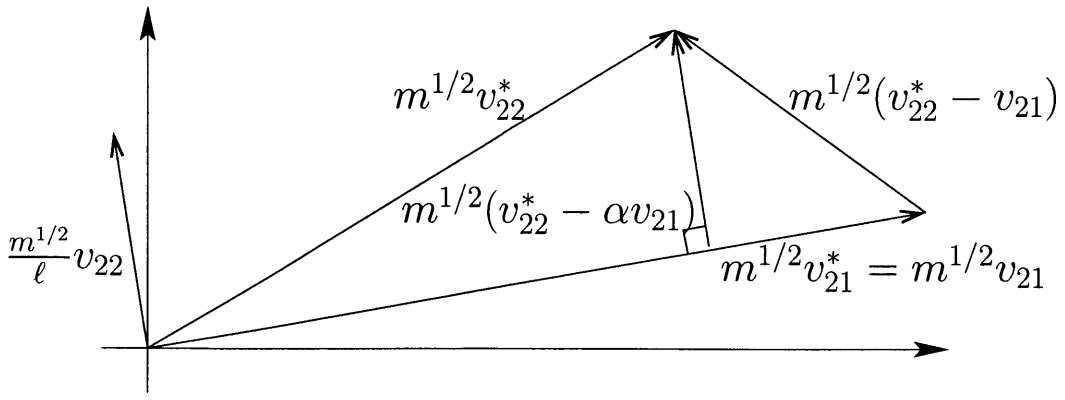

Figure D-1: Projection of mode shapes under the mass-orthogonality constraint.

ing, mode 2 has the next smallest achievable damping coefficient, and so on.) The higher modes are assigned to maximize the projection on the optimal mode v_{2p}^* and be mass-orthogonal to all previously assigned modes.

The requirement of mass-orthonormality can be written as

$$v_{2p} m v_{2q} = \delta_{pq} \tag{D.1}$$

where m is the mass matrix and δ_{pq} is the delta function given by

$$\delta_{pq} = \begin{cases} 1 & \text{if } p = q \\ 0 & \text{otherwise} \end{cases} \tag{D.2}$$

This requirement can also be written as

$$(m^{1/2} v_{2p})'(m^{1/2} v_{2q}) = \delta_{pq} \tag{D.3}$$

because the mass matrix is symmetric positive semi-definite.

The first mode is assigned its optimal mode shape $v_{21} = v_{21}^*$. The second mode shape is calculated by subtracting the component of $m^{1/2} v_{21}^*$ parallel to $m^{1/2} v_{22}^*$ from $m^{1/2} v_{22}^*$ (see Figure D-1). The resulting vector is in the direction or v_{22}. This step may be written as

$$\frac{m^{1/2} v_{22}}{\ell} = m^{1/2} v_{22}^* - \alpha m^{1/2} v_{21} \tag{D.4}$$

The scalar α is simply the cosine of the angle between the two vectors and may be written as

$$\alpha = \frac{(m^{1/2} v_{21})'(m^{1/2} v_{22}^*)}{\| m^{1/2} v_{21} \| \cdot \| m^{1/2} v_{22}^* \|} = v_{21}' m v_{22}^* \tag{D.5}$$

where we have taken advantage of the mass orthonormality in simplifying the denominator. The scalar ℓ is determined by scaling the resultant vector such that it is mass-orthonormal. The simplified result is

$$\frac{v_{22}}{\ell} = v_{22}^* - (v_{21}' m v_{22}^*) v_{21} \tag{D.6}$$

A similar procedure is followed to calculate v_{23}, which v_{23} must be mass-orthogonal to both v_{21} and v_{22}. Because v_{21} and v_{22} are already mass-orthogonal (Each vector has no projection onto the other.), we simply subtract the component of each vector that points in the same direction as $m^{1/2}v_{23}^*$. Performing the same algebra as for v_{22}, we obtain

$$\frac{v_{23}}{\ell_3} = v_{23}^* - (v_{21}' m v_{23}^*)v_{21} - (v_{22}' m v_{23}^*)v_{22} \tag{D.7}$$

The procedure is continued until all mode shapes have been determined.

Appendix E

A Note on Solvability Conditions

Throughout this thesis, solvability conditions are used to carry out the perturbation expansions. In this appendix, we briefly describe solvability conditions for linear algebraic equations. Further details are given in numerous texts including [23, 24].

Consider the system $Ax = b$ wher A is a $N \times N$ matrix and x and b are $N \times 1$ vectors. The solvability condition for this system may be stated as: If the homogeneous system $Ay = 0$ has a nontrivial solution y, then the inhomogeneous system $Ax = b$ has a solution if and only if $(b, u) = b^T \overline{u} = 0$ where u is the solution of the homogeneous adjoint problem $A'u = 0$ where $'$ indicates the complex conjugate transpose.

In this thesis, two cases are commonly encountered. First, the matrix A is symmetric and complex. Then, we say $A = A^T \neq A'$. The homogeneous adjoint problem is

$$A^T \overline{u} = A\overline{u} = 0 \tag{E.1}$$

The homogeneous solution is $y = \overline{u}$, and the solvability condition is $y^T b = 0$.

Second, the matrix A is block diagonal. For a block diagonal system, we write the equation as

$$\begin{bmatrix} A_1 & 0 \\ 0 & A_2 \end{bmatrix} \begin{pmatrix} x_1 \\ x_2 \end{pmatrix} = \begin{pmatrix} b_1 \\ b_2 \end{pmatrix} \tag{E.2}$$

where the homogeneous adjoint solustion is

$$u = \begin{pmatrix} u_1 \\ u_2 \end{pmatrix} \tag{E.3}$$

We may impose the solvability condition on each row separately to obtain

$$\begin{pmatrix} u_1' b_1 \\ u_2' b_2 \end{pmatrix} = \begin{pmatrix} 0 \\ 0 \end{pmatrix} \tag{E.4}$$

Bibliography

[1] Masato Abé and Yozo Fujino. Dynamic characterization of multiple tuned mass dampers and some design formulas. *Earthquake Engineering and Structural Dynamics*, 23:813–835, 1994.

[2] Y. Arfiadi and M. Hadi. Passive and active control of (the) three-dimensional buildings. *Earthquake Engineering and Structural Dynamics*, 29:377–396, 2000.

[3] Toshihiko Asami, Osamu Nishihara, and Amr M. Baz. Analytical solutions to h∞ and h2 optimization of dynamic vibration absorber(s) attached to damped linear systems. *Journal of Vibration and Acoustics*, 124:67–78, 2002.

[4] John E. Brock. A note on the damped vibration absorber. *Journal of Applied Mechanics*, 1946.

[5] Genda Chen and Jingning Wu. Optimal placement of multiple tune mass dampers for seismic structures. *Journal of Structural Engineering*, 127(9):1054–1062, September 2001.

[6] Stephen H. Crandall and William D. Mark. *Random vibration in Mechanical Systems.* Academic Press, 1973.

[7] Amitabha DebChaudhury. Dynamic synthesis of substructures. *Mechanics of Structures and Machines*, 18(2):239–262, 1990.

[8] J.P. Den Hartog. *Mechanical Vibrations.* McGraw-Hill, 1947.

[9] H. Frahm. Device for damping vibrations of bodies, 1909. US Patent 989958.

[10] Yozo Fujino and Masato Abé. Design formulas for tuned mass dampers based on a perturbation technique. *Earthquake Engineering and Structural Dynamics*, 22:833–854, 1993.

[11] W.-J. Hsueh. Vibration transmissibility of a unidirectional multi-degree-of-freedom system with multiple dynamic absorbers. *Journal of Sound and Vibration*, 229(4):793–805, 2000.

[12] T. Igusa and K. Xu. Vibration control using multiple tuned mass dampers. *Journal of Sound and Vibration*, 175(4):491–503, 1994.

[13] Takeru Igusa and Armen Der Kiureghian. Dynamic characterization of two-degree-of-freedom equipment-structure systems. *Journal of Engineering Mechanics*, 111(1):1–19, January 1985.

[14] Takeru Igusa and Armen Der Kiureghian. Dynamic response of multiply supported secondary systems. *Journal of Engineering Mechanics*, 111(1):20–41, January 1985.

[15] R.G. Jacquot. Optimal dynamic vibration absorbers for general beam systems. *Journal of Sound and Vibration*, 60(4):535–542, 1978.

[16] Hubert M. James, Nathaniel B. Nichols, and Ralph S. Phillips, editors. *Theory of Servomechanisms*. Mcgraw-Hill Book Company, 1947.

[17] Ming Une Jen and E.B. Magrab. Natural frequencies and mode shapes of beams carrying a two degree-of-freedom spring-mass system. *Journal of Vibration and Acoustics*, 115:202–209, April 1993.

[18] A.S. Joshi and R.S. Jangid. Optimum parameters of multiple tuned mass dampers for base-excited damped systems. *Journal of Sound and Vibration*, 202(5):657–667, 1997.

[19] K. Kawazoe, I. Kono, T. Aida, and K. Ebisuda. Beam-type(d) dynamic vibration absorber comprised of free-free beam. *Journal of Engineering Mechanics*, 124:476–479, 1998.

[20] L. Kitis, B.P. Want, and W.D. Pilkey. Vibration reduction over a frequency range. *Journal of Sound and Vibration*, 89:559–569, 1983.

[21] Chunxiang Li. Performance of multiple tuned mass dampers for attenuating undesirable oscillations of structures under the ground acceleration. *Earthquake Engineering and Structural Dynamics*, 29:1405–1421, 2000.

[22] Denys J. Mead. *Passive Vibration Control.* John Wiley & Sons, 1998.

[23] Ali Hasan Nayfeh. *Introduction to Perturbation Techniques.* Wiley-Interscience, 1981.

[24] Ali Hasan Nayfeh. *Problems in Perturbation.* 1993.

[25] H. Nishimura, K. Yoshida, and T. Shimogo. Optimal dynamic vibration absorber for multi-degree-of-freedom systems. *JSME International Journal, Series III*, 32:373–379, 1989.

[26] J. Ormondroyd and J.P Den Hartog. The theory of the dynamic vibration absorber. *ASME Journal of Applied Mechanics*, 1928.

[27] Benito M. Pacheco and Yozo Fujino. Approximate explicit formulas for complex modes of two-degree-of-freedom (2dof) system. *Structural Engineering / Earthquake Engineering*, 6(1):213–222, April 1989.

[28] Jaewook Park and Dorothy Reed. Analysis of uniformly and linearly istributed mass dampers under harmonic and earthquake excitation. *Engineering Structures*, 23:802–814, 2001.

[29] D.A. Rade and V. Steffen Jr. Optimisation of dynamic vibration absorbers over a frequency band. *Mechanical Systems and Signal Processing*, 14:679–690, 2000.

[30] H.J. Rice. Design of multiple vibration absorber systems using modal data. *Journal of Sound and Vibration*, 160:378–385, 1993.

[31] E.B. Saff and A.D Snider. *Fundamentals of Complex Analysis for Mathematics, Science, and Engineering.* Prentice Hall, second edition edition, 1993.

[32] J.C. Snowdon, A.A. Wolfe, and R.L. Kerlin. The cruciform dynamic vibration absorber. *Journal of the Acoustical Society of America*, 75(6):1792–1799, June 1984.

[33] D. Stech. An h2 approach for optimally tuning passive vibration absorbers to flexible structures. *Journal of Guidance, Control, and Dynamics*, 17:636–638, 1994.

[34] J.Q. Sun, M.R. Jolly, and M.A Norris. Passive, adaptive, and active tuned absorbers–a survey. *Transactions of ASME*, 117:234–242, 1995.

[35] Hsiang-Chuan Tsai. Green's function of support-excited structures with tuned-mass dampers derived by a perturbation method. *Earthquake Engineering and Structural Dynamics*, 22:975–990, 1993.

[36] Hsiang-Chuan Tsai. Envelope of green's function for structure response with slightly detuned vibration absorbers. *Earthquake Engineering and Structural Vibration*, 25:1–13, 1996.

[37] A.F. Vakakis and S.A. Paipetis. The effect of a viscously damped dynamic absorber on a linear multi-degree-of-freedom system. *Journal of Sound and Vibration*, 105(1):49–60, February 1986.

[38] Justin M. Verdirame and Samir A. Nayfeh. Design of multi-degree-of-freedom tuned-mass dampers based on eigenvalue perturbation. In *Proceedings of the 44th AIAA/ASME/ASCE/AHS/ASC Structures, Structural Dynamics, and Materials Conference*, Norfolk, VA, April 2003.

[39] Justin M. Verdirame, Samir A. Nayfeh, and Lei Zuo. Design of multi-degree-of-freedom tuned-mass dampers. In Gregory S. Agnes, editor, *Smart Structures and Materials 2002, Damping and Isolation*, volume 4697, pages 98–108, March 2002. 4697-11.

[40] Y.Z. Wang and S.H. Cheng. The optimal design of a dynamic absorber in the time domain and the frequency domain. *Applied Acoustics*, 28:67–78, 1989.

[41] G.B. Warburton. Optimum absorber parameters for minimizing vibration response. *Earthquake Engineering and Structural Dynamics*, 9:251–262, 1981.

[42] G.B. Warburton and E.O. Ayorinde. Optimum absorber parameters for simple systems. *Earthquake Engineering and Structural Dynamics*, 8:197–217, 1980.

[43] J.-J. Wu and A.R. Whittaker. The natural frequencies and mode shapes of a uniform cantilever beam with multiple two-dof spring-mass systems. *Journal of Sound and Vibration*, 272(2):361–381, 1999.

[44] H. Yamaguchi. Vibrations of a beam with an absorber consisting of a viscoelastic beam and a spring-viscous damper. *Journal of Sound and Vibration*, 103(3):417–425, 1985.

[45] Lei Zuo. Optimal control with structure constraints and its application to the design of passive mechanical systems. Master's thesis, Massachusetts Institute of Technology, Cambridge, Massachusetts, 2002.

[46] Lei Zuo and Samir A. Nayfeh. Design of multi-degree-of-freedom tuned-mass dampers: a minimax approach. In *43rd AIAA/ASME/ASCE/AHS/ASC Structures, Structural Dynamics, and Materials Conference.* AIAA, April 2002. AIAA 2002-1283.

[47] Lei Zuo and Samir A. Nayfeh. Design of passive mechanical systems via decentralized control techniques. In *43rd AIAA/ASME/ASCE/AHS/ASC Structures, Structural Dynamics, and Materials Conference.* AIAA, April 2002.

[48] Lei Zuo and Samir A. Nayfeh. The multi-degree-of-freedom tuned-mass damper for the suppression of single-mode vibration under randon and harmonic excitation. In *ASME 2003 Design Engineering Technical Conferences*, Chicago, September 2003.

[49] Lei Zuo and Samir A. Nayfeh. Optimization of the individual stiffness and damping parameters in multiple tuned-mass dampers. *ASME Journal of Vibration and Acoustics*, Submitted.

[50] Lei Zuo and Samir A. Nayfeh. Minimax optimization of multi-degree-of-freedom tuned-mass dampers. *Journal of Sound and Vibration*, to appear.